NASA Technical Memorandum 107551

Development of Physical and Mathematical Models for the Porous Ceramic Tube Plant Nutrifcation System (PCTPNS)

David Teh-Wei-Tsao
Chemical Engineering
Purdue University
West Lafayette, IN

Martin R. Okos
Agricultural Engineeing
Purdue University
West Lafayette, IN

John C. Sager
Biological Research and Life Support Office
J.F. Kennedy Space Center, FL

Thomas W. Dreschel
The Bionetics Corporation
J.F. Kennedy Space Center, FL

January 1992

TABLE OF CONTENTS

ABSTRACT

A physical model of the Porous Ceramic Tube Plant Nutrification System (PCTPNS) was developed through microscopic observations of the tube surface under various operational conditions. In addition, a mathematical model of this system was developed which incorporated the effects of the applied suction pressure, surface tension, and gravitational forces as well as the porosity and physical dimensions of the tubes. The flow of liquid through the PCTPNS was thus characterized for non-biological situations. One of the key factors in the verification of these models is the accurate and rapid measurement of the "wetness" or holding capacity of the ceramic tubes. This study evaluated the thermistor based moisture sensor device which has been proposed to be applied to the PCTPNS in this capacity. Due to the inconsistencies and extended response times of this device, recommendations for future research on alternative sensing devices are proposed. In addition, extensions of the physical and mathematical models to include the effects of plant physiology and growth are also discussed for further research.

LIST OF FIGURES

LIST OF TABLES

ACKNOWLEDGEMENTS

1. INTRODUCTION

1.1. Uses and Applications

The Porous Ceramic Tube Plant Nutrification System (PCTPNS) was conceived to be used primarily under a micro-gravitational (i.e. space) environment. The Controlled Ecological Life Support System (CELSS) Breadboard Project developed by the National Aeronautics and Space Administration (NASA) is based upon utilizing plant biology as an integral part of the entire system (Schwartzkopf, et al., 1989). In particular, plant biomass can be used as a major supply of food for the crew while the natural biological processes of plant growth can be utilized to recycle the air. The oxygen required can be regenerated by the plants from the carbon dioxide produced by the crew and waste recycling processes. The major problems of integrating these concepts into the CELSS Project include fluid handling, adequate delivery of nutrients to the plants, and limited growth area. In addition, a further complication arises due to the need to physically separate the nutrient solution from the atmospheric environment (Wright and Bausch, 1984; MacElroy, 1991). It has been proposed that the Porous Ceramic Tube Plant Nutrification System or a Capillary Effect Root Environment System (CERES) in general can overcome these problems and are a major candidate to be applied in a micro-gravitational environment. Typical applications of this kind include an orbiting space station, a lunar base, or a long-term space flight.

In addition to a micro-gravity application, the advantages of this system can be used in certain Earth-based situations (Olson, et al., 1989). In particular, this plant growth apparatus requires only a minimal quantity of water and growth area as compared to a soil or soil-like medium. Therefore, applications of this system to regions with low water supply and/or limited growth area could be a solution to a limited food supply. However, a major draw-back of applying this technology to these situations is that the initial costs of

setting up the required apparatus can be quite expensive. Although this is a major concern of NASA's, an alternative solution to growing plants in micro-gravity which is more advantageous has not been proposed. Other possibilities include solid substrates, nutrient film technique (NFT), solution culture, and aeroponics (Schwartzkopf, et al., 1989).

1.2. Objectives of Research

One of the major requirements of implementing the Porous Ceramic Tube Plant Nutrification System into a space application is the understanding of how the system works. Current research has been geared towards determining the responses of plants grown on such systems (Dreschel, et al., 1988; Berry, et al., 1990). However, unexplainable results such as the differential accumulation of certain plant nutrients at the tube-root interface (Dreschel, 1988; Olson, et al., 1989) have prompted the study of this system under a non-biological situation. Determination of how the physical system itself affects these results must come before the more complex biological interactions can be answered. The first step towards this goal is the conceptualization of a physical model. In particular, questions need to be answered such as what is the physical make-up or construction of this system and how does the contained fluid transfer from the internal bulk flow through the capillaries of the porous material? In order to accomplish this, a detailed view of the porous material is required along with an understanding of how this affects the flow characteristics through the system. The holding capacity or "wetness" of the ceramic material is a static situation which can be used to determine the forces involved in this physical model.

Once these effecting forces are deduced, the development of a mathematical model would be the second step towards understanding how this system works. The physical parameters affecting this mathematical equation would have to be determined in order for it to be used to predict and control this system. Here on Earth, which is a set one g-force application, a base line of results can be obtained which can be used to confirm or adjust the physical and mathematical models. In addition, these models will have to contend

for alternative gravitational environments such as those present in space. Not only is a micro-gravitational situation important to consider as mentioned previously, but so are greater than one g-force applications such as those present during lift-off. Thus gravity or the lack of gravity will have a profound influence on the flow characteristics through this system. The magnitude of the gravitational force will have to be compared to the other effecting forces such as the induced radial pressure and the surface tension of the liquid in the porous material. Once this comparison is made, settings for an on-line control device can be determined and applied to a more dynamic situation such as during the growth of plants.

One of the key elements in the development of these models is the concept of "wetness" and how to measure it. Current technology utilizes a moisture sensor device which is based upon using thermistors to measure the differences in heat dissipation in water as compared to in air (Bean, et al., 1990). The applicability of this device will have to be determined under both static and dynamic situations in order for it to be used as an on-line control device. In addition, the repeatability of the measurements will have to be used to evaluate the effectiveness of using such a device. Thus a comparison of the results to other standards of measurement such as an absorption or water potential test will have to be made. If the evaluation of this current technology proves it to be inadequate, then an alternate device will have to be designed.

2. BACKGROUND

2.1. Concept and Designs

When dealing with an altered gravitational environment, the flow characteristics of a nutrient delivery system will be seriously affected (Wright and Bausch, 1984). First and foremost, there can be no free liquid entering or leaving the system since it would literally just float away (MacElroy, 1991). Therefore, the entire nutrient solution must be in a self-contained vessel. This further complicates the ability to supply the roots with adequate aeration since normal gravity dependent gas separation processes would no longer occur. In particular, the normal functions of root aeration to supply oxygen for respiration processes (Bausch and Wright, 1985) and carry away excess carbon dioxide will cause an accumulation of these gases in the liquid phase. This accumulation will effectively interfere with the flow of the liquid as well as reduce the contact between the roots and the nutrient solution. Therefore, a complete separation of the gases from the liquid medium is required when the influences of gravity are reduced.

In order to overcome this situation, research has been conducted on the development of a nutrient delivery system which utilizes a porous membrane to separate the two essential phases (Wright and Bausch, 1984). The basic design of this system known as the Capillary Effect Root Environment System (CERES) is as follows (Bausch and Wright, 1985; Wright, et al., 1988). A microporous, hydrophilic membrane is used to physically separate the liquid phase from the gas phase. To ensure proper aeration, the roots are contained on the gas phase side of the membrane. In order to simultaneously deliver nutrients and water to these roots, they must be grown in direct contact with the porous membrane. Since surface tension forces will become dominant when gravitational forces are reduced, the use of capillary action through the pores will conceptually supply the required solution to the roots. In order to

retain the liquid phase, a slight suction must be applied to continuously draw solution from a nutrient reservoir.

Initial constructions of this type of hydroponic system utilized small 10 cm by 10 cm plates supported by a coarse plastic screen laid in the flowing nutrient solution (Wright and Bausch, 1984). A schematic design of this system is reprinted in Figure 2.1 along with an adjustment that was made to remove excess air bubbles from the solution (Bausch and Wright, 1985). In this modified design, a hydrophobic porous membrane is laid parallel to the hydrophilic membrane separated by another mesh screen. Any air bubbles existing in the nutrient solution will be drawn towards the hydrophobic plane and can be removed from the fluid stream. This can be accomplished as long as the pressure beneath the hydrophobic membrane is less than the pressure of the flowing liquid. The materials used in the construction of this CERES setup were a polysulfone hydrophilic membrane with a 0.45 micron pore size, a Teflon hydrophobic membrane with the same pore size, and polyethylene coarse mesh screens.

Several modifications such as the utilization of different membranous materials and altered geometrical designs have been made to this initial design. Problems due to the lack of durability in the materials (Dreschel, et al., 1988; Koontz, et al., 1990) as well as possible leaching of toxic substances or absorption of organic contaminants (Averner, et al., 1984) prompted a closer examination of the construction of these types of systems. Porous stainless steel plates (type 316) mounted on a polyvinyl chloride (PVC) framework were substituted into the initial design of this hydroponic nutrient delivery system (Koontz, et al., 1990). This alleviated the lack of durability of the original system and allowed for continuous reuse but also introduced the possible absorption of contaminants by the PVC. This can be particularly dangerous in that these contaminants may be released into the nutrient solution or onto the root surfaces (Averner, et al., 1984). A second problem also arose due to the uneven distribution of nutrient solution flowing underneath the plates leading to localized drying (Bausch and Wright, 1985). This led to a further modification of the flat plate design which utilized two stainless steel plates sandwiched together (No Name, 1991) . The

Membrane

Water

Screen

$r_c = \frac{\sigma}{\Delta p}$

Root

$p_{wi} < p_a$

$p_{wo} < p_{wi}$
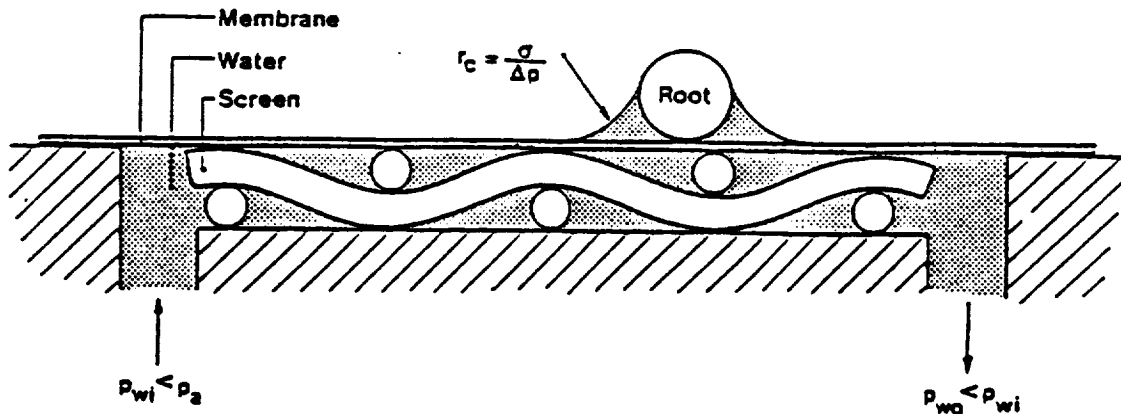
Figure 1 – A cross section illustrating the operational principles of the Capillary Effect Root Environment System.

Hydrophilic

Hydrophobic

Screen not shown

Root

$p_{wi} < p_a$

$p_{am} < p_{wo}$

$p_{wo} < p_{wi}$
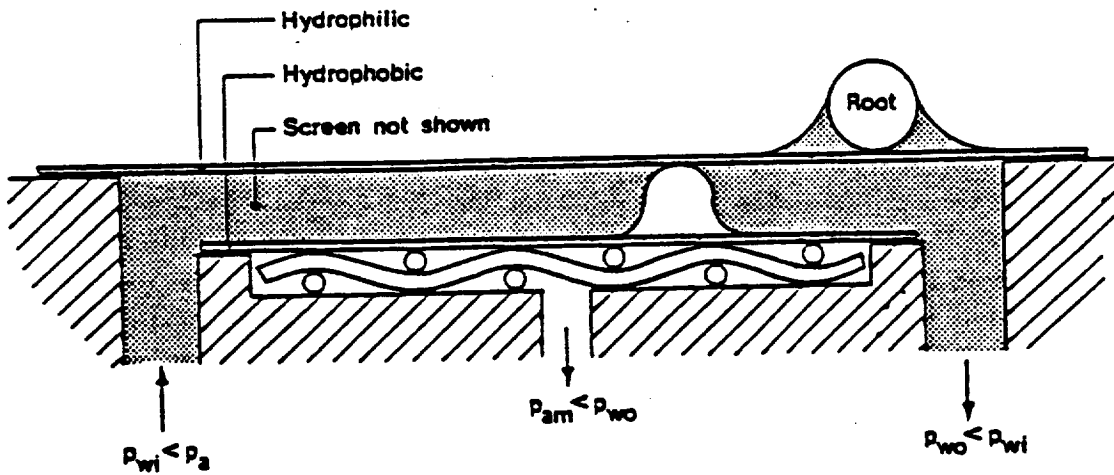
Figure 2 – The hydrophilic/hydrophobic system for removing bubbles from the hydroponic solution in microgravity.

Figure 2.1. Reprint from Wright and Bausch, 1984.

basic concept behind this design is that a second, larger pore containing plate would have a more even distribution of solution and could equalize the delivery of nutrients to the smaller pore containing plate placed above it. The thin (0.050 inch) top plate had an average pore size of 0.5 microns and was the root growth surface while the thicker (0.10 inch) bottom plate had an average pore size of 100 microns. The bulk nutrient solution flowed beneath the bottom plate and capillary action wetted each plate.

A similar adaptation to this original flat plate design utilized two parallel plates oriented with the longitudinal axis of the plant shoot instead of perpendicular (Wright and Bausch, 1984). Each plate was supplied in a parallel configuration with flowing nutrient solution with the plant roots placed in between. This supplied the necessary aeration while increasing the root growth surface area and thus, the contact area with nutrient solution. A schematic of this parallel plate design is reprinted in Figure 2.2. This particular configuration of a CERES concept was designed to specifically fit into a space shuttle middeck stowage locker (Wright and Bausch, 1984). In addition to size limitations and a complex flow control, the problem of an uneven distribution of nutrient solution also occurred.

In order to compensate for this situation, another configuration which utilized a tubular design was conceptualized (Dreschel, et al., 1987; Dreschel, et al., 1988). The initial construction of this tubular CERES setup utilized an acrylic (Versapor) membrane material formed into a tube and internally supported by a semi-rigid plastic screen. This cylindrical membrane was then encased in PVC tubing which contained a slot to accommodate emerging plants. The acrylic material provided a more durable construction (Dreschel, et al., 1988) but the PVC casing tended towards the organic contamination problem discussed earlier (Averner, et al., 1984). Other materials tested in this configuration include porous polyethylene tubes (Dreschel, et al., 1988; Dreschel, 1988; Dreschel and Sager, 1989; Dreschel, et al., 1990a) and extruded polypropylene tubes (Orbisphere Corporation, 1988; Dreschel, et al., no date). In addition to the problems involved with utilizing the PVC casings in the alternative materials, further problems could have arose due to the leaching of toxic substances particularly by the polyethylene. These
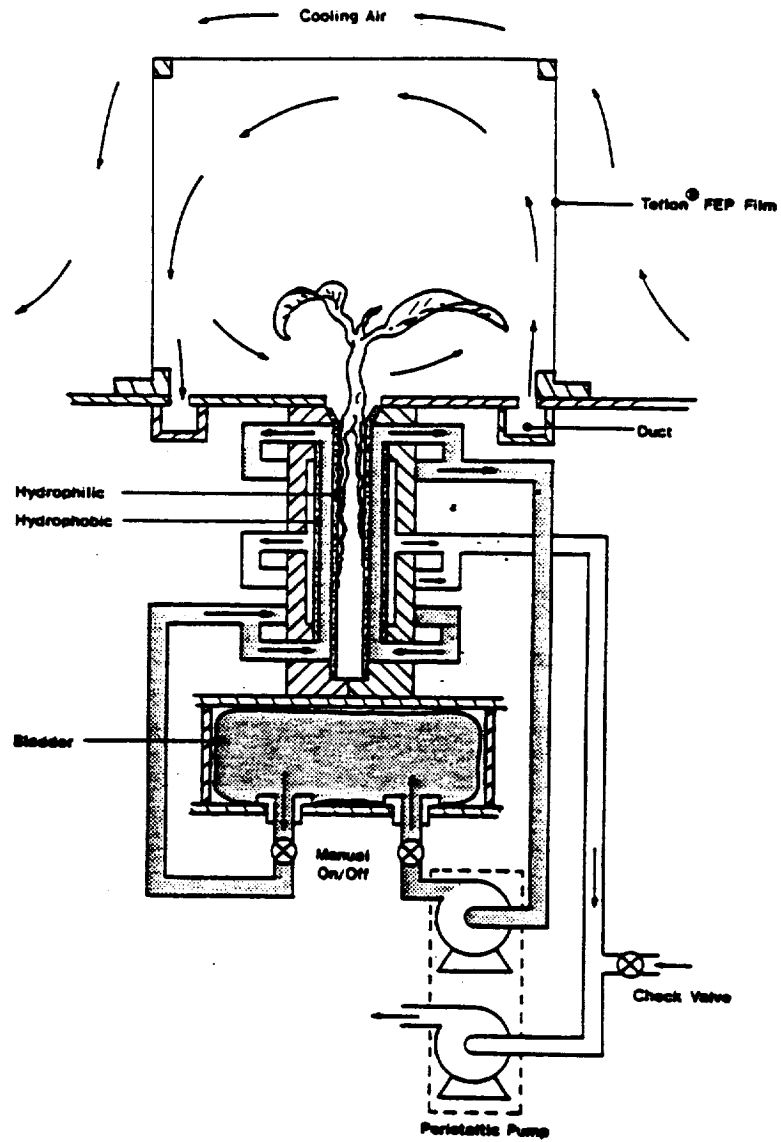
Figure 5 - Schematic diagram of a single plant growth chamber.

Figure 2.2. Reprint from Wright and Bausch, 1984.

tubes can release copper and zinc into the nutrient solution (Averner, et al., 1984) and although they are plant nutrients, their concentrations may reach toxic levels. A problem that arose when using the polypropylene material is that, by nature, it is hydrophobic (Orbisphere Corporation, 1988). In order to make these tubes wettable, a surfactant treatment must be performed which can cause complications if not done properly. An exploded view of the various generations of this tubular nutrient delivery system is reprinted in Figure 2.3.

Of the more recent porous materials currently being tested in this tubular CERES configuration, porous stainless steel (type 316) and ceramic tubes have proven to be quite successful. At the Wisconsin Center for Space Automation and Robotics (WCSAR), the stainless steel tubes (20 micron pore size) are currently being examined in conjunction with a non-organic rooting medium (Tibbitts, et al., 1989). The external medium used is typically Arcellite (kitty litter) and is maintained in direct contact with the tubes. In this nutrient delivery system, the stainless steel tubes compensate for the fluid handling problems present in a microgravity environment while the non-organic medium provides a simulated soil environment for the plant roots. The basic concept behind using this external medium is that simultaneous contact of the plant roots with nutrient solution and air can be maintained. In particular, capillary action through the stainless steel tubes and into the soil-like medium will fill the smaller pore spaces while the larger pores will remain open. Thus, the plant roots will obtain the necessary root aeration. The advantages of this type of system include a rigid, durable tubular construction, an even distribution of liquid, and a root environment similar to soil. The disadvantages of utilizing this type of system is that the extraction of the roots from the medium at times of harvest may be difficult and time consuming. In addition, the stainless steel which is inherently hydrophobic can introduce possible toxic elements such as Cr, Ni, and Mo (Koontz, et al., 1990). Although initial tests with this material revealed only very low levels of these elements (Koontz, et al., 1990), long-term or continuous plant growth may cause these levels to reach more deleterious concentrations.

Tubular membrane plant growth unit

FITTING FROM NUTRIENT SUPPLY

SOLID TUBE WITH HOLES

MEMBRANE TUBE

OPEN TUBULAR SUPPORT

FITTING TO PUMP AND NUTRIENT SUPPLY

SOLID TUBE

MEMBRANE TUBE

OPEN TUBULAR SUPPORT

NUTRIENT SOLUTION

AIR SPACE FOR ROOTS

ASSEMBLED CROSS SECTION
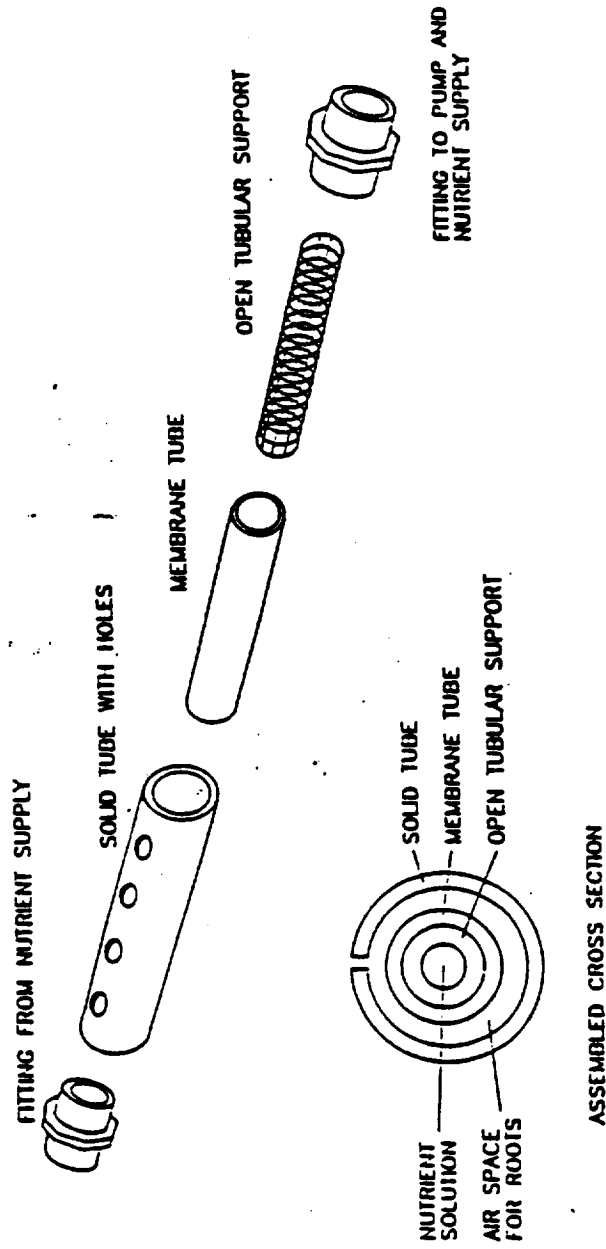
Figure 2. Schematic diagram of the tubular membrane plant growth unit (original design)

Figure 2.3. Reprint from Dreschel, et al., 1988.

Porous tube plant growth unit

FITTING FROM NUTRIENT SUPPLY

SOLID TUBE WITH HOLES

POROUS MATERIAL TUBE

SPACER

SPACER

FITTING TO PUMP AND NUTRIENT SUPPLY

SOLID TUBE

POROUS TUBE

NUTRIENT SOLUTION

AIR SPACE FOR ROOTS

ASSEMBLED CROSS SECTION
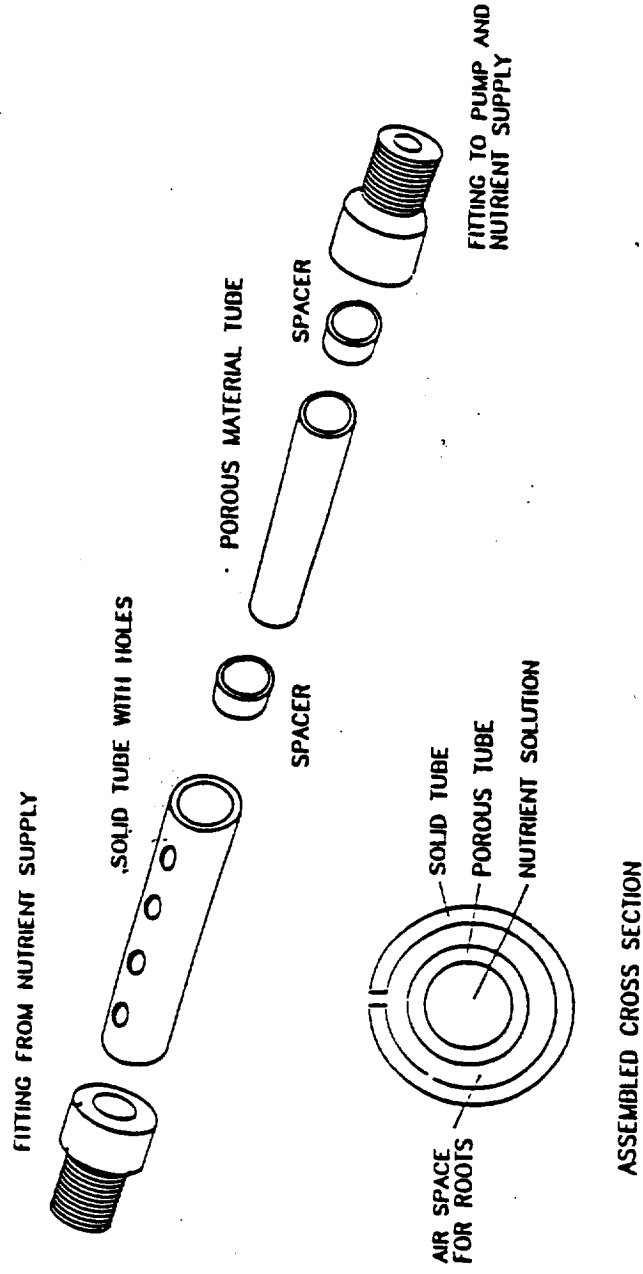
Figure 3.   Schematic of the first design of the porous tube plant growth unit.

Figure 2.3.   Reprint from Dreschel, et al., 1988.

Porous tube plant growth unit

FITTING FROM NUTRIENT SUPPLY

OUTER OPEN TUBULAR SUPPORT WITH SLOT

POROUS MATERIAL TUBE

WHITE/BLACK POLYETHYLENE

FITTING TO PUMP AND NUTRIENT SUPPLY

WHITE/BLACK POLYETHYLENE

SPACE FOR SEEDS

OUTER OPEN TUBULAR SUPPORT WITH SLOT

POROUS TUBE

NUTRIENT SOLUTION

AIR SPACE FOR ROOTS

ASSEMBLED CROSS SECTION
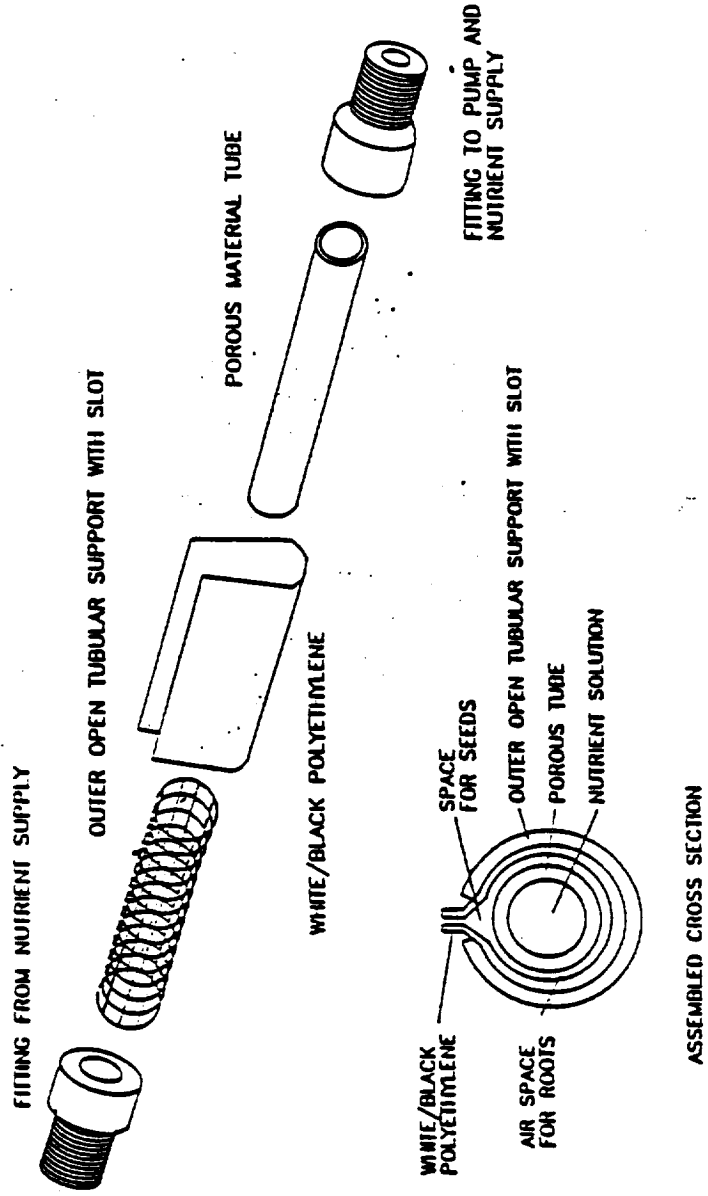
Figure 4. Schematic diagram of the second design of the porous tube plant growth unit.

Figure 2.3. Reprint from Dreschel, et al., 1988.

The Porous Ceramic Tube Plant Nutrification System (PCTPNS) which is currently being tested at the Kennedy Space Center (KSC) is configured in the same manner as the second tubular design given previously in Figure 2.3. The materials used in the construction of these ceramic tubes are listed as highly purified inorganic oxides and high temperature fluxing agents (Osmonics, Inc. Product Bulletin, 1988). They come in various tube lengths, diameters, and pore sizes (0.3 to 25 microns) which allows for a wide variation in applications. Other advantages include extreme rigidity and durability as well as being hydrophilic in nature (Dreschel, et al., 1988; Dreschel, et al., 1990b). In addition, plants can be grown with their roots in direct contact with the ceramic tube and do not require an external rooting medium. Thus, the extraction of the plant roots is considerably simplified as compared to the system utilized at WCSAR. As for the release of toxic substances or the interaction with certain nutrients, no definite results have been obtained for this ceramic material.

2.2. Plant Growth Tests

Although various plants have been grown successfully on each of the CERES based hydroponic systems, an exact account of the biomass production results will not be mentioned here. However, the effects of the physical design and construction of these nutrient delivery systems on their ability to support plant growth will be given. For the designs utilizing the flat plate configuration, the plant growth results were compared to plants grown in vermiculite (Bausch and Wright, 1985) as well as at different applied suction pressures (Koontz, et al., 1990). As for the tubular CERES designs, direct comparisons of the effects of different applied suction pressures (Dreschel, et al., 1987; Dreschel, et al., 1988; Dreschel, 1988; Dreschel and Sager, 1989; Berry, et al., 1990; Dreschel, et al., 1990a), pore sizes (Dreschel, et al., 1988; Dreschel, et al., 1990a; Dreschel, et al., 1990b), and membranous materials (Dreschel, et al., 1988) were made. In addition, plant growth results were compared on factors such as membrane versus soil growth methods and direct germination instead of transplantation (Orbisphere Corporation, 1988).

Tomato plants (*Lycopersicum esculentum*) were grown from 1 cm tall seedlings for two weeks in the flat polysulfone plate design depicted in Figure 2.2. In addition, seedlings were simultaneously grown under the same conditions except that they were maintained in styrofoam cups containing vermiculite wetted daily with nutrient solution. In both cases, the plants appeared healthy and were of comparable size after the two week growth period. Thus, these experiments gave a direct indication that the CERES concept was a successful means of supporting plant growth with results similar to those of a conventional hydroponic growth method (Bausch and Wright, 1985). An additional study of the plant growth capabilities of the CERES based systems utilizing flat plates was conducted on 'Ruby Conn' loose-leaf lettuce plants (*Lactuca sativa* L.). In this situation, the plants were maintained on stainless steel (type 316) with an orientation perpendicular to the plates (see Figure 2.1). By reducing the applied negative pressure below the membrane plate from 25 mm of water to just below zero, an average increase of 58% in the top fresh weights of the plants was exhibited. Therefore, the applied suction pressure was shown to have a profound influence on the abilities of this plant growth system (Koontz, et al., 1990).

Similar results of the variation in plant biomass production as influenced by the applied suction pressure was exhibited in several of the tubular designs. For example, when wheat plants (*Triticum aestevum* L. cv. Yecora Rojo) were grown from seed to maturity (72 days) on acrylic tubes, the three suction pressures of 8, 12, and 40 cm of water resulted in the greatest to lowest accumulation of plant dry matter, respectively. It was postulated that the increased suction pressures caused the nutrient solutions contained within the tubes to become less available for the roots to absorb (Dreschel, et al., 1987). In other words, the competition between the absorption by the plants and the containment by the negative internal pressure became amplified at the greater suction pressures. Support for this result was later given for these wheat plants grown not only on the acrylic membranes (Dreschel, et al., 1988; Dreschel, et al., 1990a) but also on the polyethylene tubes (Dreschel, et al., 1988; Dreschel, et al., 1990a) and on the ceramic tubes (Berry, et al., 1990). In addition, similar findings were reported for lettuce plants (*Lactuca sativa* L. cv. Waldman's Green) cultivated on these three materials (Dreschel,

et al., 1988; Dreschel, et al., 1990a). The suction pressures tested in these tubular systems ranged from -0.20 to -3.00 kPa with the total dry mass per plant and seed mass per plant measured. Trends showed a non-linear relationship between these parameters for both the wheat and lettuce experiments.

In a more extensive study of the effects of the applied suction pressure on a tubular CERES configuration, more specific growth parameters which express the variations in nutrient translocation were measured (Dreschel, et al., 1988; Dreschel and Sager, 1989). These parameters include the root, straw, chaff, and seed masses in addition to the total mass (all in units of grams per plant) of the wheat plants. The three negative pressures tested were 0.40, 1.48, and 2.58 kPa and in all of the measurements, the trends supported the previous findings. The only exception was in the root mass which gave the highest result at -0.40 kPa, the lowest at -1.48 kPa, and an intermediate value at -2.58 kPa. This type of trend was also exhibited when the seed mass to total mass ratio was calculated. This indicated that although the total masses decreased as the suction became greater, there was a variation in the allocation of nutrients particularly to the roots and seeds.

In other measurements which further supported the dependence of plant growth on the pressure head, the effects of these variations on the uptake of nutrients were examined (Dreschel, 1988; Dreschel and Sager, 1989). To accomplish this task, the concentrations of the various nutrients that accumulated on the root mass were monitored at harvest time. At the lowest suction pressure of 0.40 kPa used in these measurements, the nitrate-nitrogen supplied to the roots appeared to be insufficient while at greater negative pressures, this was alleviated. As for the accumulation of calcium, potassium, magnesium, zinc, and iron, the results showed that although variations did exist between the pressures, the differences were not significant and showed no general trends. Similarly, this conclusion can also be made for the phosphate-phosphorus and copper contents; however, the general trends of these nutrients revealed a continuous decrease in accumulation as the suction pressure increased. Perhaps the greatest effect of this factor on the micro-nutrient availability was exhibited

on the accumulation of manganese. The trend of this element was an inverse of that measured for the macro-nutrient nitrate-nitrogen concentrations. Although these measurements were made after the fact, they revealed that the delivery of nutrients was, in general, non-limiting. However, the reasons behind these nutrient flux phenomena have as of yet to be explained.

Other physiological plant processes which exhibited variations due to an altered applied pressure head include the leaf equilibrium water potential, stomatal conductance, and water use efficiency (Berry, et al., 1990). At higher suction pressures, the leaf equilibrium water potential decreased possibly due to the relatively restricted root growth volume. In addition, since only one side of the root system is in contact with the meniscus of nutrient solution which forms between the root and tube surface (see Figure 2.1), then the surface area in contact would be greatly altered by the pressure beneath the tube. This explanation can also be used to account for the exhibited decrease in stomatal conductance and corresponding increase in water use efficiency. Since less nutrient solution would be available for the plant roots at a more negative suction pressure, then a lower amount of potassium ions would be available for the stomata (Humble and Raschke, 1971). Similarly, these conditions would cause the plants to use the available water in a more efficient manner.

Another factor which affects the nutrient solution availability is the average pore size of the membrane tubes. For the wheat plants grown on the acrylic tubes, a direct comparison was made between a 0.2 and a 5.0 micron pore size tube (Dreschel, et al., 1988). The total mass per plant and the seed mass per plant were both significantly higher on the larger pore size tube even though the applied suction pressure was maintained at -0.4 kPa on both tubes. Similar trends were exhibited in the various parts of the wheat plants such as in the chaff and straw (Dreschel, et al., 1990a). However, the fresh and dry weights of the roots showed an inverse relationship to these trends which, again, would seem to make sense. Since the larger pore size would permit a larger volume of nutrient solution to pass through the tube, then a smaller root system would be required to maintain absorption. A similar experiment was

conducted on the ceramic tubes containing various sized pores (0.3, 0.7, 2.0, and 10.0 microns) supporting wheat and maize plants (Dreschel, et al.,1990b). Although the trends of the results were less conclusive than the acrylic tubes, a dependence upon the pore size of the ceramic tubes was evident. For the wheat trial, the 0.7 micron tube supported the greatest growth as measured by the total weight of the plant while the 2.0 micron tube gave the lowest result. As for the tubes with the extreme pore sizes (0.3 and 10.0 microns), their results were intermediate. A slightly better trend was exhibited in the maize trial except that the results showed an inverse relationship as compared to the acrylic tubes. Possible explanations for greater growth resulting from a smaller pore sized tube include the differences in the water requirements of the plant species grown or the variations due to different membranous materials.

In order to compare the capabilities of the acrylic, polyethylene, and ceramic tubes to support plant growth, each of these were run under constant pressure using the polyethylene tube as the standard (Dreschel, et al., 1988). Lettuce plants were grown for 25 days on each of these tubes and the total and seed masses per plant measured afterwards. In a side-by-side experiment involving the acrylic and polyethylene tubes, the suction pressure was set at -0.4 kPa and the growth parameters measured. Results showed that the acrylic tube could support the lettuce plants four times better than the polyethylene counterpart. Similarly, when the polyethylene material was compared to the ceramic tube, the latter material resulted in a doubling of the cell mass accumulations. Although both of these materials proved to be superior to the polyethylene, a direct comparison between these two cannot be made. The suction pressure for the experiment involving the ceramic tube was different from that of the aforementioned -0.4 kPa. In addition, no mention was made as to what the average pore sizes were of the three tubes. Thus, these results are subject to some speculation.

Another construction material which has been tested in this tubular CERES design is polypropylene (Orbisphere Corporation, 1988). In these experiments, lettuce and cabbage plants were grown on these nutrient delivery tubes as well as in soil. A comparison between these two growth methods showed that the lettuce was

superior on the membrane tube while the inverse was true for the cabbage. These results indicate that the preferred growth method is greatly species dependent. This conclusion has been supported by other researchers (Dreschel, et al., 1988). Another objective of this comparison in growth methods was to determine whether seeds preferred to be germinated directly on the porous tubes or transplanted after germination. Experiments conducted on lettuce, basil, and parsley plants revealed that direct germination of all of these plants on the membrane tubes resulted in superior growth. The reason behind this result is due to the removal of the effects of transplantation shock (Resh, 1987).

2.3. "Wetness" Sensing

There have been two methods which have been used to determine the water transfer or holding capacity for the porous ceramic tube system. The first is the use of a root mimicking absorbant material such as sections of germination paper which are placed under a weight on the tube for a specified length of time (Dreschel, et al., 1990b). Absorption of solution from the tube and into the germination paper was measured by weighing the wet and dry masses of the absorbant. The calculated water flux rates were shown to have a dependency upon both the applied suction pressure and the average pore size of the ceramic tubes. From data provided by Thomas Dreschel of the Bionetics Corporation, John F. Kennedy Space Center, Florida, the results of these experiments are given in Figure 2.4. In addition to this water flux data, the results of the second possible method of quantifying the "wetness" were provided. This second method utilizes the thermistor moisture sensing device mentioned previously and the results were compared to the absorbant material measurements. Figures 2.5.1 to 2.5.4 graphically show the results of this comparison. As can be seen, the voltage readings of the thermistor based sensor are also pressure dependent and generally follow the results of the absorption by the germination paper. However, deviations between these two methods did occur on the smallest pore size tube (0.3 microns).
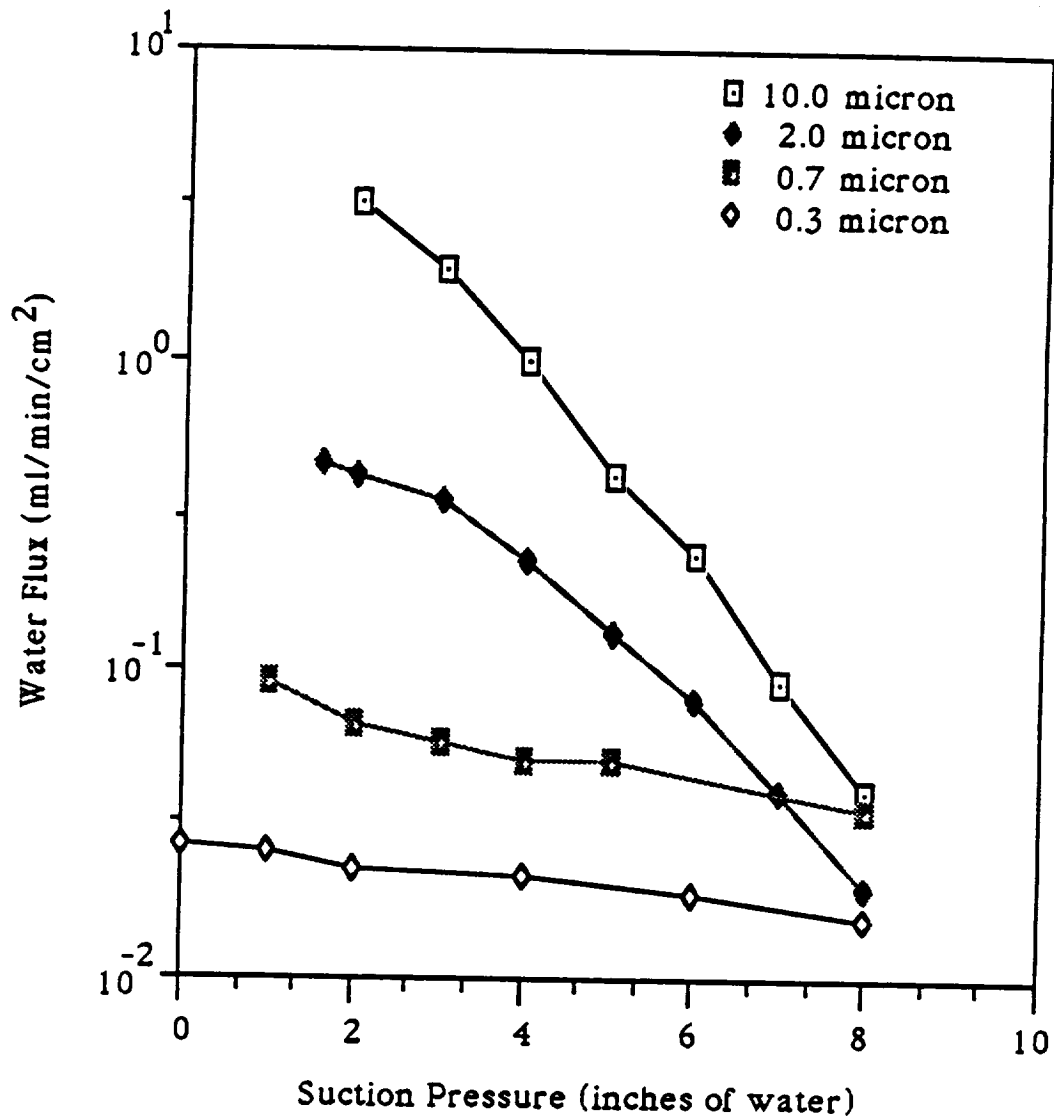
Figure 2.4. Semi-Log Plot of the Water Flux Rate vs. the
Applied Suction Pressure as Determined by
the Germination Paper Absorption Tests
(Data Obtained from Thomas Dreschel)
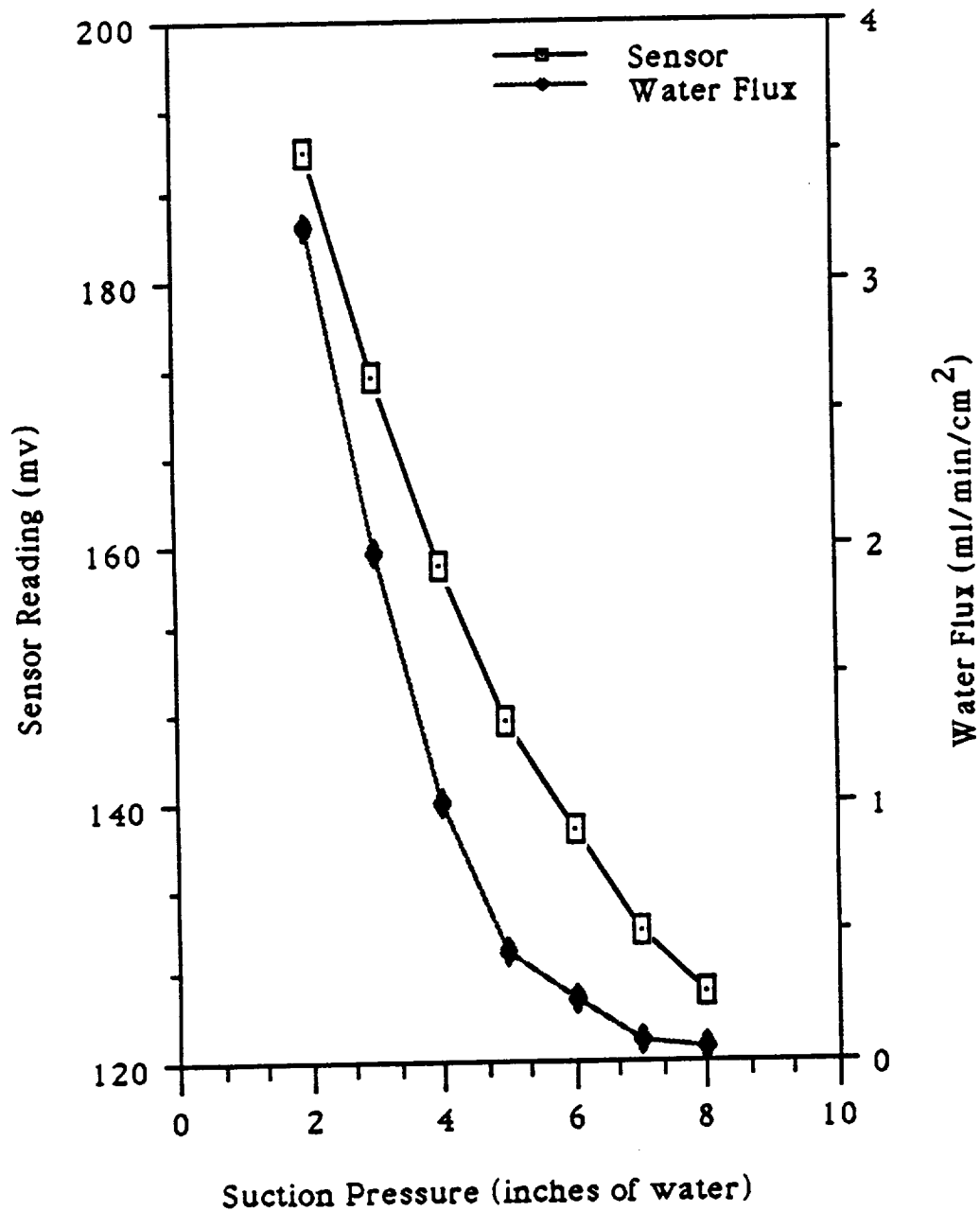
Figure 2.5.1. Moisture Sensor Reading and Water Flux
Measurements on the 10.0 Micron Pore
Size Tube (Data from Thomas Dreschel)
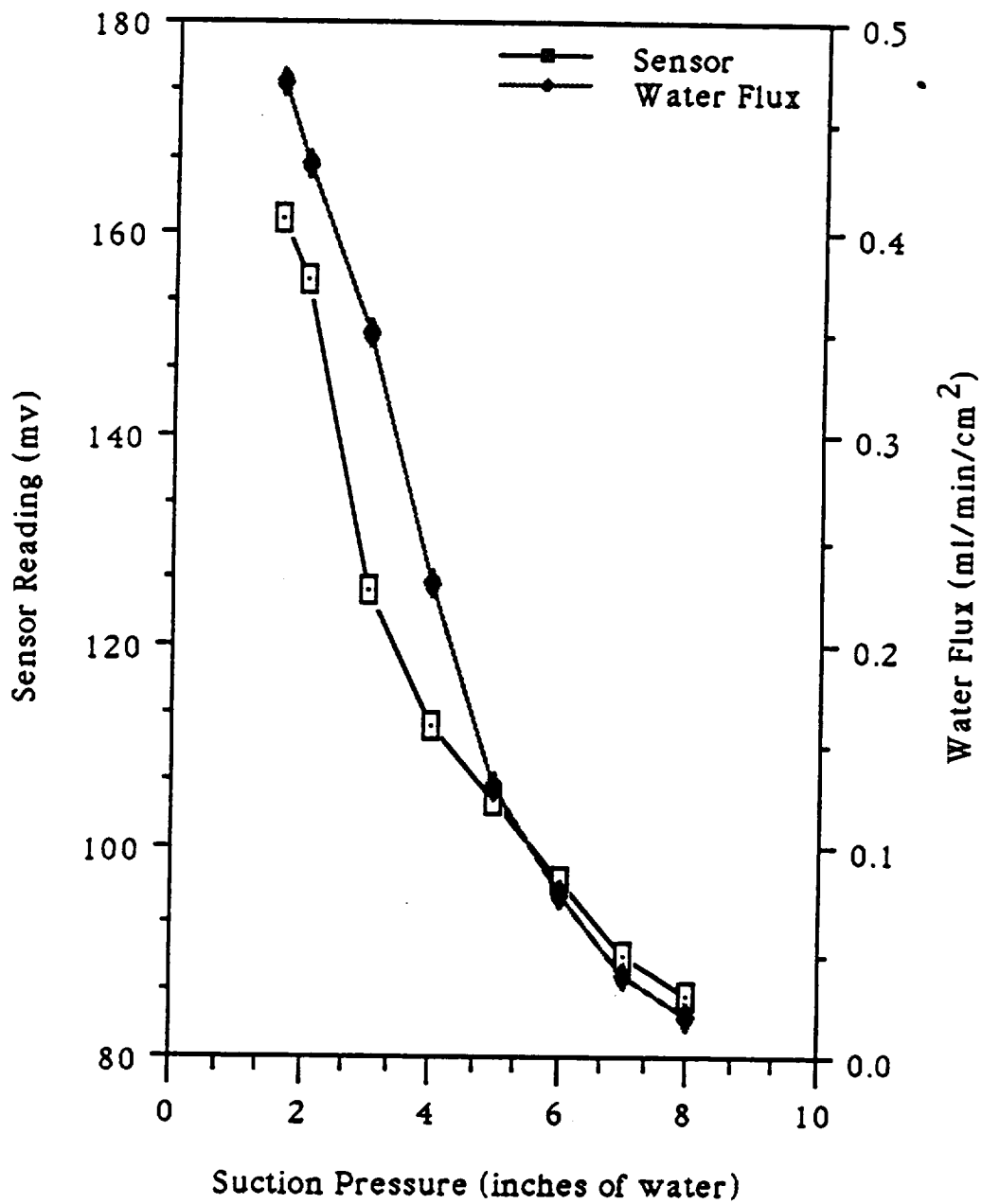
Figure 2.5.2. Moisture Sensor Reading and Water Flux
Measurements on the 2.0 Micron Pore
Size Tube (Data from Thomas Dreschel)
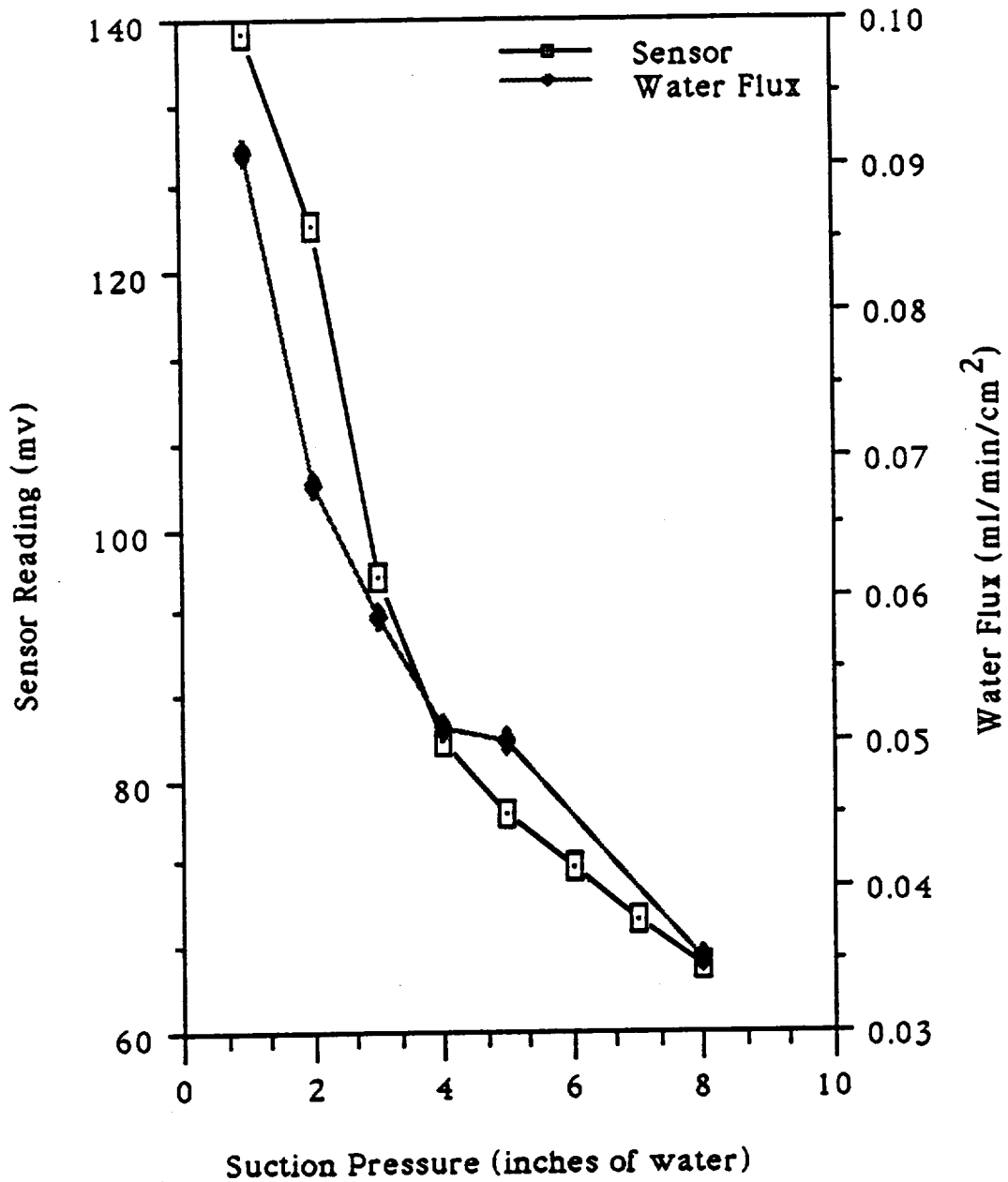
Figure 2.5.3. Moisture Sensor Reading and Water Flux
Measurements on the 0.7 Micron Pore
Size Tube (Data from Thomas Dreschel)
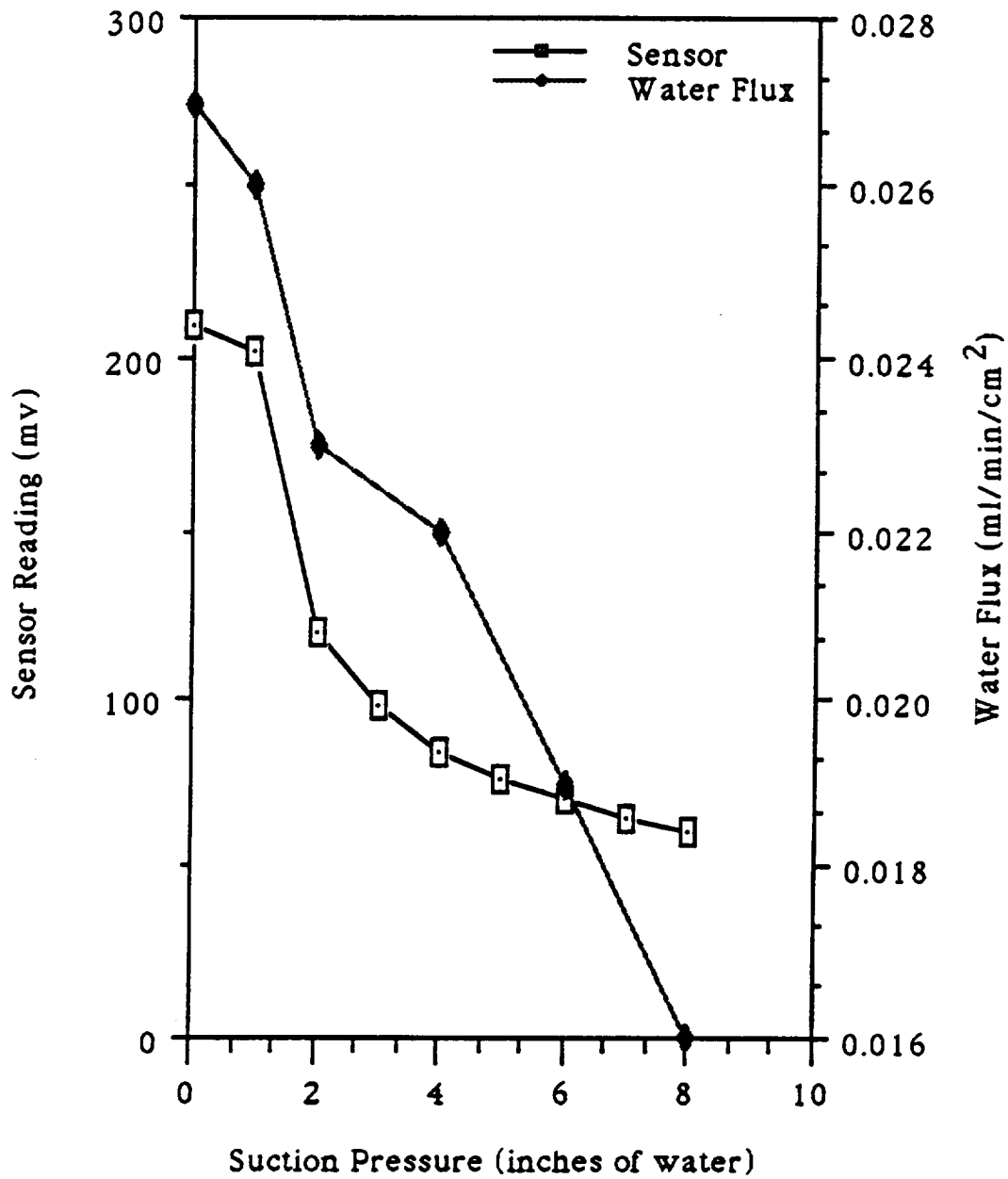
Figure 2.5.4. Moisture Sensor Reading and Water Flux
Measurements on the 0.3 Micron Pore
Size Tube (Data from Thomas Dreschel)

The conceptualization and design of this moisture sensor device is based upon the differences in thermal properties that exist between liquid and air (Bean, et al., 1990). Using a constant heating source, the degrees of heat dissipation from a moist ceramic tube can be differentiated if various liquid contents exist within the pores of the tube. An increase in moisture content of the ceramic material would require a smaller temperature gradient to dissipate the constant quantity of heat. Thus placing a heating element between two thermistors could be used to measure these differences where one would remain constant exposed to only air while the other would change after contact is made with the tube. In order to insure that a more accurate measurement of moisture content is achieved, the device was designed to have a relatively rapid reaction time (approximately 45 seconds for a constant reading). The speed of measurements is important so that drying of the tube from the constant heat source does not become significant. Although this device does not quantify the actual amount of liquid contained in the ceramic tube or measure the flux rate, the results of Figures 2.5.1 to 2.5.4 show that it does merit further investigation. As for the relationship between water flux rate and the dissipation induced voltage change, no clear explanation has been provided.

3. MATERIALS AND METHODS

3.1. Porous Ceramic Tube Plant Nutrification System (PCTPNS)

The experiments to test the PCTPNS were conducted on a lab-top version of this hydroponic system provided by Thomas Dreschel. A schematic diagram of this apparatus is shown in Figure 3.1 which illustrates the major components of this system. Four different types of Porous Ceramic Tubes were tested and had average pore sizes of 0.3, 0.7, 2.0, and 10.0 microns. The lengths of these membrane cylinders were 12.7 cm (5 inches) while the outer diameters were all 1.6 cm (5/8 inches). As for the internal diameters, this value ranged from 1.1 to 1.3 cm with no dependence upon the average pore size. As stated previously, the ceramic material was constructed out of highly purified inorganic oxides and high temperature fluxing agents (Osmonics, Inc. Product Bulletin, 1988). Unfortunately, the exact chemical composition of these manufacturing materials was not provided and should be deduced.

A constant speed peristalic Suction Pump was used to draw solution from the Porous Ceramic Tube and into the Reservoir Diaphragm (see Figure 3.1). This expandable/contractible reservoir allowed for various pressures to be set in this plant nutrification system. In order to change the pressure, solution was injected from the 50 ml Pressure Adjustment Syringe (Coarse Control) to decrease the applied negative pressure. Conversely, to increase the suction (make more negative), solution was withdrawn by using this same syringe. A second Pressure Adjustment Syringe was optionally used to obtain a Fine Control of the applied pressure. In order to determine the value of the suction pressure that existed within the system, a Negative Pressure Gauge which could measure upto -8.0 inches of water pressure was placed at the exit of the Porous Ceramic Tubes. A second method which could have been used to control the applied pressure was to change the screw setting on the Flow Control Valve. However, since this method proved to be difficult in obtaining
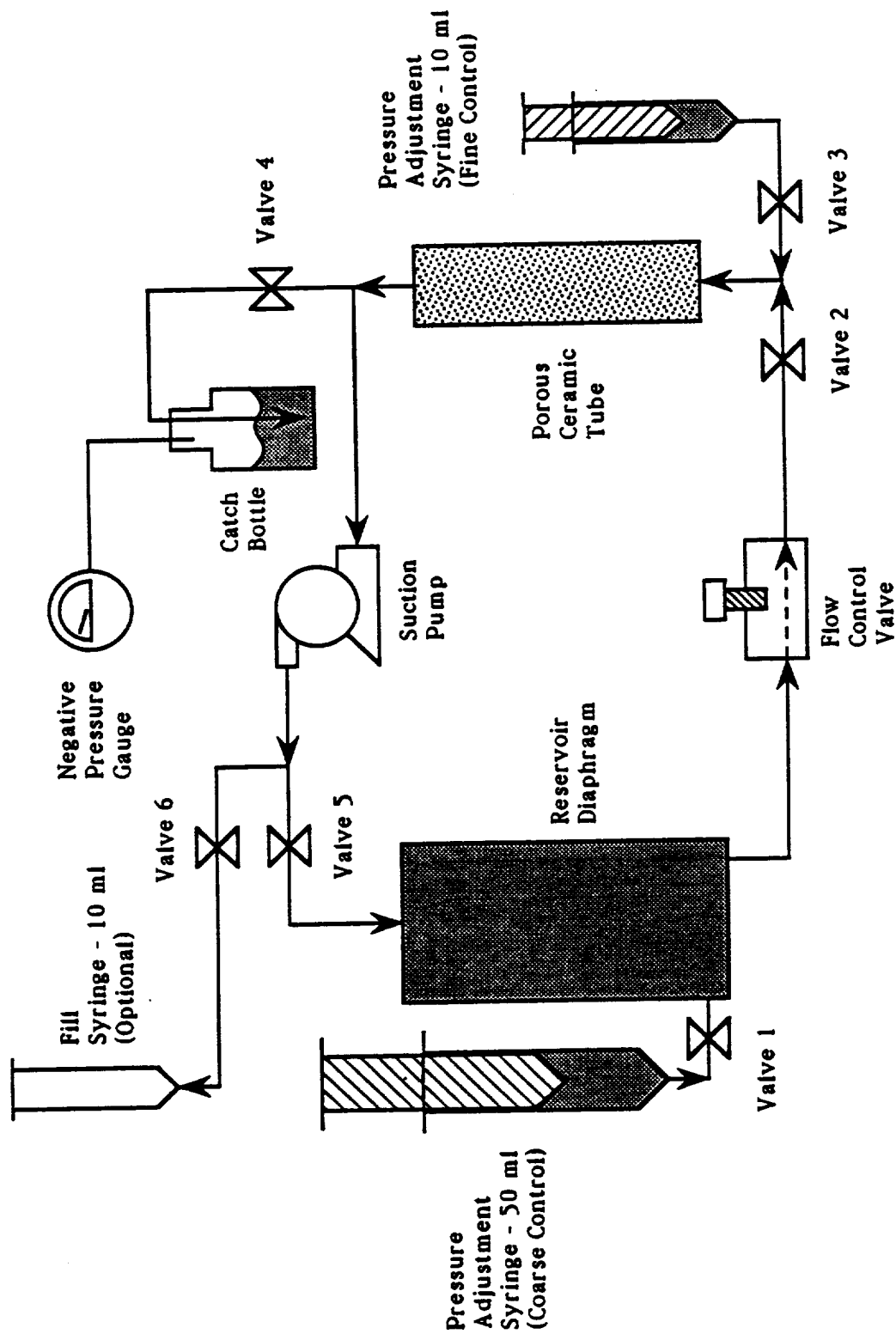
Figure 3.1. Porous Ceramic Tube Plant Nutrification System (PCTPNS)

exact pressures, it was not utilized but remained fully opened in the experiments. Elaboration of this decision will be made in a later section.

A final component of this plant nutrification system which was optionally put in to determine the flow rate through the system was the 10 ml Fill Syringe. After priming the system by withdrawing any trapped air bubbles using the Pressure Adjustment Syringes (Valve 1 and 3 open), the pressure was set using the procedure mentioned previously (Valves 2,4,5 open; Valve 6 closed). Once a steady pressure reading was obtained, Valves 1 and 3 were closed and the flow rate measurements taken. In order to accomplish this, Valve 5 was closed and Valve 6 immediately opened to allow solution to enter the Fill Syringe. The time required to fill 10 ml was measured and the flow rate could then be calculated. The results of this flow rate measurement procedure are listed in the Results Section as Experiment 1.

The second experiment conducted on the PCTPNS was to determine the effective permeability coefficient using Darcy's equation for flow through porous media. The procedure used in this experiment consisted of first priming the system as described earlier and then setting the suction pressure to the desired level. Various values were tried on each different pore sized tube with typical ranges from near zero to -2.0 inches of water. One condition that was desired regardless of the tube type and pressure setting was that the flowing liquid must weep from the tube. This weeping condition occurs when the amount of suction used is too small to contain the liquid within the tube. The liquid that wept from the ceramic material was collected in a catch pan and the amount weighed after a known length of time. This provided a means to measure the radial flow rate from the tube interior to the external environment. This radial velocity is used in Darcy's equation and will be discussed later.

In order to determine the percent void volumes of the ceramic tubes, comparisons of their weights after oven drying at 100 °C and after saturation in water were made. Before being placed in the oven, the porous tubes were washed in ethanol to remove oils that

might be present on the surfaces. After this ethanol wash, the tubes were rinsed thoroughly in distilled water and then placed in the drying oven for one day. Once this was accomplished, the ceramic tubes were allowed to cool after which they were weighed and then submerged in water. Since the time required for complete saturation to occur was not known, the tubes were withdrawn from the water bath, shaken to remove drops, weighed, and then re-submerged to make a second measurement. A comparison of the successive wet weights revealed whether complete saturation had occurred. Due to the results of this experiment (see Results Section - Experiment 3), a second means to establish the saturation was conceived. Utilizing two miniature pumps, water was forced into both ends of the ceramic cylinders leaving the porous matrix as the only exit. Again, successive measurements were made with the results being more stable.

3.2.   Porous Ceramic Disks and Visualization Apparatus

As stated in the objectives of this research, a physical model of the ceramic material is desired. Due to the cylindrical construction of the porous tubes, microscopic observations were more easily made on 30 mm diameter by 0.32 cm thick disks. These experimental tools were also obtained from Osmonics, Inc. as were the tubes and had average pore sizes of 0.7, 2.0, and 10.0 microns. As with the tubular counterparts, the porosity of the ceramic disks were calculated using the washing and submersion procedures outlined for the tubes. Again, complete saturation was not known clearly so the submersion time was extended to over 12 hours with liquid constantly running over the disks. The results of these measurements are given in the Results Section as Experiment 4.

In addition to these results, the observations of the ceramic surfaces are also provided. The apparatus used to make these empirical observations included a stereo microscope and an inverted dissecting scope. The stereo microscope was used to visualize to top of the disks (and tubes) while the dissecting scope was physically turned upside down to observe the under side of the disks. A photograph of this inverted scope is shown in Figure 3.2.
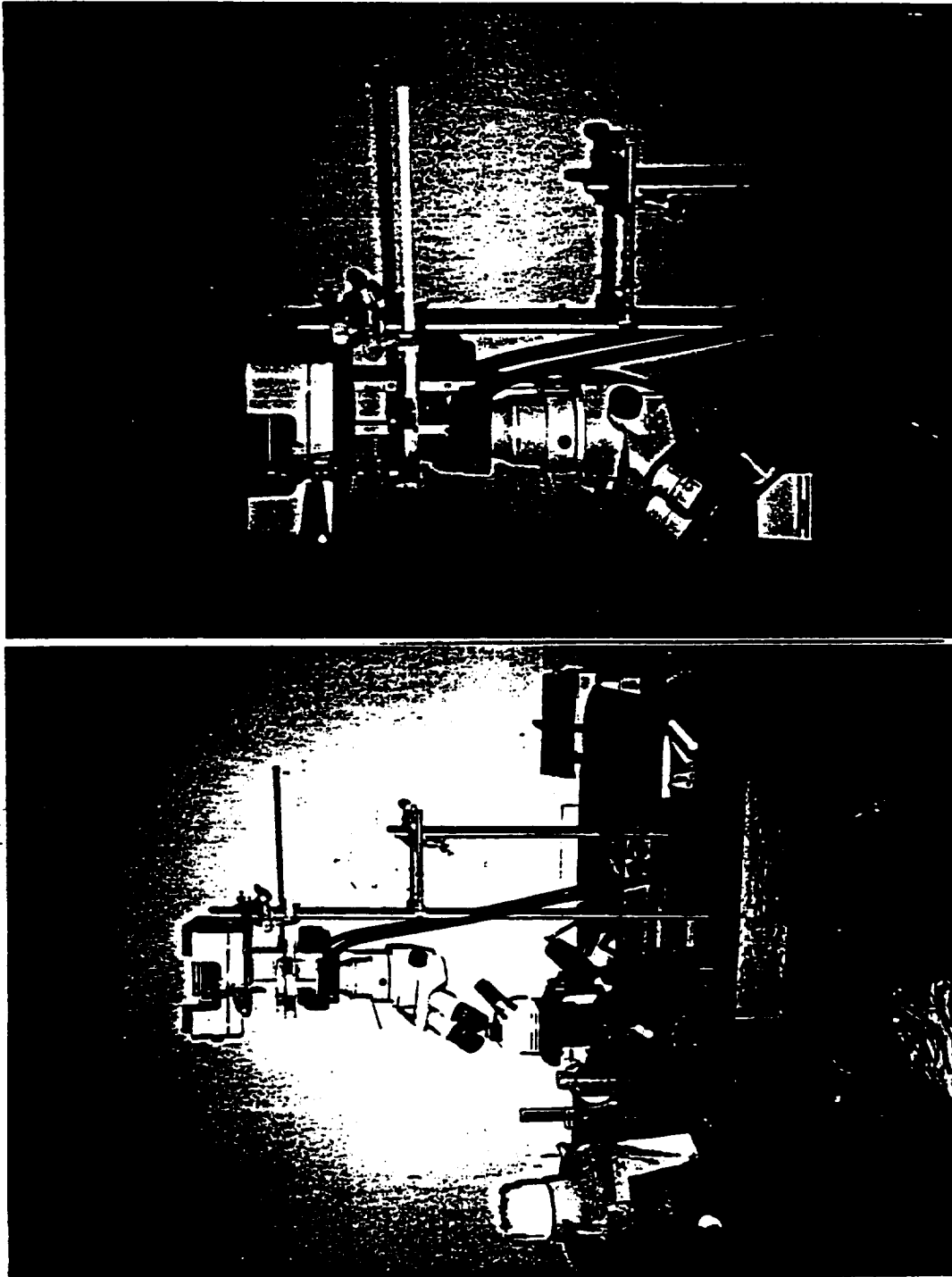
Figure 3.2. Inverted Dissecting Microscope Setup

The observations made at approximately 70x magnification using these microscopes included the absorption rate or affinity of the ceramic material for water, the surface features of the disks as liquid flowed vertically, and the horizontal spread pattern through the disks. In order to determine the effects of gravity on the flow characteristics through the ceramic material, observations were made in both the upstream and downstream view points. In particular, the flow of liquid upwards was achieved by placing the disks on a tripod submerged in water so that the bottom of the test element was just even with the liquid level. Once contact with the liquid was made, the gravity opposing flow of water through the ceramic material was visualized using the overhead stereo microscope. Since there was complete contact between the water and the disk surface, then this observation only represented upwards vertical flow with little horizontal variations. From this viewpoint, the surface features of the ceramic were seen along with how aqueous solutions distributed in the "hills and valleys" of the porous material. In order to determine the differences in magnitude between the gravitational and affinity attraction forces, the upwards flow characteristics were compared to flow in the reverse direction (i.e. with gravity). This second set of observations was accomplished by dropping water on the disk from a pipette and viewing the underside of the disk using the inverted scope setup. In addition to the downwards vertical flow characteristics, this second visualization procedure was used to view the horizontal spread pattern of water through the ceramic material. These observations were made from both the top and bottom of the disks using the overhead and inverted scopes, respectively. Using these techniques, the physical model of the PCTPNS was conceptualized as will be discussed in the Discussion Section.

As was evident from the background research reviewed earlier, there is a strong dependence of the "wetness" of the tubes on the magnitude of suction applied beneath the ceramic material. In order to actually see this phenomenon, the overhead stereo microscope was situated such that a tube in the PCTPNS was observable. The changes in the level of liquid distributed in the "hills and valleys" of the tubular porous material was directly visualized when a sudden change in the suction pressure was

produced. This change was accomplished by injecting and withdrawing liquid through the 50 ml Pressure Adjustment Syringe.

3.3. Thermistor Moisture Sensor Device and Absorption Tests

The final objective of this research is to evaluate the applicability of the thermistor based moisture sensor device for use with the PCTPNS. The test protocol utilized to examine this device involved the determination of the stability and consistency in the voltage readings as well as to investigate the variations due to the location along the length of the tubes. The first experiment conducted with this device utilized tubes with the four different pore sizes. Each in turn was hooked up to the apparatus depicted in Figure 3.1 and ran under pressures ranging from -2.0 to -8.0 inches of water. Four replicates of the voltage readings were taken for each applied suction pressure used in order to determine the stability of the measurements. As for the consistency in the voltage readings, this experiment was conducted again on another day to determine whether similar values could be obtained. In addition, these values were compared to those obtained by Thomas Dreschel (see Background Section 2.3). The results of this experiment are reported in the Results Section as Experiment 5.

In taking the readings of this moisture sensor device for the results of Experiment 5, the thermistor was placed at relatively the same location on top of the tubes. This was to insure that the values obtained were not influenced by the pressure drop that existed along the length of the tube. However, this factor was tested in the next set of experiments which utilized the physical dimensions of the thermistor holding case to give four locations along the top of the ceramic tubes. A schematic diagram of the thermistor casing and test locations along the tubes is provided in Figure 3.3. After a constant pressure reading was obtained in the PCTPNS, voltage readings at the four locations were taken one at a time. The results and statistical significance analyses are reported as Experiment 6 in the Results Section.
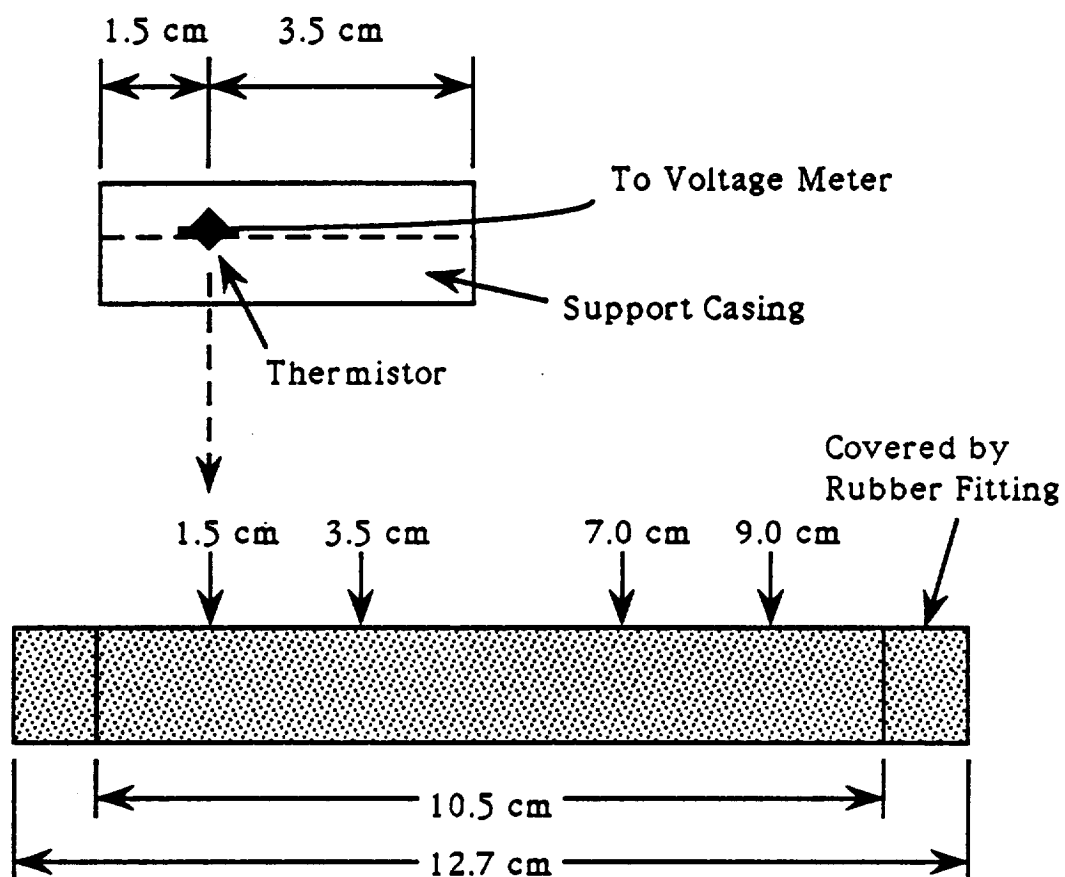
Figure 3.3. Schematic Diagram of the Thermistor Casing and
the Locations of the Moisture Sensor in Relation
to the Porous Ceramic Tube

In order to calibrate this instrument, the thermistors were placed on each of the tubes while they were still dry. The reading on the voltage meter was then adjusted until a relatively constant value of zero was obtained. The reason behind calibrating this device on a dry tube instead of in the air is because there is a difference in the thermal properties between these two mediums (Bean, et al., 1990). In addition, the pore size of the tubes was exhibited as having an effect on this calibration procedure and was therefore conducted separately on each tube. This differentiation was due to the air/ceramic ratio at the surface of contact which is directly related to the void fraction of the porous material. After this instrument was zeroed on the dry ceramic, it was removed after which time, the voltage reading achieved a negative value. Once the particular tube was attached to the nutrient recirculation system (see Figure 3 .1) and the moisture sensor placed on the tube, measurements of the voltage readings were recorded. It was observed that the time required for the voltage reading to reach a constant value varied as the applied suction pressure was altered. This phenomenon was then examined in more detail using as ceramic tube with an average pore size of 10.0 microns. The three pressures applied to the system were -2.0, -5.0, and -8.0 inches of water with measurements taken of the time required for the maximum reading. The results of this third moisture sensor device analysis experiment are given in the Results Section as Experiment 7.

In order to determine the applicability of this device to be used with the PCTPNS, a comparison study was also performed using the germination paper absorption test. The design of this experiment was based after the procedure used to obtain the results presented earlier in Figures 2.5.1 to 2.5.4. However, an expansion of this procedure was implemented to test the effects of different surface areas of contact and the amount of weight placed on the germination paper. The two different sized sections of the absorbant material tested were 1.0 x 5.8 cm and 1.5 x 5.8 cm while the weights tested were 23.6 and 42.4 grams. The weights were constructed out of a semi-cylinder of PVC tubing with an additional weight optionally attached to it. The suction pressures used were the same as those for the thermistor based sensor and the contact times were predetermined to allow a substantial increase in the measured wet

weights. The change in the weights between the dry and wet germination paper sections were then used to calculate the water flux rate. These experiments were conducted on both the 0.3 and 10.0 micron tubes and the results are presented in the Results Section as Experiment 8.

4. RESULTS

4.1. Experiment 1 - Flow Rate Measurements

In order to determine the flow rate through the PCTPNS, the time required to completely fill the 10 ml Fill Syringe was measured. The four tubes containing the different pore sizes were each hooked up to the system and ran under pressures of -2.0, -4.0, -6.0, and -8.0 inches of water. In order to relate the time measurements to the volumetric flow rate, the following equation was used.

$$Q = V / t \tag{1}$$

In Equation (1), the flow rate, Q, is a function of the time, t, while the total volume, V, was maintained at a constant value of 10 ml. The results of these calculations are presented in Figure 4.1 which illustrates the dependence of Q on the applied suction pressure, P_S, and the average pore size of the tubes, d. A regression analysis of each data set was performed with the results also provided in the figure. For the 10 micron pore size tube, the relationship exhibited between Q (in ml/min) and P_S (in inches of water) was calculated to be the following.

$$Q = -0.38 \, P_S + 74.1 \tag{2}$$

Likewise, the linear regressions for the 2.0, 0.7, and 0.3 micron porous tubes are given in Equations (3), (4), and (5), respectively.

$$Q = -0.36 \, P_S + 73.1 \tag{3}$$

$$Q = -0.61 \, P_S + 72.4 \tag{4}$$

$$Q = -0.53 \, P_S + 71.4 \tag{5}$$
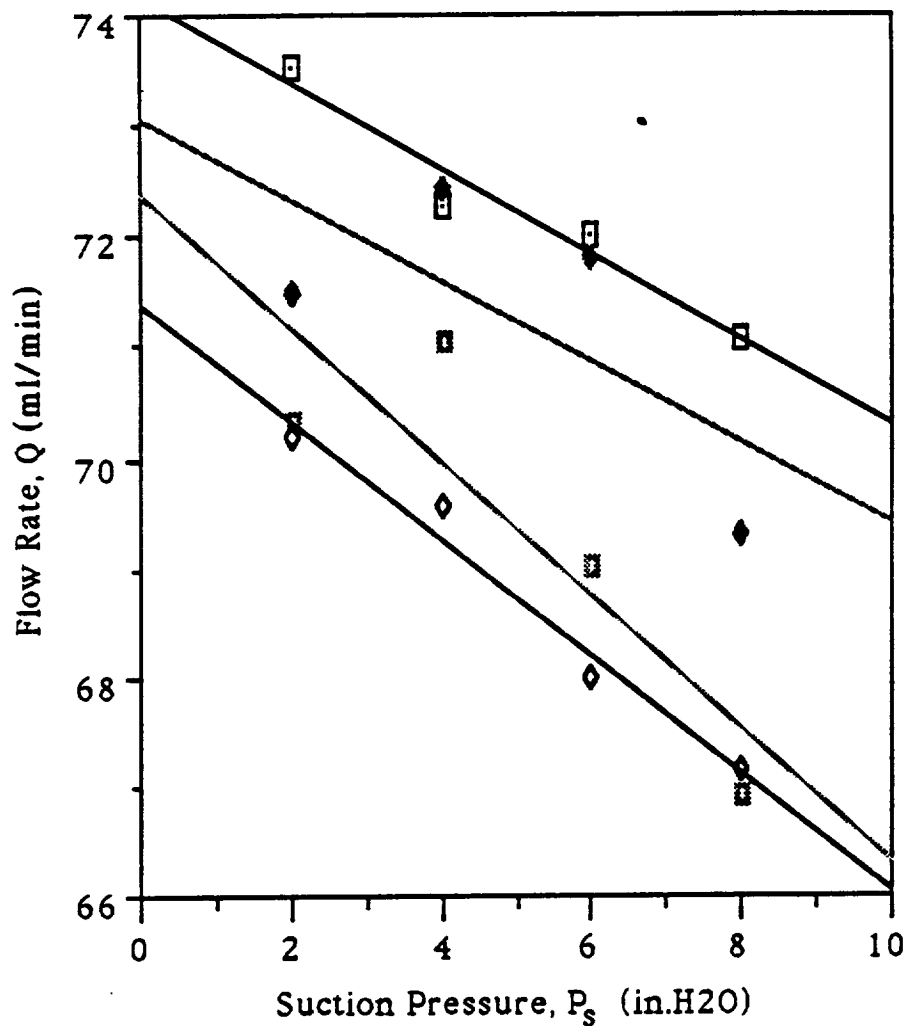
Figure 4.1. Flow Rate, Q, Plotted Against the Applied Suction
Pressure, P_s , for the Four Different Pore Sized
Ceramic Tubes with Regression Lines

▣ 10.0 micron	$Q = 74.1 - 0.38\ P_s$	$R^2 = 0.948$
● 2.0 micron	$Q = 73.1 - 0.36\ P_s$	$R^2 = 0.474$
▩ 0.7 micron	$Q = 72.4 - 0.61\ P_s$	$R^2 = 0.757$
◆ 0.3 micron	$Q = 71.4 - 0.53\ P_s$	$R^2 = 0.973$

Each data point in this figure represents the averages of two replicates.

4.2. Experiment 2 - Permeability Coefficient Measurements

The procedure of this experiment required the measurement of the amount of water wept from the ceramic tubes after a recorded length of time had elapsed. In order to obtain this desired weeping condition, the four different pore sized tubes were ran at very small suction pressures. In particular, the 10.0 micron porous tube was ran under -0.6, -1.0, and -1.4 inches of water pressure while the experiment on the next smallest pore sized tube (2.0 microns) was conducted at -0.4, -0.8, and -1.2 inches. Since the range of suction pressures resulting in weeping decreased as the average pore size became smaller, even lower suctions were used on the remaining two tubes. The 0.7 micron tube experienced pressures of -0.2, -0.4, and -0.6 inches of water whereas the 0.3 micron tube required pressures of only -0.2 and -0.4 inches to cause the weeping. Higher pressures than these did not give the desired result and therefore could not be used. In order to calculate the permeability coefficients for the tubes, Darcy's Equation for flow through porous material was used (Bird, et al., 1960).

$$\bar{v}_r = \frac{k}{\mu}\left(\frac{dp}{dr} - \rho g \cos\theta\right) \tag{6}$$

Rearranging and solving for the permeability coefficient, k, gives,

$$k = \frac{-\bar{v}_r \mu}{dp/dr - \rho g \cos\theta} \tag{7}$$

The radial velocity, $\bar{v}_r$, was calculated from the data collected as mentioned above using the following equation.

$$\bar{v}_r = \frac{Q_r}{\pi D_o L} = \frac{V_r}{\pi D_o L t} \tag{8}$$

In Equation (8), V_r, represents the volume of liquid collected in the catch pan while t is the time of collection. The physical parameters D_o and L represent the outer diameter (1.6 cm, 5/8 in.) and effective length (10.5 cm) of the porous tubes, respectively. Note that this effective length is shorter than the actual tube length (12.7 cm) due to the rubber fittings used in the apparatus which covered the ends of the tubes. In order to determine the radial pressure differential, dp/dr, an approximation was made using the discrete changes of the form, $\Delta p / \Delta r$. Since the applied suction pressure is measured from atmospheric conditions, then Δp is equivalent to P_s. Therefore, the following equation for the pressure differential can be used in Equation (7).

$$\frac{dp}{dr} = \frac{\Delta p}{\Delta r} = \frac{-2P_s}{D_o - D_i} \qquad (9)$$

In these experiments, the internal diameters, D_i, were 1.20, 1.30, 1.15, and 1.10 cm for the 0.3, 0.7, 2.0, and 10.0 micron pore sized tubes, respectively. Substituting Equations (8) and (9) into Equation (7) gives the final equation for the permeability coefficient.

$$k = \frac{-V_r (D_o - D_i)\, \mu}{[-2P_s - \rho g \cos\theta\, (D_o - D_i)][\, \pi D_o L t]} \qquad (10)$$

A semi-log plot of k versus P_s is given in Figure 4.2 for each of the four different porous ceramic tubes. The values plotted in this figure represent the average between the maximum and maximum values possible due to the $(\cos\theta)$ term. When $\theta = 0$ $(\cos\theta = 1)$, the permeability coefficient becomes a minimum while the inverse is true when $\theta = \pi$ radians $(\cos\theta = -1)$. These are the cases since $-P_s$ will only obtain a negative value.
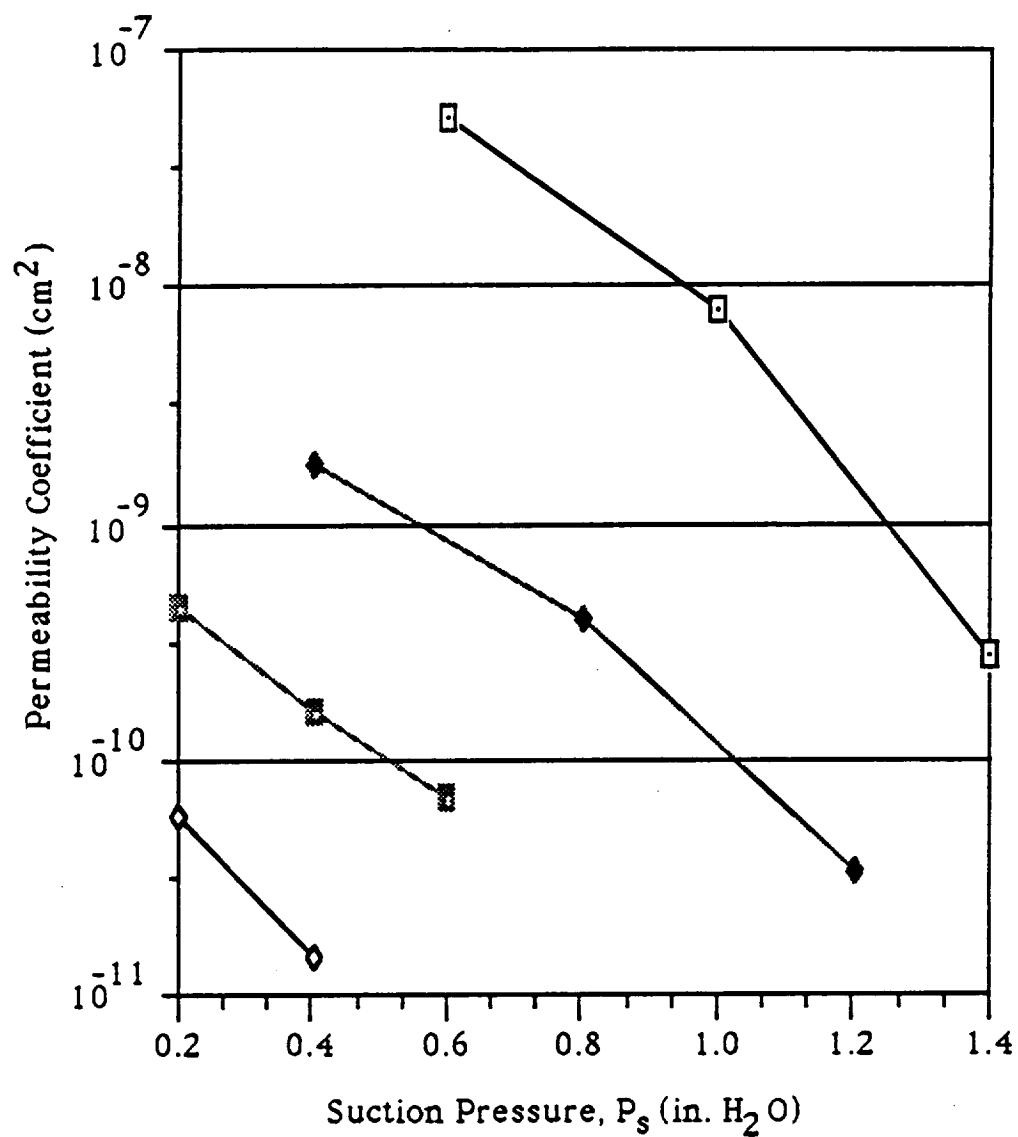
Figure 4.2. Semi-Log Plot of the Permeability Coefficient,
k, as a Function of the Suction Pressure, P_s ,
for the Four Different Pore Sized Ceramic Tubes

10.0 micron
2.0 micron
0.7 micron
0.3 micron

4.3. Experiment 3 - Void Fraction Determinations for the Ceramic Tubes

The first step in the determination of the void fraction of the porous tubes was to calculate the total volume by measuring the physical dimensions. The length, L, internal diameter, D_i, and external diameter, D_o, were measured separately for each cylinder and the total volume calculated as below.

$$V_{total, \, tube} = (\pi/4)(D_o - D_i)^2 L \qquad (11)$$

In addition, the wet weights of the tubes after saturation in water were compared to the dry weights which lead to the determination of the void volumes.

$$V_{void} = (x_w - x_d)/\rho_w \qquad (12)$$

In Equation (12), x represents the wet (w) and dry (d) weights whereas ρ_w is the density of water which was assumed to be equal to unity (in g/cm^3). Therefore, the void fraction, ϕ_v, was determined by taking the ratio of the void volume to the total volume.

$$\phi_v = V_{void}/V_{total} \qquad (13)$$

When possible, several tubes containing each different pore size were used in order to obtain an average void fraction. The results of these calculations are provided in Table 4.1 and illustrate the independence of ϕ_v on the pore size. For the 10.0 micron tubes, the average value for ϕ_v was determined to be 41.5% while the 2.0, 0.7, and 0.3 micron tubes were calculated respectively to have average void fractions of 59.6, 49.7 and 33.9%.

Table 4.1. Void Fractions of the Four Different Pore Sized
            Ceramic Tubes

10.0 micron Tube	V_{total} (cm^3)	V_{void} (cm^3)	ϕ_v (%)
1	13.360	5.604	42.0
2	13.360	5.543	41.5
3	13.360	5.439	40.7
4	13.360	5.644	42.3
Ave			41.5%

2.0 micron Tube	V_{total} (cm^3)	V_{void} (cm^3)	ϕ_v (%)
1	15.389	7.996	52.0
2	14.074	7.596	54.0
3	11.260	7.402	65.7
4	11.260	7.265	64.5
Ave			59.6%

0.7 micron Tube	V_{total} (cm^3)	V_{void} (cm^3)	ϕ_v (%)
1	13.466	6.774	50.3
2	13.745	7.027	51.1
3	12.792	5.753	45.0
4	11.525	5.941	51.6
Ave			49.7%

0.3 micron Tube	V_{total} (cm^3)	V_{void} (cm^3)	ϕ_v (%)
1	11.172	3.782	33.9
Ave			33.9%

4.4. Experiment 4 - Void Fraction Determinations for the Ceramic Disks

As with the previous experiment, the physical dimensions of each disk were measured in order to determine the total volume of the ceramic material. The equation used to calculate this parameter took the form,

$$V_{total,\ disk} = (\pi/4)D^2H \qquad (14)$$

where d is the diameter and H is the height or thickness of the disks. The void volume of each disk was determined by using the saturation procedure described earlier in conjunction with Equation (12). Again, Equation (13) was used in order to calculate the fraction of void space present in the ceramic matrix. The average values for ϕ_v were respectively calculated to be 25.0, 54.8, and 46.7% for the 10.0, 2.0, and 0.7 micron disks. The results of these calculations are presented in Table 4.2 along with the values of the experimental measurements. Note that no measurements of a 0.3 micron pore size containing disk were made since none were available.

Table 4.2. Void Fractions of the Three Different Pore Sized Ceramic Disks

10.0 micron Disk	V_{total} (cm^3)	V_{void} (cm^3)	ϕv (%)
1	2.462	0.634	25.8
2	2.574	0.643	25.0
3	2.322	0.586	25.2
4	2.427	0.570	23.5
5	2.384	0.609	25.6
Ave			25.0%

2.0 micron Disk	V_{total} (cm^3)	V_{void} (cm^3)	ϕv (%)
1	2.326	1.264	54.3
2	2.233	1.238	55.4
3	2.201	1.196	54.3
4	2.240	1.209	54.0
5	2.281	1.271	55.7
Ave			54.8%

0.7 micron Disk	V_{total} (cm^3)	V_{void} (cm^3)	ϕv (%)
1	1.867	0.987	52.9
2	2.083	0.887	42.6
3	2.104	0.982	46.7
4	1.950	0.899	46.1
5	2.037	0.961	47.2
Ave			46.7%

4.5.   Experiment 5 - Stability and Consistency Measurements of the Thermistor Moisture Sensor Device

The data collected to evaluate the thermistor moisture sensor device consisted of four replicates of the voltage readings when the PCTPNS was maintained at a particular operating condition.   In addition to testing the different ceramic tubes containing the pores of various sizes, the suction pressure was altered from -8.0 to -2.0 in increments of one inch of water.   The voltage readings for a particular tube were taken sequentially starting at the greatest suction (-8.0 inches of water) and ending at the other end of the test range (-2.0 inches).   This process was then reversed by beginning at -2.0 and ending at -8.0 and then this whole procedure was repeated to obtain the total of four replicates.   Since the measurements at one pressure setting were not taken one after the other, this represents a stability test for the sensory device.   The results of these experiments are presented in Figures 4.3.1 to 4.3.4 for the 10.0, 2.0, 0.7, and 0.3 micron tubes, respectively.   The standard deviations associated with these results ranged from ±14.0 to ±3.0, ±5.0 to ±0.8, ±5.4 to ±2.6, and ±15.3 to ±1.2 for the four different tubes, respectively.   In addition to the averages of the four replicates, the original data provided by Thomas Dreschel is given as a comparison. This comparison can be used to establish the consistency of the thermistor based sensor since each set of data was obtained by independent researchers and at different times.   In addition, some of the results of the next experiment (variations due to the sensor location on the tube) can be used to evaluate this factor as well.   At suction pressures of -3.0 and -7.0 inches of water, the average voltage readings obtained from Experiment 6 are also provided on Figures 4.3.1 to 4.3.4.

As can be seen from these figures, the results of this research yielded roughly a linear relationship between the voltage readings and the applied negative pressures.   Using linear regression, least square lines were drawn for each of the porous tubes tested.   The results of these analyses are given in Equations (15), (16), (17), and (18) for the 10.0, 2.0, 0.7, and 0.3 micron tubes, respectively.

$$V = -10.0\, P_S + 251.4 \tag{15}$$
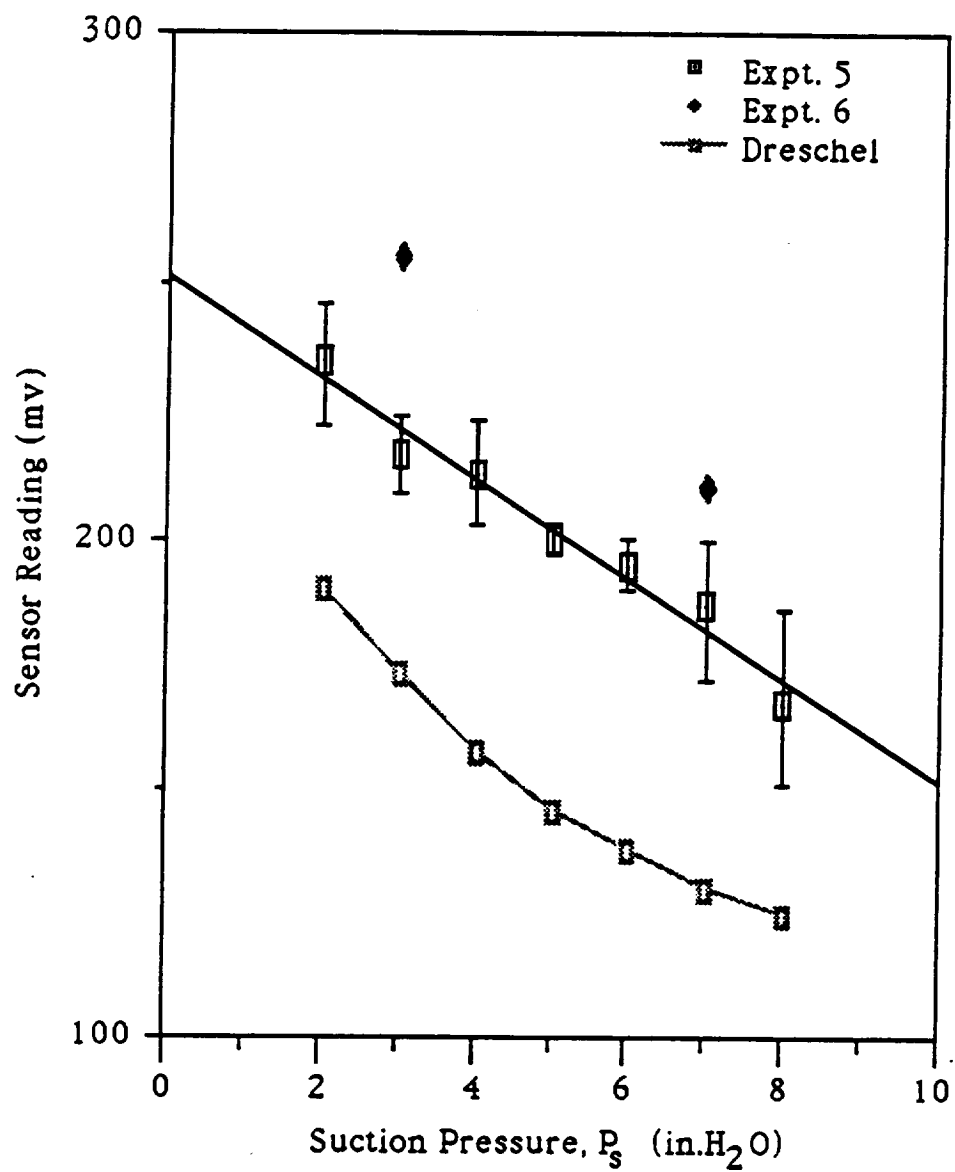
Figure 4.3.1. Sensor Reading as a Function of Suction Pressure, P_s, on a 10.0 Micron Pore Sized Ceramic Tube (Data from Expt. 5, Expt. 6, and Thomas Dreschel)

Sensor Reading = 251.4 - 10.0 P_s R^2 = 0.970
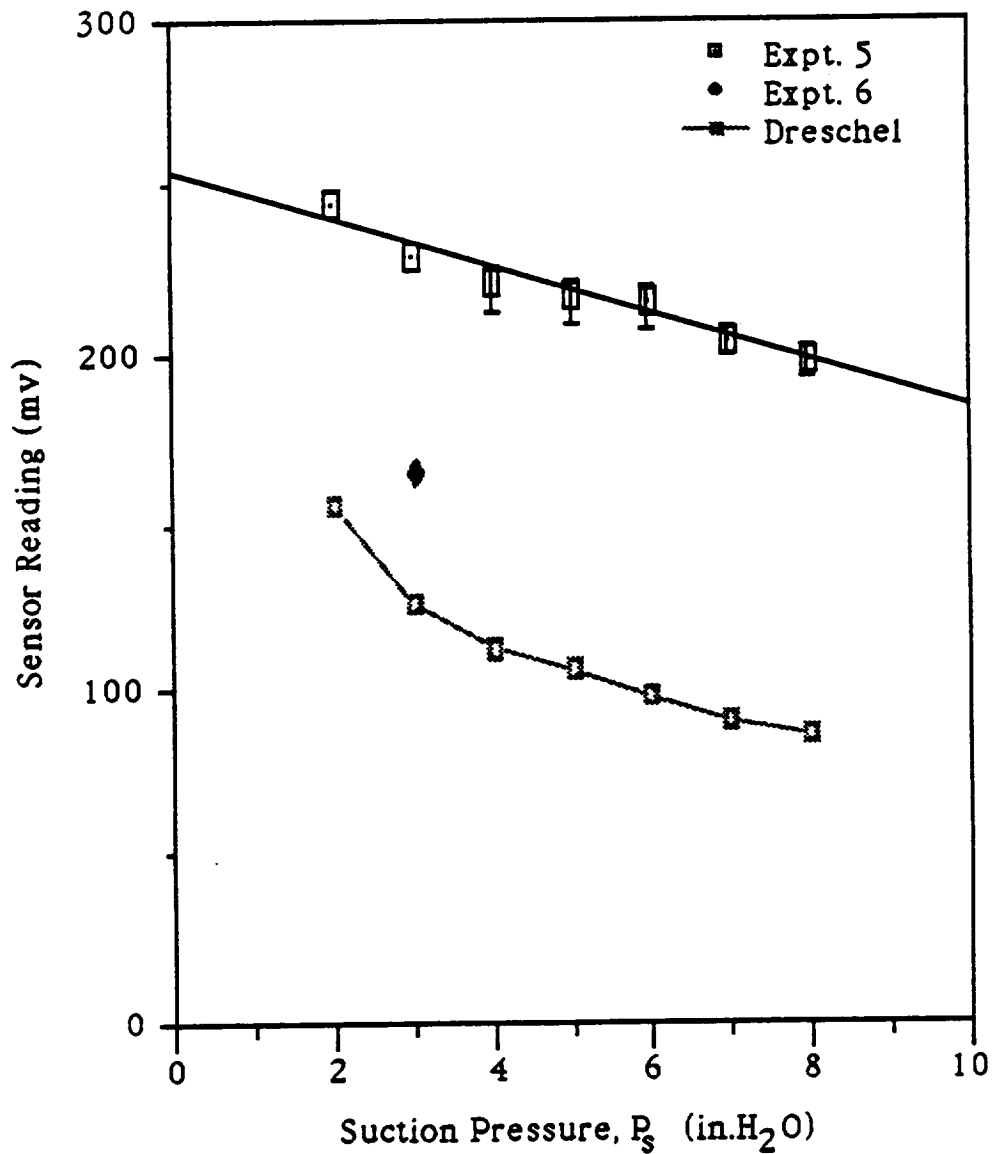
Figure 4.3.2. Sensor Reading as a Function of Suction Pressure, P_s, on a 2.0 Micron Pore Sized Ceramic Tube (Data from Expt. 5, Expt. 6, and Thomas Dreschel)

Sensor Reading = 254.6 - 7.2 P_s R^2 = 0.947
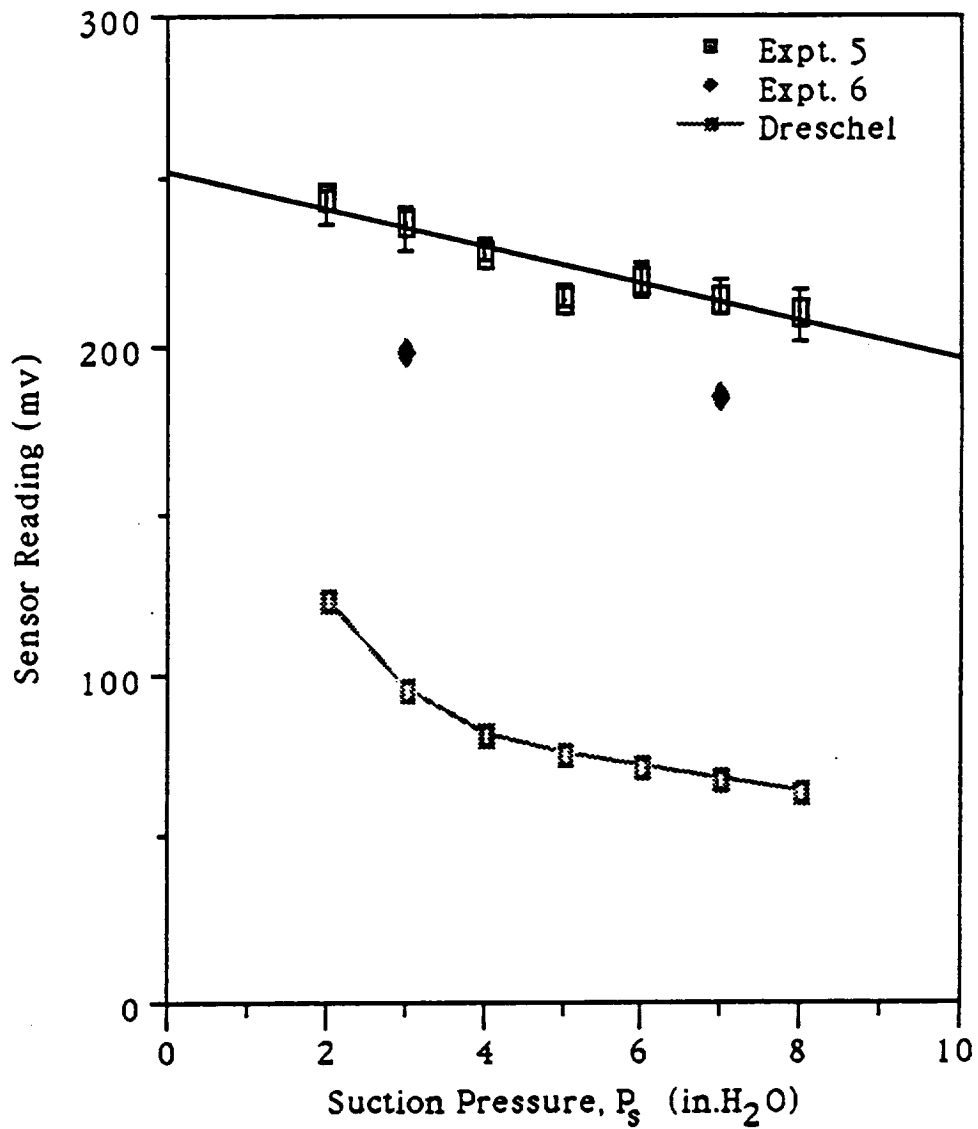
Figure 4.3.3. Sensor Reading as a Function of Suction
Pressure, P_s, on a 0.7 Micron Pore Sized
Ceramic Tube (Data from Expt. 5, Expt. 6,
and Thomas Dreschel)

Sensor Reading = 253.3 - 5.9 P_s R^2 = 0.882
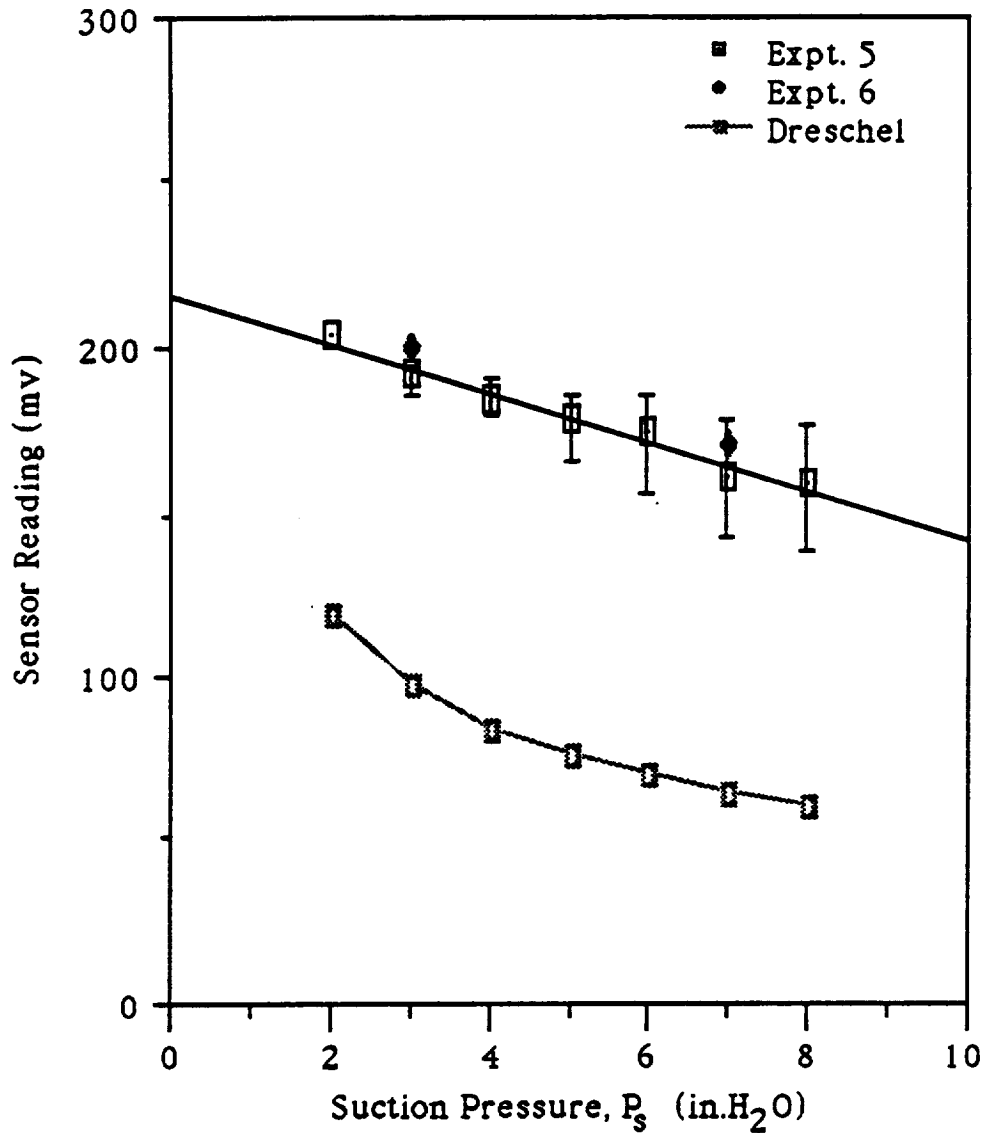
Figure 4.3.4. Sensor Reading as a Function of Suction
Pressure, P_s , on a 0.3 Micron Pore Sized
Ceramic Tube (Data from Expt. 5, Expt. 6,
and Thomas Dreschel)

Sensor Reading = $216.5 - 7.5\ P_s$ $R^2 = 0.986$

$$V = -7.2\ P_S + 254.6 \tag{16}$$

$$V = -5.9\ P_S + 253.3 \tag{17}$$

$$V = -7.5\ P_S + 216.5 \tag{18}$$

Using these equations to estimate the expected voltage readings leads to the standard error according to the following equation (Spiegel, 1961).

$$\text{Standard Error} = \left[\frac{\sum_i (x_{i,obs} - x_{i,exp})^2}{n-2}\right]^{1/2} \tag{19}$$

In Equation (19), $x_{i,obs}$ is the experimentally obtained value for the voltage reading while $x_{i,exp}$ is determined from Equation (15), (16), (17), or (18). The results of such calculations where n is the number of observations on the 10.0, 2.0, 0.7, and 0.3 micron tubes were ± 8.4, ± 5.1, ± 5.9, and ± 8.9 mv, respectively. These error ranges should account for 68% of the sample points but, as can be seen from Figures 4.3.1 to 4.3.4, these standard errors of the estimates cannot account for the results obtained by Thomas Dreschel and in general do not account for the results of Experiment 6. In addition, a doubling or tripling of this standard error which would account for 95 and 99.7% of the sample points, respectively (Spiegel, 1961), still does not encompass the alternate experimental results.

4.6. Experiment 6 - Pressure Drop Effects on the Moisture Sensor Device

The flow through any conduit is accomplished by a corresponding pressure drop along its length (Bird, et al., 1960). In order to determine the effect of this phenomenon on the voltage readings obtained by the thermistor based moisture sensor device, measurements at four different locations on the tops of the tubes were taken. Specifically, the thermistors were located at 1.5, 3.5, 7.0, and 9.0 cm from the entrance end of each of the four porous tube types (see Figure 3.3). The two pressures of -3.0 and -7.0 inches of water were tested on each of these tubes for four replicates obtained non-sequentially. In other words, after the desired pressure was set in the PCTPNS, voltage readings at the four locations were taken at increasing lengths from the entrance, one at a time. This process was then reversed (i.e. decreasing lengths) and then the entire procedure repeated again to obtain the four replicates. The results of these experiments are presented in Tables 4.3.1 to 4.3.4 along with the average readings obtained for the four sensor locations. For the 0.7 and 2.0 micron tubes, complete results were not obtained due to the degradation in the sensor readings; voltage readings fell well below the previously achieved values.

The largest variation in the average voltage readings due to the location on the tubes was 18 mv obtained for each test pressure on the 10.0 micron pore sized tube. However, in both cases, the differences were not exhibited between the ends of the tubes but occurred at random locations on the tube. Similar results were obtained on the other pore sized tubes thus illustrating the independence of the voltage readings on the sensor location. In addition, an analysis of the standard deviations of the four replicates (see Tables 4.3.1 to 4.3.4) revealed that in general, the errors associated with a single location could cancel the variations exhibited along the length of the tube.

Table 4.3.1. The Effect of the Location of the Moisture
Sensor on the Sensor Readings

10.0 Micron Tube:

	Sensor Reading (mv)			
P_s (in.H_2O)	1.5 cm	3.5 cm	7.0 cm	9.0 cm
-3.0 ->	252	237	252	245
-3.0 <-	256	227	251	253
-3.0 ->	257	238	251	253
-3.0 <-	254	244	263	260
Ave	255±2.2	237±7.1	254±5.9	253±6.1

	Sensor Reading (mv)			
P_s (in.H_2O)	1.5 cm	3.5 cm	7.0 cm	9.0 cm
-7.0 ->	210	211	213	216
-7.0 <-	212	193	215	224
-7.0 ->	212	205	210	213
-7.0 <-	206	185	221	215
Ave	210±2.8	199±11.7	215±4.7	217±4.8

Table 4.3.2.   The Effect of the Location of the Moisture
Sensor on the Sensor Readings

2.0 Micron Tube:

P_S (in.H_2O)	Sensor Reading (mv)			
	1.5 cm	3.5 cm	7.0 cm	9.0 cm
-3.0 ->	161	160	167	174
-3.0 <-	166	166	171	173
-3.0 ->	168	166	175	164
-3.0 <-	---	---	---	---
Ave	165±3.6	164±3.5	171±4.0	170±5.5

P_S (in.H_2O)	Sensor Reading (mv)			
	1.5 cm	3.5 cm	7.0 cm	9.0 cm
-7.0 ->	---	---	---	---
-7.0 <-	---	---	---	---
-7.0 ->	---	---	---	---
-7.0 <-	---	---	---	---
Ave	Sensor Readings Degraded			

Table 4.3.3.   The Effect of the Location of the Moisture
Sensor on the Sensor Readings

0.7 Micron Tube:

P_S (in.H_2O)	Sensor Reading (mv)			
	1.5 cm	3.5 cm	7.0 cm	9.0 cm
-3.0 ->	191	193	199	198
-3.0 <-	201	197	202	206
-3.0 ->	202	199	200	206
-3.0 <-	198	200	204	196
Ave	198±5.0	197±3.1	201±2.2	202±4.4

P_S (in.H_2O)	Sensor Reading (mv)			
	1.5 cm	3.5 cm	7.0 cm	9.0 cm
-7.0 ->	189	191	195	194
-7.0 <-	180	187	194	197
-7.0 ->	---	---	---	---
-7.0 <-	---	---	---	---
Ave	185	189	195	196

Table 4.3.4. The Effect of the Location of the Moisture
Sensor on the Sensor Readings

0.3 Micron Tube:

	Sensor Reading (mv)			
P_S (in.H_2O)	1.5 cm	3.5 cm	7.0 cm	9.0 cm
-3.0 ->	200	192	194	180
-3.0 <-	200	194	196	189
-3.0 ->	202	200	195	194
-3.0 <-	197	197	199	196
Ave	200±2.1	196±4.4	196±2.2	190±8.8

	Sensor Reading (mv)			
P_S (in.H_2O)	1.5 cm	3.5 cm	7.0 cm	9.0 cm
-7.0 ->	181	180	170	178
-7.0 <-	173	174	180	189
-7.0 ->	167	184	177	168
-7.0 <-	164	173	162	191
Ave	171±7.5	178±5.2	172±8.0	182±10.7

4.7. Experiment 7 - Time Dependent Measurements of the Moisture Sensor Device

While conducting Experiments 5 and 6, it was observed that the time required to reach a constant voltage reading on the moisture sensor device was dependent upon the applied negative pressure. Experiments were conducted on the 10.0 micron pore sized tube at pressures of -2.0, -5.0, and -8.0 inches of water with the time required to reach a maximum voltage reading measured. In addition, the voltage readings themselves were recorded so that a correlation with the time could be produced. Four replicates at each pressure were taken with the averages calculated and plotted as in Figure 4.4. In addition, linear least squares regression calculations were performed on both the maximum sensor reading obtained and the time required for this maximum as influenced by the suction pressure. The results of these analyses are also presented in Figure 4.4. The relationship between the sensor reading and the pressure is given in Equation (20) while time versus pressure is given in Equation (21).

$$\text{Sensor Reading} = -8.8\ P_S + 131.5 \tag{20}$$

$$t = 1.13\ P_S + 17.98 \tag{21}$$

In order to relate the sensor reading to the time required, Equations (20) and (21) were combined to give the following linear relationship.

$$t = -0.128 \times \text{Sensor Reading} + 34.87 \tag{22}$$

Equation (22) illustrates the maximum time of approximately 35 seconds which is required to reach a steady value on the sensor device placed on a 10.0 micron porous tube. This result confirms the previous findings that the response of this device occurred between 30 and 45 seconds after being placed on a moist surface (Bean, et al., 1990).
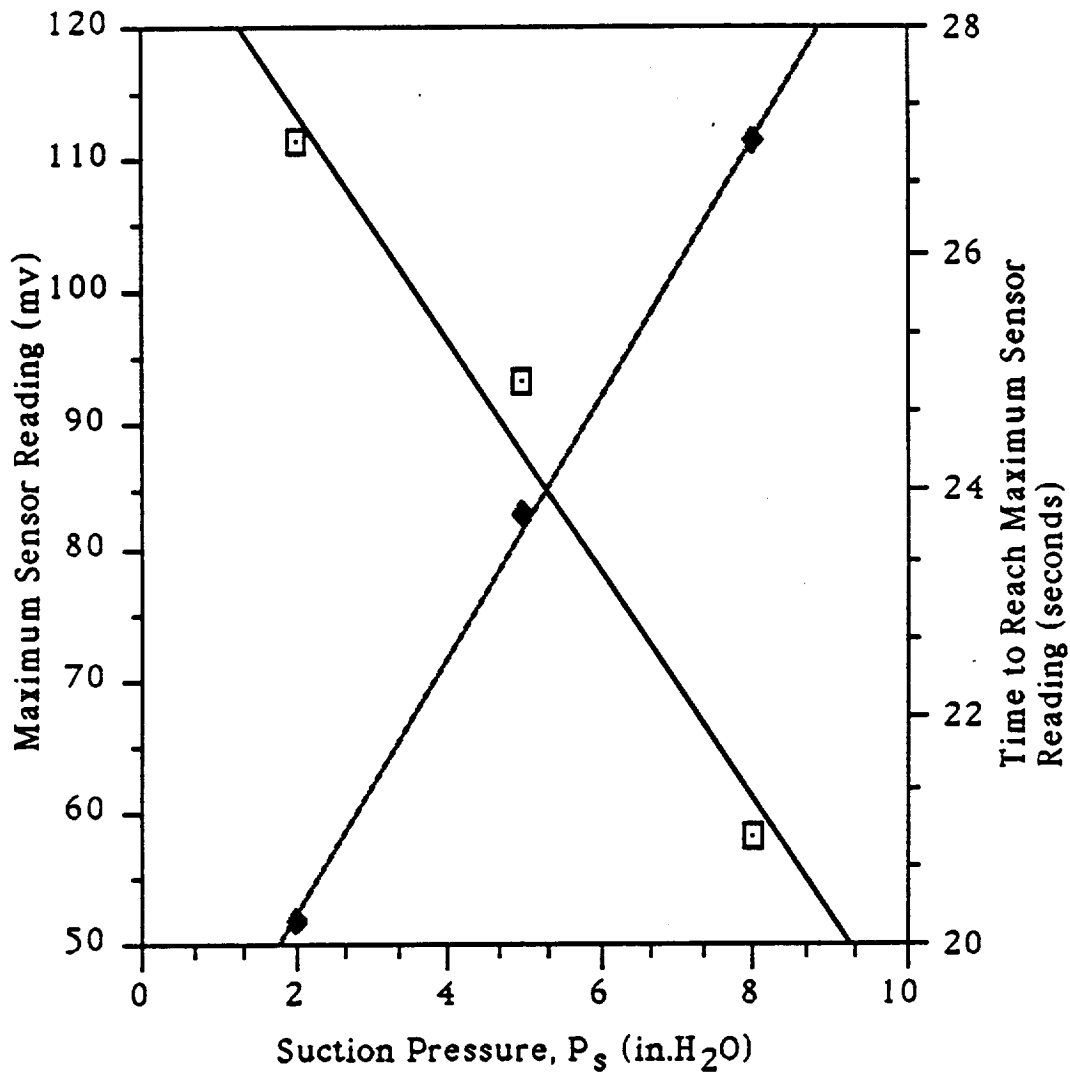
Figure 4.4. The Maximum Sensor Reading and the Time
Required for the Moisture Sensor Device to
Reach this Maximum as Influenced by the
Suction Pressure, P_s

Sensor Reading = 131.5 - 8.8 P_s R^2 = 0.969
Time = 17.98 + 1.13 P_s R^2 = 0.999

4.8. Experiment 8 - Water Flux Determinations

This experiment was conducted as a comparative study for the thermistor based moisture sensor device. The water flux rate was determined by measuring the wet and dry weights of the absorbant material placed for a known length of time in direct contact with a ceramic tube. The tubes tested contained pores with average sizes of 10.0 and 0.3 microns and were examined at the same pressures as the moisture sensor device (-2.0 to -8.0 inches of water in increments of one). As stated in the Materials and Methods Section, two external weights were tested in conjunction with two different surface areas of contact. In order to calculate the flux, F, in these experiments, the following equation was used.

$$F = \frac{\rho_w (x_w - x_d)}{A\, t} \tag{23}$$

In this equation, F (in ml/min/cm^2) was calculated on the basis of the per unit area of surface contact, A, of the absorbant material. For the 10.0 micron pore sized tube, neither this factor nor the amount of external weight placed on the germination paper sections had an effect on the water flux rate. This situation can be seen in Figure 4.5.1 which plots the averages of two replicates for each of the four possible experimental conditions (2 weights, 2 areas). Similarly, the results involving the 0.3 micron pore sized tubes are provided in Figure 4.5.2 but reveal a wide variation in responses, unlike the 10.0 micron counterpart.
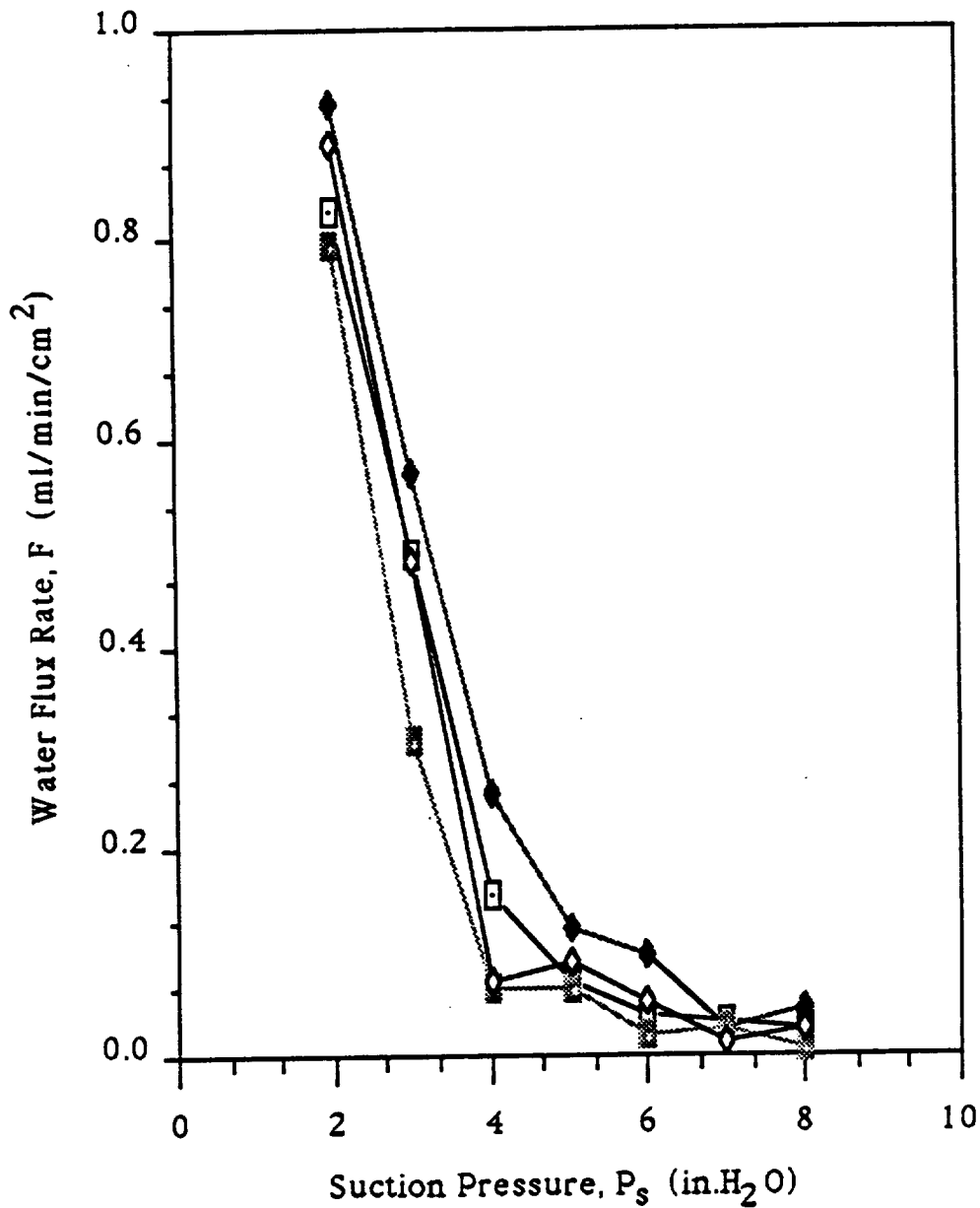
Figure 4.5.1. Water Flux Rate, F, as Determined by the
Germination Paper Absorption Test for
the 10.0 Micron Pore Sized Ceramic Tube

Weight = 23.6 g, Area = 1.0 cm x 5.8 cm
Weight = 42.4 g, Area = 1.0 cm x 5.8 cm
Weight = 23.6 g, Area = 1.5 cm x 5.8 cm
Weight = 42.4 g, Area = 1.5 cm x 5.8 cm
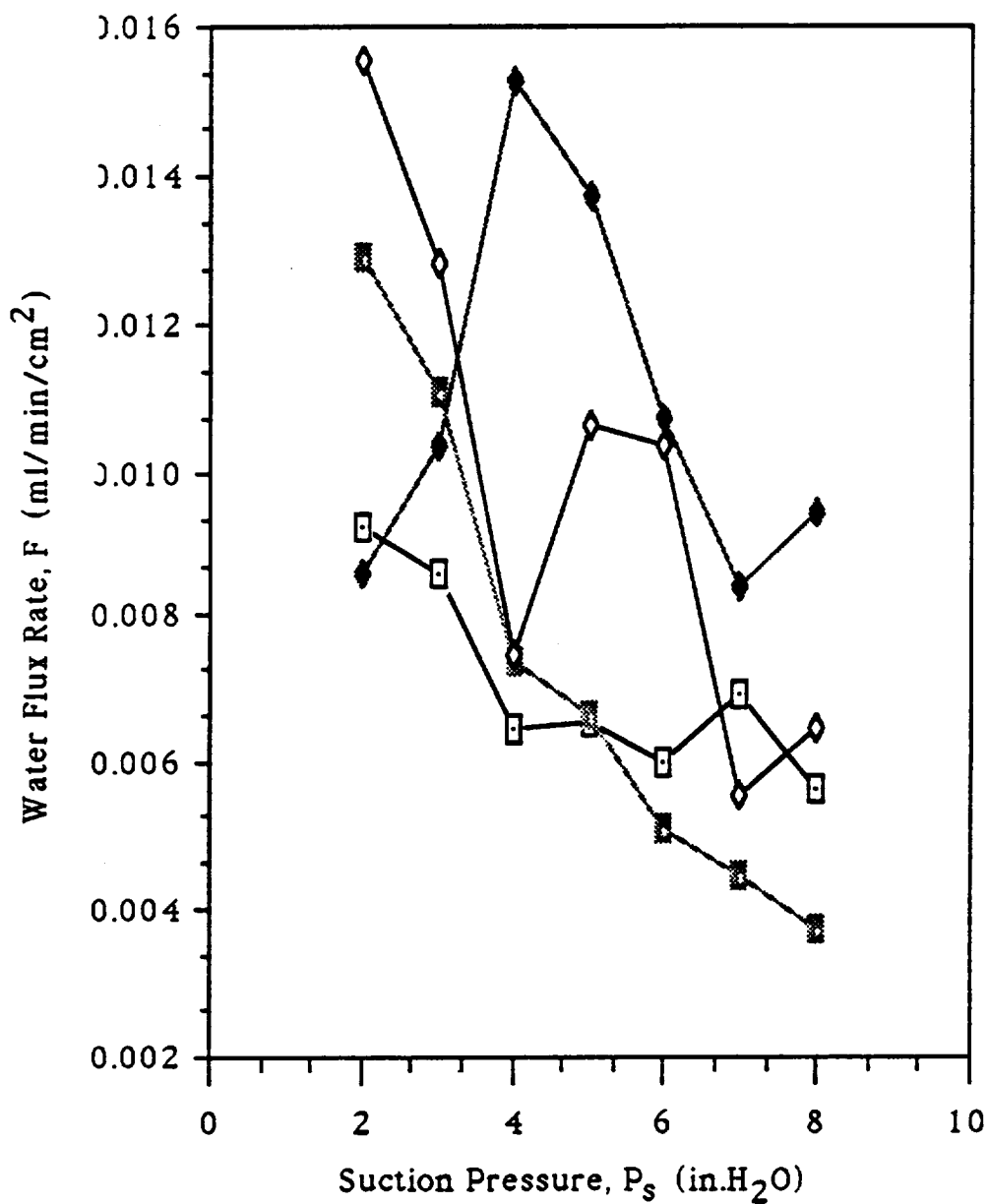
Figure 4.5.2. Water Flux Rate, F, as Determined by the Germination Paper Absorption Test for the 0.3 Micron Pore Sized Ceramic Tube

Weight = 23.6 g, Area = 1.0 cm x 5.8 cm
Weight = 42.4 g, Area = 1.0 cm x 5.8 cm
Weight = 23.6 g, Area = 1.5 cm x 5.8 cm
Weight = 42.4 g, Area = 1.5 cm x 5.8 cm

5. DISCUSSION

5.1. Concept and Definition of "Wetness"

The concept of the "wetness" of the ceramic material, either in disk or tube form, has been used to describe the qualitative state of the porous material. When run in the PCTPNS, the porous tubes would be considered very wet when weeping conditions occurred. Conversely, when cavitation or the inward flux of air into the tubes occurred, this would be considered a state where the ceramic was not very wet. However, in the intermediate pressure range between these two extreme conditions, it would be quite difficult to quantify the "wetness" of the tubes. Using the microscopic observations obtained in Experiment 4 of this research paper, a clearer definition of this catch-all word under these intermediate conditions can be obtained. In particular, the vertical flow-through experiments conducted on the ceramic disks illustrated the uneven distribution of liquid in the "hills and valleys" of the surface features. As time progressed after contact was made between the liquid and the dry disks, certain regions of void spaces or "valleys would fill first and then others would follow later as more liquid was introduced. As for the visualizations of the horizontal spread pattern within these disks, it was revealed that the rate of flow through the porous matrix was not even. Once a drop of liquid was placed on top of the disks, it would spread out fairly rapidly and be absorbed into the voids of the ceramic. However, direct observations using the overhead microscope showed that the spread pattern was not in a perfect circular expansion from the initial drop radius. Therefore, due to the random convolutions of the porous material which appeared as compressed granular particles, and by analogy to the horizontal flow, the flow in the vertical direction would not be as a single level of liquid. Instead, a variable distribution dependent upon the surface tension that existed between specific regions of these two mediums would result. In other words, the appearance of liquid in certain

regions of the disk surfaces and not in others was not solely dependent upon the depths of the "valleys."

Another factor which was observed as having an influence on the degree of "wetness" of the ceramic material was the suction pressure applied within the porous tube. When the negative pressure was altered from a higher to a lower suction, it was directly observable under the microscope that the average level of liquid distributed amongst the "hills and valleys" would increase. Or, stated in another way, the ceramic tube would become more wet as the suction pressure was decreased. Again, the distribution of liquid in the porous matrix was visualized as a variance of the region. Therefore, it would appear that the forces due to the pressure differential affect the overall "wetness" of the ceramic while the surface tension forces are mainly only a local influence making one region wetter than another.

From a scientific and engineering point of view, a definition of "wetness" on a quantitative basis would be more applicable to the development of physical and mathematical models. Since the void fractions of the tubes and disks were calculated, one possible measure of the overall "wetness," W, would be the percentage of void space that contains liquid.

$$W = \frac{V_{void, filled}}{V_{void, total}} = \frac{V_{void, filled}}{\phi_V V_{total, tube}} \tag{24}$$

Using Equation (11) for $V_{total, tube}$ in Equation (24) gives,

$$W = \frac{V_{void, filled}}{\phi_V (\pi/4)(D_o - D_i)^2 L} \tag{25}$$

Knowing that a distribution of liquid levels exists at the tube surface, an average level, h, measured from the internal tube wall can be used to convert the numerator of Equation (25) into a more measurable form.

$$W = \frac{\phi_v (\pi/4)[(D_i + 2h)^2 - D_i^2]L}{\phi_v \ (\pi/4)(D_o - D_i)^2 L} \qquad (26)$$

Simplifying Equation (26) leaves the mathematical definition of the "wetness" of the ceramic tube in a PCTPNS.

$$W = \frac{(D_i + 2h)^2 - D_i^2}{(D_o - D_i)^2} \qquad (27)$$

Thus, Equation (27) illustrates that the overall "wetness" is solely dependent upon the average level of liquid contained in the matrix of the ceramic material.

5.2. Development of a Physical Model

The development of a physical model for the PCTPNS involved the elucidation of the physical make-up of the ceramic tubes in addition to the determination of the various forces affecting the radial flow. From the microscopic observations on the tubes as well as on the disks, at least two different materials appeared to be used in the construction of the porous ceramics. In addition, the product bulletin (Osmonics, Inc., 1988) stated that more than one inorganic oxide was used. As for the forces involved in controlling the flow of liquid through the porous ceramic matrix, three substantial effectors have been identified. The two that have already been mentioned are the surface tension force holding the liquid in the porous matrices and the net pressure differential force pulling liquid into the bulk flow. The directional vector of these two forces is independent of the location on the tube. The final force involved in the control of the flow of liquid through the ceramic tubes is the ever present gravitational force. This particular force differs from the other two in that it is uni-directional only in the negative z - coordinate. The effects of this force would be different on top of the tubes as compared to the underside. Specifically, this force would cause

inward flow at the top of the tubes while underneath the tubes, gravity would force liquid outwards.

A depiction of the developed physical model is provided in Figure 5.1 which illustrates the forces involved at both the top and bottom of a ceramic tube in addition to the use of at least two granular particle types. Included in this diagram are illustrations of the various liquid levels distributed between the uneven surface features of the ceramic and the average liquid level used in the quantification of the "wetness." One feature which could be slightly different in this model for the four different pore sized tubes would be the grain size of the inorganic oxide particles. Under the microscope, the size of the particles used to construct each tube type was proportional to the reported average pore size (Osmonics, Inc. Product Bulletin, 1988). This relationship makes sense since smaller particles can make a more intimate fit with its neighboring particles thus decreasing the average pore size. Conversely, larger particles would have a higher degree of steric hindrances with its neighbors thus resulting in larger pore sizes. These conclusions are analogous to the structuring of compounds on the atomic scale (Morrison and Boyd, 1986).

Another parameter which should follow this trend, keeping all other factors constant, is the void fraction contained within each tube type. However, the results of Experiment 3 showed that ϕ_v was not proportional to the pore size. Specifically, the largest void fraction was found to be contained in the 2.0 micron tube while the 10.0 micron tube which, intuitively, should of had the largest ϕ_v gave an intermediate result instead (see Table 4.1). This same phenomenon was exhibited in the ceramic disks as well (see Table 4.2). Possible reasons for this discrepancy could lie in either the construction procedure used or in the materials themselves. At the 70x magnification used to visualize these ceramic materials, a difference could be seen in the uniformity of the granular particles. In the 10.0 micron tube, the grain sizes varied significantly while in the smaller pore sized tubes, this became less evident. The method used to form these granular particles into the tubes and disks may have been different depending upon the abilities of the various sized and shaped particles to adhere. In other words, the 10.0 micron
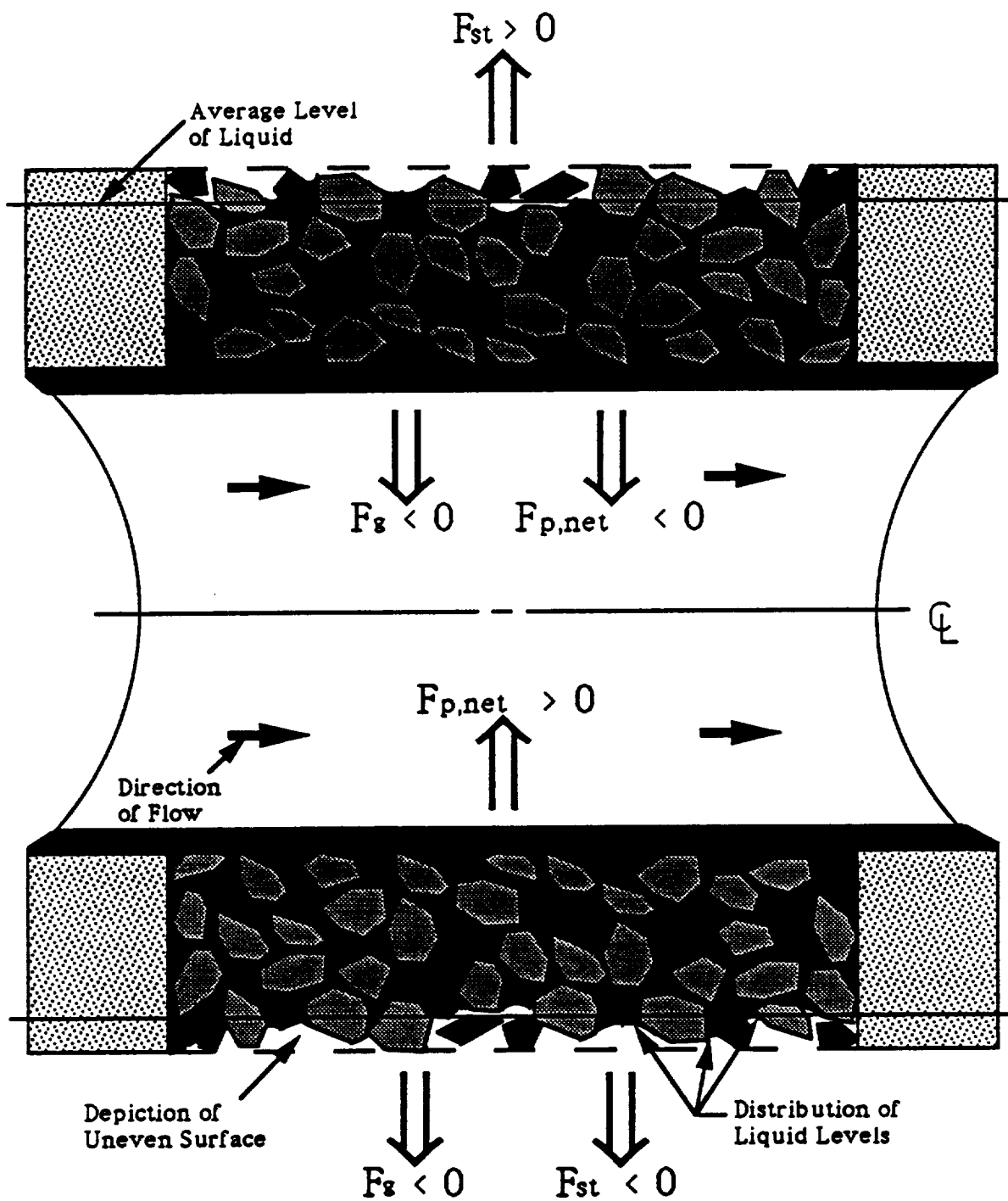
Figure 5.1. Developed Physical Model of the Porous Ceramic Tube
Plant Nutrification System (PCTPNS)

tube may have required a higher degree of compression in order to maintain the desired shape. In addition, the ratio of the different inorganic oxides used may have been altered to meet certain strength and durability requirements for each of the different tube types. In order to determine an exact reason for these differences in void fractions, a clearer understanding of the construction materials and methods would be required.

5.3. Development of the Mathematical Model

From the physical model and the definition of the "wetness" of the ceramic material developed in the previous discussions, a mathematical model of the PCTPNS can be formulated. The three major forces influencing the "wetness" of the PCTPNS are the forces exerted by the surface tension, F_{st}, the net pressure differential, $F_{p,net}$, and gravity, F_g. The surface tension of water in the radial direction, $\gamma\cos\phi$, is given in units of force per unit length (Bromberg, 1984). Therefore, this term applies to the contact length between the water and the circumference of the pore spaces in the ceramic material. This differs for the force exerted by the applied negative pressure, $-P_s$, which is the difference between the internal and external pressures. The units of this term are measured on a force per unit area basis and would be applied to the surface area of the air-liquid interface. As for the specific gravity, $-\rho g\cos\theta$, the total liquid volume contained in the porous matrix as well as in the bulk fluid flow within the tube must be used since this term is given in a force per unit volume measure.

In order to relate all of these forces together, a balance can be performed which would describe the PCTPNS under static conditions. Before this can be accomplished, the appropriate unit factors must be derived. The volume of liquid contained in the porous ceramic matrix, $V_{void, filled}$, was expressed earlier as the following.

$$V_{void, filled} = \phi v(\pi/4)[(D_i + 2h)^2 - D_i^2]L \qquad (28)$$

Another method which could be used to describe this parameter utilizes a theoretical number of pores, n, and the average diameter of

the pores, d. At a given average liquid level, h, in the ceramic tube, $V_{void,\ filled}$, can be written as follows.

$$\bullet\ V_{void,\ filled}\ =\ n\pi d^2 h/4 \tag{29}$$

Since the total circumference of the pore spaces at this given level, h, can be expressed as,

$$C_{void,\ filled}\ =\ n\pi d \tag{30}$$

then Equation (30) can be related to Equation (29) in the following manner.

$$C_{void,\ filled}\ =\ 4V_{void,\ filled}/hd \tag{31}$$

Similarly, the total interfacial surface area, $A_{void,\ filled}$, at the average liquid level can be related to the filled void volume as follows.

$$A_{void,\ filled}\ =\ n\pi d^2/4\ =\ V_{void,\ filled}/h \tag{32}$$

Therefore, the surface tension and pressure differential forces can be expressed using Equations (31) and (32), respectively.

$$F_{st}\ =\ \gamma\cos\phi[4V_{void,\ filled}/hd] \tag{33}$$

$$F_{p,net}\ =\ -P_s[V_{void,\ filled}/h] \tag{34}$$

For the gravitational force, since the entire volume of liquid in the porous matrix and within the tube itself must be taken into account then, F_g, can be written as follows.

$$F_g\ =\ -\rho g\cos\theta[V_{void,\ filled}\ +\ (\pi/4)D_i^2 L] \tag{35}$$

Under steady state conditions, these forces should be equivalent to zero and the forces should balance. Therefore,

$$F_{st}\ +\ F_{p,net}\ +\ F_g\ =\ 0 \tag{36}$$

Substituting Equations (33), (34), and (35) into Equation (36) gives this force balance in terms of the void volume.

$$\gamma\cos\phi \ [4 \ V_{void,\ filled}/hd] - P_s \ [\ V_{void,\ filled}/h]$$
$$- pg\cos\theta[V_{void,\ filled} + (\pi/4)D_i^2L] = 0 \qquad (37)$$

Simplifying this equation,

$$[4\gamma\cos\phi/hd - P_s/h - pg\cos\theta]V_{void,\ filled}$$
$$- pg\cos\theta(\pi/4)D_i^2L = 0 \qquad (38)$$

Finally, substituting Equation (28) for $V_{void,\ filled}$ gives,

$$[4\gamma\cos\phi/hd - P_s/h - pg\cos\theta]\phi v(\pi/4)$$
$$[(D_i + 2h)^2 - D_i2]L - pg\cos\theta(\pi/4)D_i^2L = 0 \qquad (39)$$

Equation (39) represents the mathematical model of the PCTPNS under steady state conditions. Figure 5.2 is a cross-sectional drawing of a ceramic tube and illustrates the essential parameters used in this mathematical model.

From the observations of Experiment 4, the force due to the surface tension of water contained in the porous matrix of the ceramic tubes seems to be mainly controlled by the regional characteristics. However, since the exact ceramic density and fluid content cannot be determined specifically for each region, the surface tension force would need to be averaged over the entire tube surface and over the various distributions of liquid levels. Therefore, the average liquid level was used in the derivation of the total surface tension force given in Equation (33). In this equation, γ represents the surface tension of water which is controlled by the cohesiveness of the liquid for itself. In addition, the contact angle, ϕ, between the meniscus of water and the sides of the ceramic pores is controlled by the adhesive interaction between these two mediums. Therefore, assuming a static situation, these two parameters are generally referred to as constants that are dependent only on the properties of the materials involved and not on other controlled factors such as the applied pressure. A typical value of γ was found to be 72.75 dyne/cm at 20°C (Bromberg, 1984) while the contact angle between the water and the ceramic material is related by Equation (39). Since γ and ϕ are constants as are the density of the liquid, p, and the diameter of the pores, then the height of the liquid
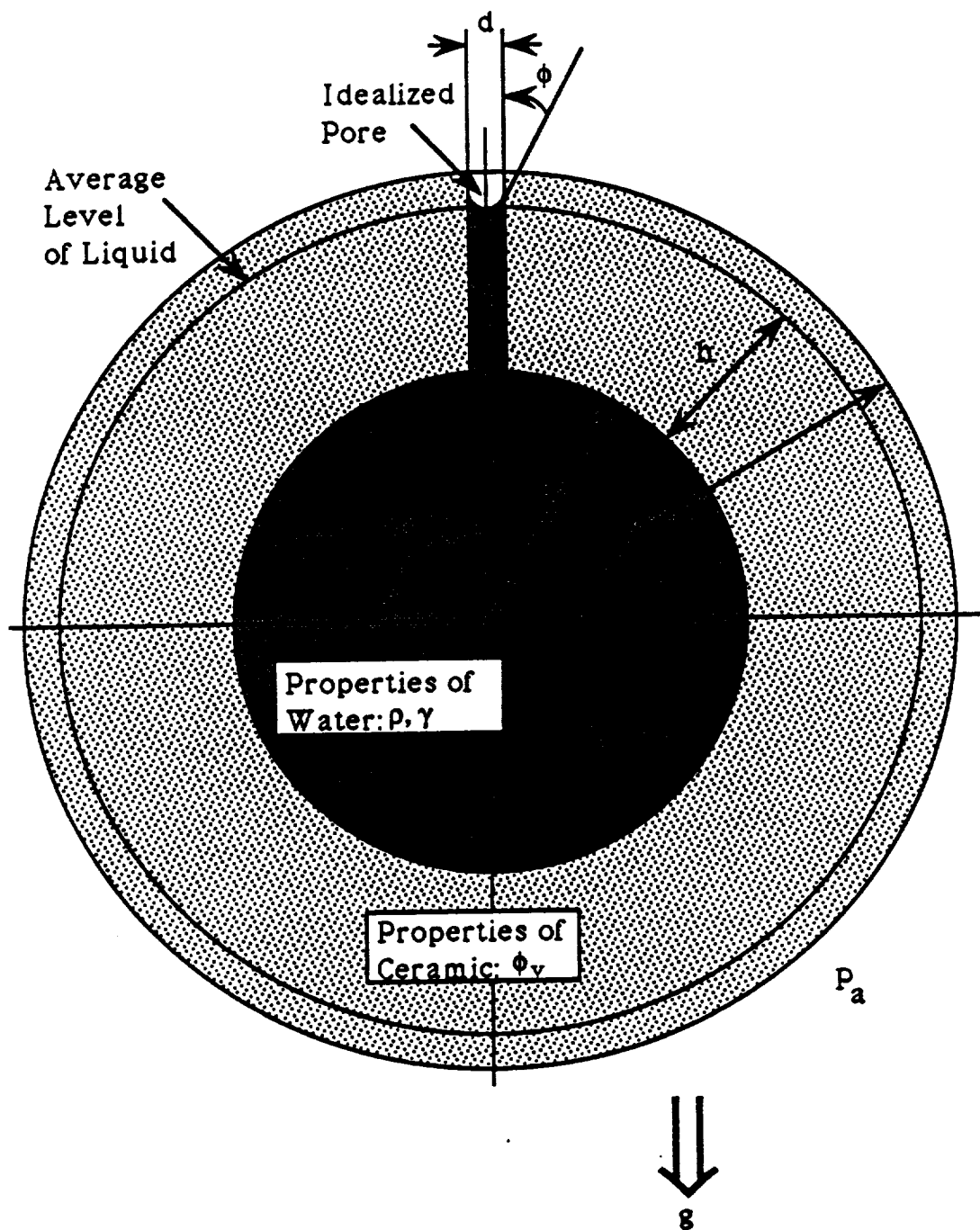
Figure 5.2. Cross-Sectional Drawing of a Porous Ceramic
Tube Illustrating the Essential Parameters
Used to Develop the Mathematical Model

in the capillary, h, would only be dependent upon the suction pressure. This equation was originally derived assuming that the specific gravity, g, was constant as is accepted here on Earth. However, in the variable gravity of space, when the gravitational contribution can become negligible, then Equation (39) would reduce to the following.

$$[4\tau\cos\phi/hd - P_s/h]\phi_v \ (\pi/4)[(D_i + 2h)^2 - D_i^2]L = 0 \quad (40)$$

Simplifying and rearranging,

$$4\tau\cos\phi = P_s d \quad (41)$$

Therefore, Equation (41) illustrates that a change in pressure must cause a change in either the surface tension of water for itself or the contact angle between the two mediums. Whether one or both of the parameters are changed cannot be exactly determined until a design of an experiment with variable gravity can be performed. However, since the surface tension is based upon the molecular interactions of the water (Bromberg, 1984), one would suspect that would be more likely to be altered. This can even be visually seen when an unsteady state pressure is applied to a liquid contained within a tube or capillary. For example, drawing water into a syringe causes a transient convex meniscus until the suction is halted and the usual concave meniscus results. Therefore, under these assumptions, the contact angle between the water and the sides of the ceramic pores would be defined by the amount of pressure applied to the system.

In the static mathematical model of the PCTPNS given in Equation (39), the contribution due to the net pressure differential did not take into account the pressure drop that would exist between the ends of the tubes. According to the Hagen-Poiseuille Equation (Bird, et al., 1960),

$$Q_z = \frac{\pi D_i^4(P0 - PL)}{128\mu L} \quad (42)$$

flow in the longitudinal direction, Q_z, is induced in conduits due to the pressure gradient along the length, $(P_o - P_L)$. For flow to occur, P_o at the tube entrance must be greater than P_L at the tube exit. Since the applied suction pressure, P_s, was measured from atmospheric conditions at the tube exit, then $P_L = -P_s$ (see Figure 3.1). Therefore, according to Equation (42), P_o should be greater than P_s (less negative and the pressure along the length of the tube should approach P_s as the distance to the exit of the tube is decreased. The justification for not including this phenomenon in the model equation lies in the fact that in tubes of such small length, the pressure drop is relatively negligible in comparison to the magnitude of the applied pressure itself. From the results of Experiment 1, the longitudinal flow rate was calculated to be approximately between 67 and 74 ml/min for the various tube types. Using Equation (42) and setting $P_L = -P_s$, the pressure at the tube entrance and thus, the total longitudinal pressure drop can be determined. The results of such calculations for each tube at the extreme pressures (-2.0 and -8.0 inches of water) are provided in Table 5.1. As can be seen, the drops in pressure from one end of the tube to the other are approximately three orders of magnitude smaller than the pressures applied to the system.

Table 5.1. Pressure Drops Along the Lengths of the
Various Pore Sized Tubes (10.0, 2.0, 0.7,
and 0.3 microns)

| Tube Pore Size (μm) | P_s = -2.0 in.H_2O | | P_s = -8.0 in.H_2O | |
	Q_z (ml/min)	P_o - P_L (in.H_2O)	Q_z (ml/min)	P_o - P_L (in.H_2O)
10.0	73.5	1.602×10^{-3}	71.1	1.550×10^{-3}
2.0	71.5	1.305×10^{-3}	69.3	1.265×10^{-3}
0.7	70.4	7.866×10^{-4}	67.0	7.486×10^{-4}
0.3	70.2	1.080×10^{-3}	67.2	1.034×10^{-3}

This factor may become more predominant if the lengths of the tubes are increased or the internal diameters decreased assuming that the flow rates are maintained. In order to account for the situations where these pressure drops can greatly affect the net pressure differential in the radial direction, the following adjustments would have to be made to Equation (34).

$$F_{p,net} = -[P_s + \Delta P/2][V_{void, filled}/h] \qquad (43)$$

In Equation (43), ΔP represents the pressure drop, $P_o - P_L$, which is equal to $P_o - P_s$ and can be calculated in the same manner as the results of Table 5.1. Therefore, the overall force balance can be written to include a substantial longitudinal pressure drop should one be shown to exist.

$$[4\gamma\cos\phi/hd - (2P_s + \Delta P)/2h - \rho g\cos\theta]\phi v(\pi/4)$$
$$[(D_i + 2h)^2 - D_i^2]L - \rho g\cos\theta(\pi/4)D_i^2L = 0 \qquad (44)$$

This alternative force balance may prove to be more applicable to the experimental apparatus of this research even though the results of Experiment 1 and Table 5.1 show that ΔP is negligible. After an evaluation of the experimental design of the flow rate measurements, the procedure used to obtain the results may have been inappropriate. The major problem with the methodology used in these determinations was that the conditions of the PCTPNS was altered from a steady state to a dynamic situation. When the pressure was set and maintained at a constant value, the entire nutrient recirculation system was closed off from the environment. Since the speed of the pump was constant then the flow rate through this closed system should have been the same regardless of the value of the pressure measured at the tube exit. As described in the Materials and Methods Section of this report, the desired negative pressure was obtained by injecting or withdrawing liquid from the Nutrient Reservoir using the 50 ml Pressure Adjustment Syringe (see Figure 3.1). This method of pressure control simply changes the internal pressure of the entire system relative to the atmosphere (as read on the Negative Pressure Gauge) but should not have altered the pressure drop between the ends of a particular tube as was indicated in the results of Experiment 1 and Table 5.1. The reasons

behind these results stem from the fact that the flow measurements commenced when Valve 5 was closed and Valve 6 opened, caused the system to become open to the environment. Thus, the internal pressure would tend towards an equilibrium with the atmospheric pressure and the time required would be dependent upon the initial, steady state pressure setting. This explains why there were slopes in the flow rate versus time graphs in Figure 4.1.

In order to explain the differences in the intercepts of each of the plots of Figure 4.1, the Hagen-Poiseuille Equation (Equation 42) can be used. Since Q_z should be constant due to the constant speed pump, then the pressure drop through each tube would only be dependent upon the internal diameters of the tubes. As stated previously, D_i varied from one tube to another and could be the reason behind the variations in the intercept values. These differences in the pressure drops for each tube would translate into differences in the internal pressure of the entire system even though the pressure read on the Negative Pressure Gauge remained the same. The pressure at one particular point in the system (i.e. the tube exit) can be set to an equivalent value for each tube but the pressures at other points may not be the same when compared between tubes. This is particularly true for the Nutrient Reservoir Diaphragm which would act as a pressure buffer for the system since it can expand and contract (change its diameter) as well. A hypothetical plot of the "pressure situations" in the PCTPNS for different tube internal diameters is provided in Figure 5.3 to aid in this explanation. In this figure, three different tube diameters, $D_{i,1} < D_{i,2} < D_{i,3}$, have three different pressure drops between the ends of the tubes. Each of these pressure drops is compensated for at the Nutrient Reservoir Diaphragm where its effective diameters are in the order, $D_{d,1} > D_{d,2} > D_{d,3}$. When the system is opened to the atmosphere at the Fill Syringe, the expandable/contractible Nutrient Reservoir Diaphragm would become an additional controlling factor in the time required for system equilibration. In other words, the diaphragm would act similarly to a second pump imparting a pressure whose magnitude and sign would depend upon its initial state. If it were initially expanded, then its consequent contraction during the unsteady conditions would force liquid out faster while in
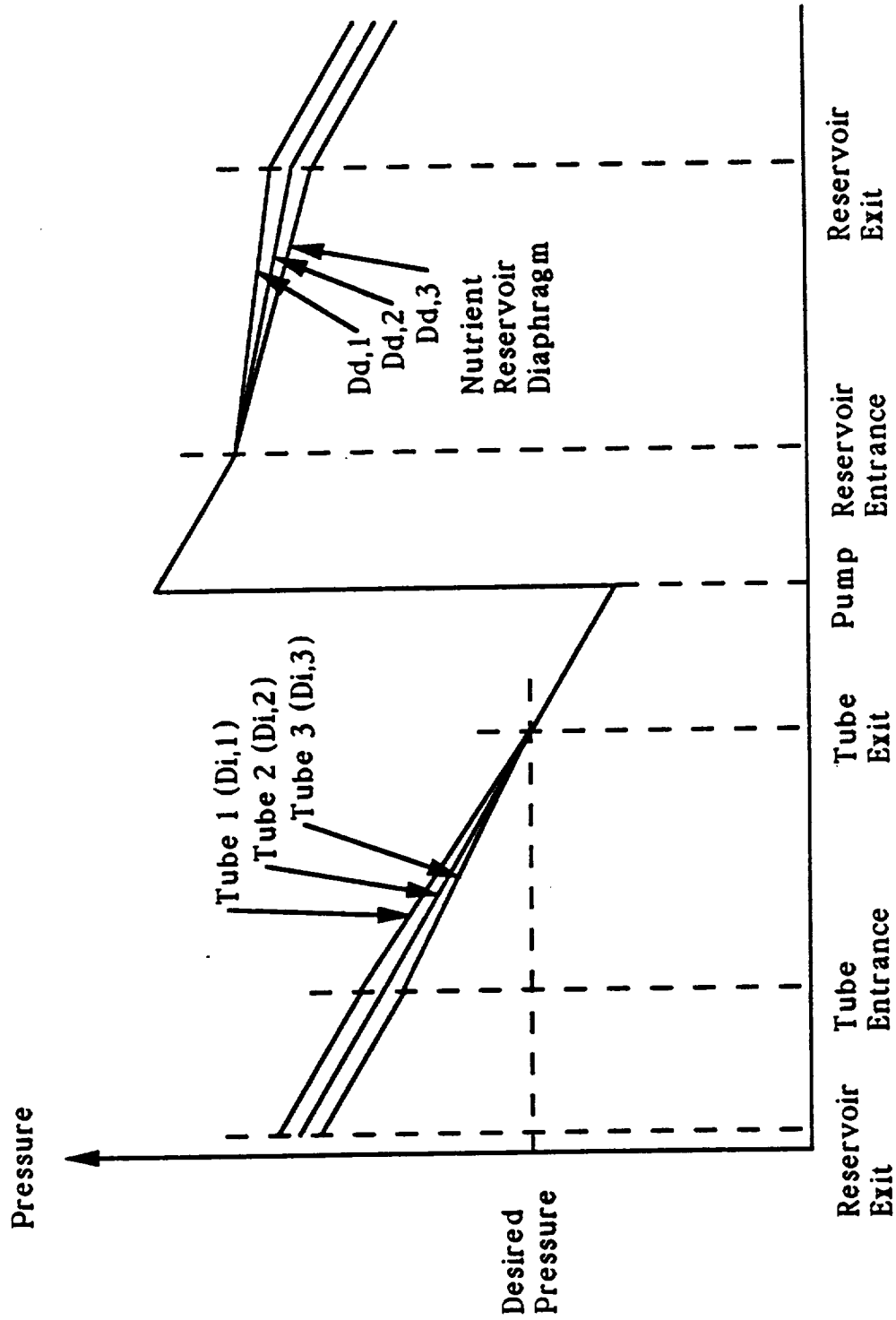
Figure 5.3. Hypothetical Plot of the "Pressure Situation" in the PCTPNS for Three Tubes with Different Internal Tube Diameters ($D_{i,1} < D_{i,2} < D_{i,3}$)

the reverse situation; its expansion from an initially contracted state would slow the liquid flow.

These same arguments can be used to explain the results of Experiment 2. Specifically, the determinations of the permeability coefficients were conducted under an unsteady state condition since liquid wept continuously from the tubes. Intuitively, this parameter should not have varied as the suction pressure was altered since the permeability coefficient is a function of the properties of the porous medium (Geankoplis, 1983). However, the results depicted in Figure 4.2 seem to contradict this conclusion and can possibly be explained by the unsteady state situation of the experiment. At near zero suction pressures, the rate at which the liquid was collected in the Catch Pan would have been greater than liquid collected at larger suction pressures. In addition, this loss of liquid would have resulted in a greater change in the suction pressure as the experimental time continued. Therefore, the pressure, P_s, used in Equation (10) which only represented the initial pressure setting should have been replaced by a term which took into account the total change. By altering the denominator of this equation, the larger variations exhibited at the smallest initial suctions would have caused the results of the permeability coefficients to decrease. In other words, the changes in the rate of loss of liquid, V_r/t, between each initial pressure setting would have been compensated for by the differences in the pressure changes. However, since the total change in the suction was not recorded, then new calculations of the permeability coefficients cannot be performed.

In order to verify the mathematical model of the PCTPNS as given in Equation (39), the results of Experiment 2 can be used. Specifically, since the rate of weeping from the smallest pore sized tube (d = 0.3 microns) at a suction pressure of -0.2 inches of water was extremely slow (Q_r = 0.042 ml/min), then this situation roughly approximates a steady state condition. The presence of weeping at this fairly slow rate would be indicative of a contact angle, ϕ, being slightly greater than $\pi/2$ radians. In addition, the average height of liquid in the porous matrix, h, would be equivalent to the level at the outer diameter, D_o, of the ceramic tube.

$$h = (D_o - D_i)/2 \tag{45}$$

Thus, substituting Equation (45) into Equation (39) and solving for $\emptyset$ gives,

$$\cos\emptyset = \frac{(D_o - D_i)d}{8\gamma} \left[\frac{pg\cos\theta D_i{}^2}{\phi_v(D_o{}^2 - D_i{}^2)} + \frac{2P_s}{D_o - D_i} + pg\cos\theta \right] \tag{46}$$

Using the physical dimensions of the tube, $D_o = 1.6$ cm, $D_i = 1.2$ cm, and the void fraction, $\phi_v = 0.339$ (see Experiment 3 Results) along with the properties of water such as the density, $p_w = 1.0$ g/cm^3 and the surface tension, $\gamma = 72.75$ dyne/cm, the contact angle can be calculated. Of course, since this is an Earth-bound application where the specific gravity, g, is constant at 980.6 cm/s^2, then the contact angle at the top ($\cos\theta = 1$) and at the bottom ($\cos\theta = -1$) of the tube would be slightly different. The results of these calculations yield a contact angle at the top of the tube which is slightly less than $\pi/2$ radians at 89.992°. However, at the underside of the tube where the effects of gravity are the largest, the corresponding contact angle was greater than $\pi/2$ radians at 90.003°. Therefore, this result confirms that weeping should occur under these operational conditions albeit at a slow rate. In addition, this further verifies that the model equation can be used to describe the flow characteristics of the PCTPNS.

5.4. Evaluation of the Moisture Sensor Device

The measurement of "wetness" of the ceramic material is an important aspect in using the mathematical model developed in this paper to explain the characteristics of the PCTPNS. As stated earlier, the definition of "wetness" is the amount of liquid contained in the total void space of the ceramic matrices. Therefore, this characterizing definition is directly related to the average height of liquid, h, in the porous material. In the verification calculations for the mathematical model, this parameter was set equivalent to half the distance between the internal and external tube diameters (see Equation 45). For operational conditions far from weeping, this parameter must be measured in order for the calculations to be completed. The one method which has been proposed to aid in accomplishing this requirement is the use of the thermistor based moisture sensor device.

In order to evaluate the applicability of this device to achieve the goal of measuring h, the following criteria were tested. First, the stability of this instrument was examined by calculating the standard deviations of the non-successive measurements of Experiment 5. The average standard deviations for each of the four decreasing pore sized tubes were ± 7.4, ± 3.5, ± 4.2, and ± 8.4, respectively. These deviations represent less than 5% of the average sensor readings and therefore indicate a satisfactory stability in the instrument. The second criteria test was to determine how consistent this device was when measurements were taken during different trials and by different experimenters. The results of Figures 4.3.1 to 4.3.4 for the 10.0, 2.0, 0.7, and 0.3 micron pore sized tubes, respectively, revealed that these standard errors associated with the linear regression lines could not account for the other trial results. In addition, tripling the error estimates which should account for 99.7% of the results (Spiegel, 1961) still could not achieve this. Therefore, although the measurements by this moisture sensor device were relatively stable, repeated use did not reveal a satisfactory consistency.

A third means of evaluating this moisture sensor device was to test the resulting voltage readings against established physical occurrences. Since the pressure has a direct influence on the average

liquid level in the porous tube, the moisture content would be similarly affected. Therefore, the requirement of the pressure drop along the length of the tubes (Bird, et al., 1960) should have yielded a correction as measured by the sensor device. This is based on the premise that this device differentiates between the rates of heat dissipation in air and in liquid (Bean, et al., 1990). However, the results of Experiment 6 (see Tables 4.3.1 to 4.3.4) show that this device could not discern between the changes in pressure due to the longitudinal flow through the tubes. In fact, the standard deviations of the sensor measurements reveal that a pressure rise could not have occurred through these tubes. This phenomenon is illustrated in Figures 5.4.1. to 5.4.4 for the 10.0, 2.0, 0.7, and 0.3 micron tubes, respectively. As can be seen from these figures, no clear correlation can be obtained between the voltage and location of the sensor along the tubes. One note that should be pointed out in favor of possibly applying this device to the PCTPNS is that the pressure drops through these tubes are very small and the deviations may just be due to the sensor instabilities.

The two situations when the moisture sensor device can be applied to the PCTPNS are static and dynamic conditions. Although the readings at one location on the tubes were precise in that they were repeatable, readings at different locations (i.e. radial pressure differentials) show this sensor was not necessarily accurate. In addition, each time that this device is used a new calibration procedure would have to be performed since the voltage readings obtained would not be consistent with past results. Therefore, the applicability of the moisture sensor device to measuring h in the PCTPNS under static conditions appears to be quite limited. The fallacies and inconsistencies in the sensor itself would lead to inconsistent measurements of h. However, the one consistent phenomenon that was observed while testing this instrument was that the time required to reach a maximum voltage reading varied with the magnitude of the applied suction. This dynamic characteristic of the sensor is illustrated in the results of Figure 4.4 which shows that longer measurement times are required for greater suction pressures.

Figure 5.4.1. Sensor Reading as a Function of the Location
of the Moisture Sensor Device Along the Length
of the 10.0 Micron Tube

———□——— 3.0 in.H2O

———◆——— 7.0 in.H2O

Figure 5.4.2. Sensor Reading as a Function of the Location of the Moisture Sensor Device Along the Length of the 2.0 Micron Tube

3.0 in.H2O

Figure 5.4.3. Sensor Reading as a Function of the Location
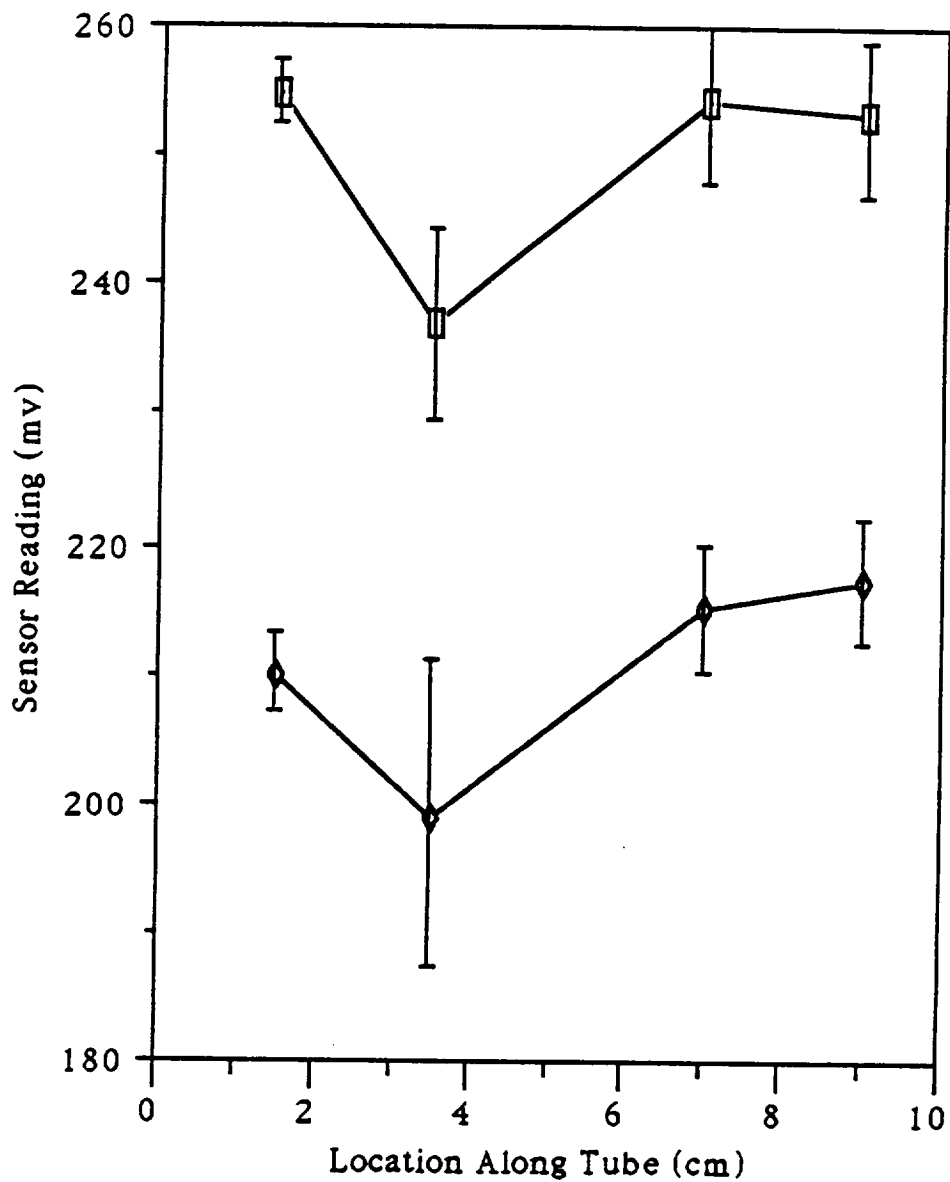of the Moisture Sensor Device Along the Length
of the 0.7 Micron Tube

Figure 5.4.4. Sensor Reading as a Function of the Location of the Moisture Sensor Device Along the Length of the 0.3 Micron Tube
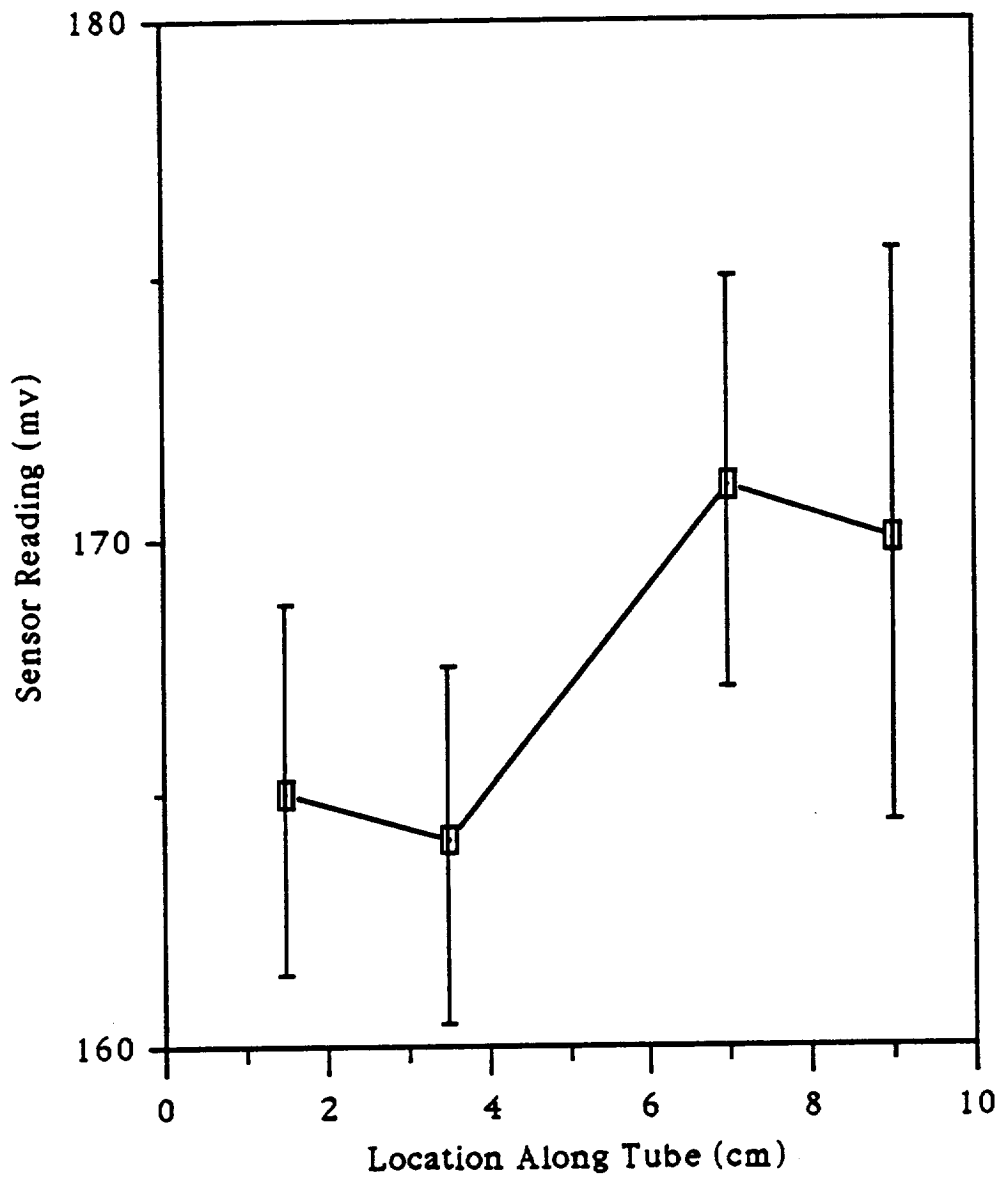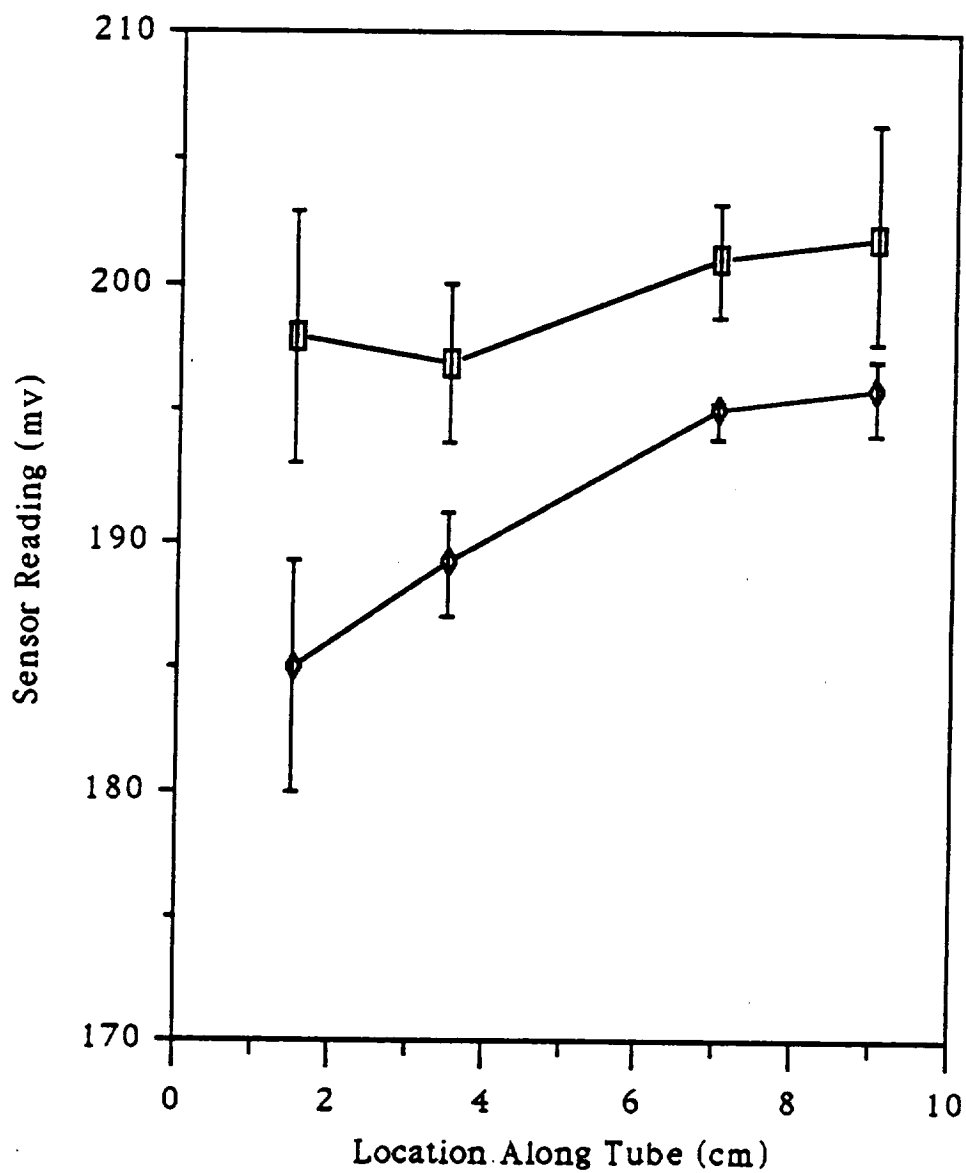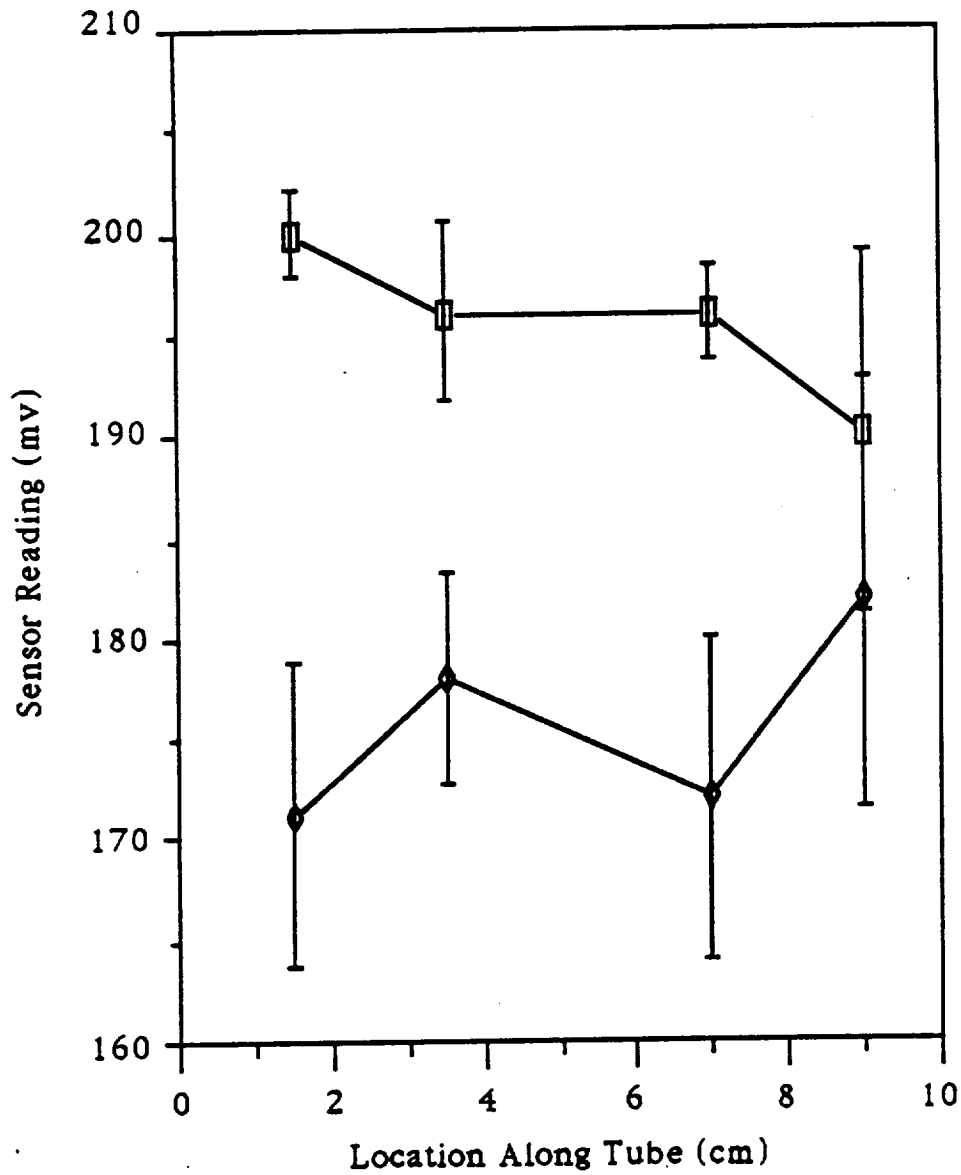
3.0 in.H2O

7.0 in.H2O

In order to explain this trend, the concepts of liquid wetted surfaces needs to be combined with the concepts behind the development of the models for the PCTPNS. When the thermistor is placed in contact with the moist tube, an extra surface to which the liquid can wet is introduced into the system. In other words, the thermistor itself becomes an additional wall of the external pore spaces to which liquid can cling. Therefore, the flow rate of liquid into a capillary space which depends upon the initial state would directly affect the rate at which heat was dissipated from the constant heat source of the sensor. Since the initial steady state conditions (i.e. before sensor contact) are dependent upon the applied suction pressure, as illustrated in the mathematical model, then the time required for the liquid to rise to the thermistor would be correspondingly dependent. Therefore, a correlation between the time required and the applied suction pressure should exist and is shown in Figure 4.4 to be a linear relationship for the 10.0 micron pore sized tube. In addition, this result shows that the thermistor based moisture sensor device may be applicable to a more dynamic operation of the PCTPNS. However, the initial condition of the liquid height in porous matrices would still need to be determined by some other means in order for these unsteady state measurements to be meaningful. Therefore, this device cannot be successfully applied as a method to measure the average liquid level, h, in the porous tubes which is required to further verify the mathematical model.

In order to determine whether the voltage readings of the moisture sensor device corresponded to the water flux onto sections of a root-like absorbant, the experiments of Thomas Dreschel were repeated. For the 10.0 and 0.3 micron pore sized tubes, the water flux rates, F, plotted against the applied suction pressures are presented in Figures 4.5.1 and 4.5.2, respectively. Correspondingly, the sensor readings as a function of the negative pressures are plotted as well and are shown in Figures 4.3.1 and 4.3.4 for the two different pore sized tubes. In order to compare these results, the water flux rate at a given suction pressure was plotted against the corresponding value obtained by the moisture sensor. The results of these comparisons for the 10.0 and 0.3 micron tubes are provided in Figure 5.5.1 and 5.5.2, respectively. As can be seen in these plots, the average flux at each pressure is linearly correlated to the sensor
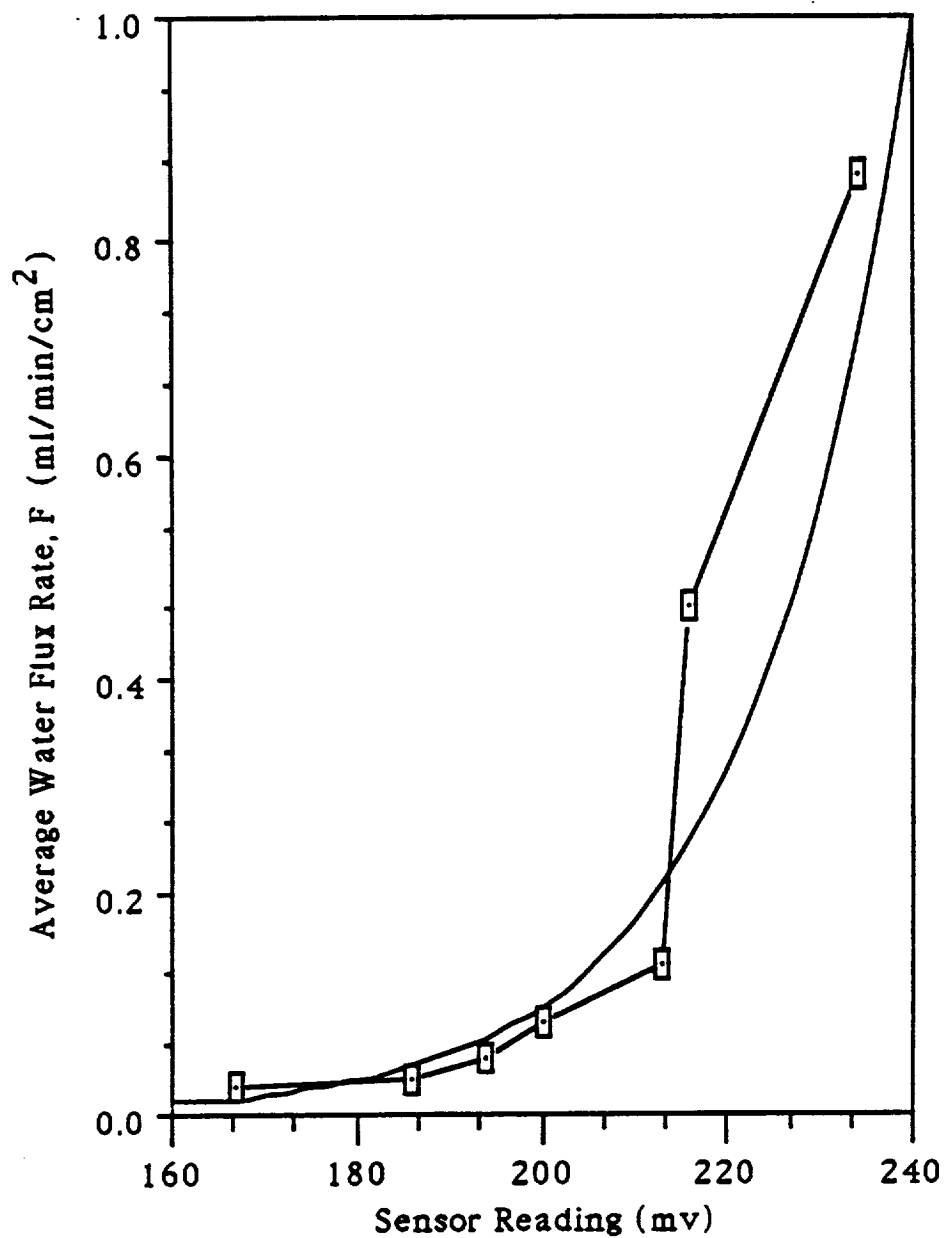
Figure 5.5.1. Non-Linear Correlation Between the Average
Water Flux Rate and the Sensor Reading
Obtained from the 10.0 Micron Pore Sized
Tube

F = 9.78e-7 * 10^(2.51e-2 Sensor Reading)   R^2 = 0.894
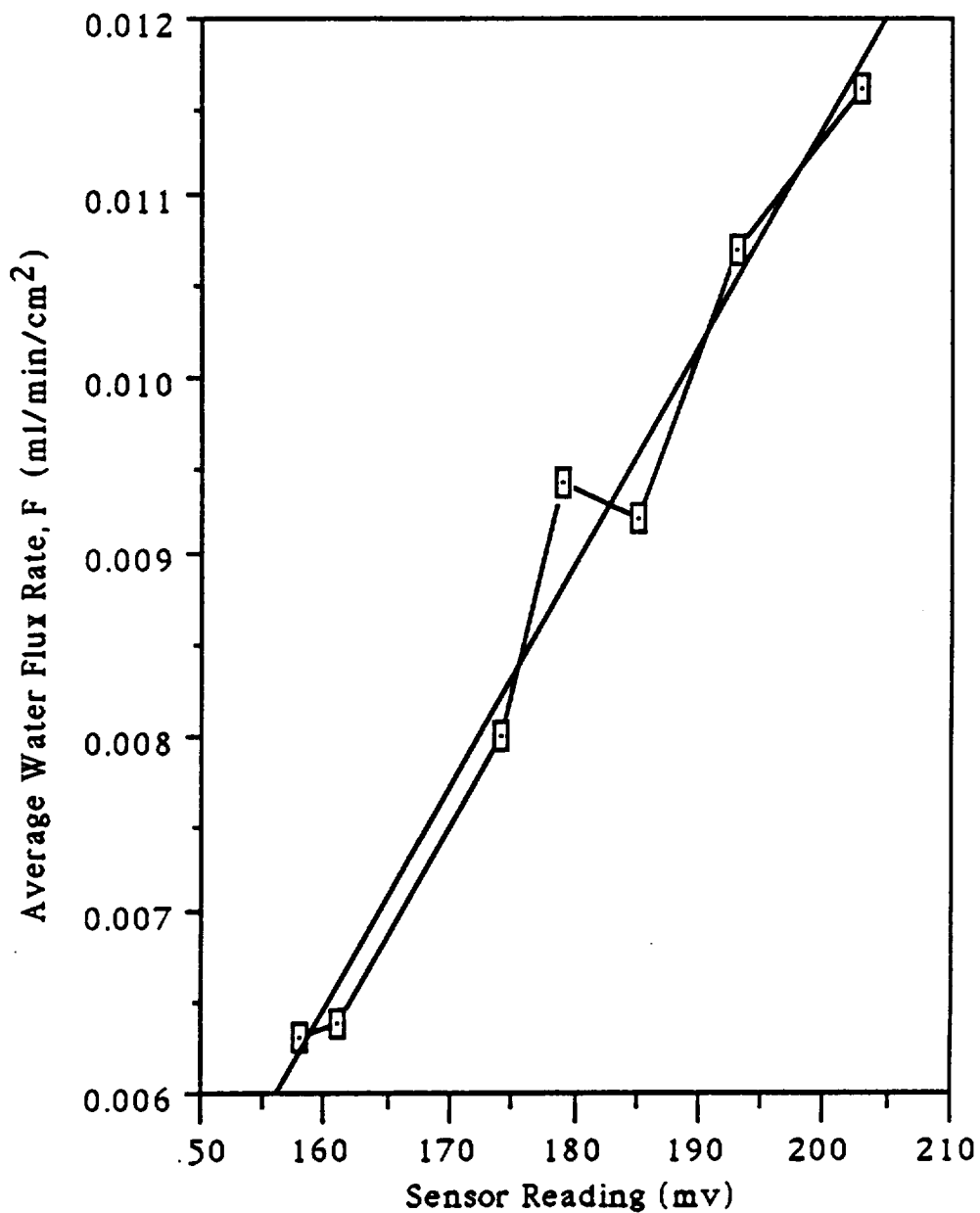
Figure 5.5.2. Linear Correlation Between the Average
Water Flux Rate and the Sensor Reading
Obtained from the 0.3 Micron Pore Sized
Tube

$$F = -1.31e\text{-}2 + 1.23e\text{-}4 \text{ Sensor Reading} \quad R\hat{}2 = 0.975$$

readings for the 0.3 micron tube while there exists a non-linear relationship for the 10.0 micron tube. However, in the range between approximately 160 and 200 mv, the results are both fairly linear with the deviations for the 10.0 micron pore sized tube occurring at higher voltages. Therefore, a more nonlinear relationship may exist in the smaller pore sized tube as well as at near zero suction pressures. This illustrates that the thermistor based moisture sensor device may still be an applicable system to the PCTPNS but would require more clarifying tests.

C-2

6. RECOMMENDATIONS

6.0. Future Research

This section of this research paper is devoted to an overview of the recommendations for future research conducted on the PCTPNS. First and foremost, the tube composition and the plant nutrient solution elements need to be examined. The procedures for these tasks need to be conducted prior to any biological influences in order to determine whether these considerations contain any independent influences. Secondly, the operation and design of the experimental apparatus needs to be improved to alleviate the problems encountered in this research. In particular, the PCTPNS and the "wetness" sensing device need to be redesigned and reevaluated in order to make the control and measurement of the operating conditions more easily obtainable than was possible in this research. These operational considerations will lead to further verifications and possible adjustments to the physical and mathematical models developed. The third recommendation involves incorporating the considerations of plant physiology in the physical and mathematical models. Specifically, the root-tube interface needs to be visualized qualitatively and the elemental interactions determined quantitatively. The requirements of these three considerations are outlined in the last portion of this section and are a prelude to conducting the future research objectives. All or part of these can be performed as a doctoral research topic for the principal investigator of this paper depending upon the availability of each requirement.

6.1. Material Considerations

The physical model of the PCTPNS as depicted in Figure 5.1 was developed through the observations of the liquid-ceramic material interactions under various operational conditions. In particular, the change in the average level of liquid or the "wetness" of the ceramic was influenced by the applied suction pressure and the local surface tension interactions. In defining how these phenomena affect the movement of liquid in this system, the physical make-up and construction methods of the ceramic tubes need to be clarified. In particular, the hydrophilic nature of the inorganic oxides along with their material interactions with the nutrient elements needs to be determined. In addition, any effects of the construction techniques used to form these ceramic tubes should be examined as well. This information would be available from the suppliers of this product, Osmonics, Inc., and is the first recommendation for furthering the research on the PCTPNS.

The quantities and types of inorganic oxides used in the formation of these various pore sized tubes need to be determined in order to quantify the hydrophilic nature of the material. Once the exact composition is known, an investigation of the water bonding capacity of the materials could be accomplished. The tasks involved in this investigation would include talking with Osmonics, Inc. in order to obtain this specific information or even samples of the granular particles used in the construction of the tubes. Perhaps the most important aspect of these materials is whether or not water will adhere stronger to these particles or to water itself cohesively. The degree of hydrophilic attraction has a direct effect on the surface tension forces as a whole and would be functionally related to the contact angle, ϕ. If the attraction between these two mediums is greater in magnitude than the cohesion of water for itself, then o will be close to zero. On the other hand, if the cohesive surface tension of water is greater than the attraction, then ϕ will be far from zero degrees (see Figure 5.2 for reference). Since this parameter in the model equation (Equation 39) is a relative unknown except in cases such as under weeping conditions, determining the functionality of the adhesive interaction would be desirable. Not only could this lead to further verifications of the model equation at least at 1-g force, but

a determination of the relative magnitudes of all of the affecting forces can be done. This will be of particular importance when the forces due to gravity are substantially reduced and new operational conditions defined.

From the literature review, construction materials interacting with the nutrient elements of a hydroponic solution can lead to some problems. In particular, the leaching of toxic compounds or the absorption of essential nutrients from the solution by the porous medium can lead to some nutritional disorders (Averner, et al., 1984). This situation is supported in the plant growth tests by the analyses of the composition of the solution between the tube and the roots. Certain elements were shown to accumulate in this region while others did not (Dreschel, 1988; Olson, et al., 1989). Whether or not the inorganic oxides of the ceramic material have binding capacities for some of the nutrient elements has yet to be determined. Again, this information may be available from Osmonics, Inc., but if not, running the nutrient elements through columns packed with the granular particles could lead to this determination. An atomic analysis of the solution after it passed through the column would have to be compared to the original composition in order to make this determination. These types of experiments are recommended to be conducted prior to plants being cultivated on the PCTPNS.

Another factor which needs to be clarified is the influence of the construction techniques used to form these tubes on the porosity of the material. The lack of correlation between the average pore size and the void fraction of the ceramic tubes and disks suggests that different protocols for construction may have been used. The effect of this factor on the flow of liquid through the PCTPNS can be realized through the use of Equations (28), (33), (34), and (35). For a given average liquid level, h, in the cylindrical tubes, the void volume that is actually filled with liquid is directly proportional to the void fraction (see Equation 28). According to Equations (33) and (34), o_v would also have a direct proportional influence on the magnitudes of the surface tension and pressure differential forces, respectively. However, the force due to gravity is only partially affected by o_v since the bulk fluid flow in the tube interior must also

be included. The internal diameters of the tubes have also been shown not to correlate with the average pore sizes of the tubes. Therefore, in order to compare the relative magnitudes of the contributing forces, a clearer understanding of the techniques used to form these cylinders is required.

The information required would include the average grain size of the inorganic oxides, the type of fluxing agent used, and the amount of compression used in forming the various shapes. This type of information should also be available from the suppliers of these tubes. Once these are obtained, the production process could possibly be controlled by specifying desired ϕ_v and D_i values so that F_{st} and $F_{p, net}$ would be optimized while the influences of the gravitational force would be reduced. This particular situation would be desired since the changes in gravity such as those present in space travel are uncontrollable. Therefore, if the magnitude of F_g is reduced, then the changes in the operational settings corresponding to the changes in g would be less dynamic and easier to control. In other words, if the magnitudes of F_{st} and $F_{p, net}$ can be designed on Earth to be considerably larger than F_g, then the changes in gravity present in space would have a smaller effect on the entire operation of the PCTPNS.

6.2. Operational Considerations

A redesign of the experimental apparatus and procedures is recommended before further tests are conducted on the PCTPNS itself. In particular, tighter control and measurement of the applied system pressures and corresponding flow rates need to be obtained which were not present in this research. In addition, the acquisition of "wetness" sensing data needs to be improved in order to facilitate this tighter control of the system. With these adjustments to the current PCTPNS, verifications of the physical and mathematical models can be accomplished for both short and long-term operations. This will lead to any required adjustments that should be made to the current models developed.

The pressure drop and flow rate measurements such as those in Experiment 1 (see Figure 4.1 and Table 5 .1) need to be improved. The major fault of the method used in this research was that the system was altered from a steady to an unsteady state condition when the experiment commenced. This led to unsteady state flow rate data which was not indicative of a continuously operated system as was desired. In order to overcome this problem, the flow rate measurements can be made from a flow meter installed somewhere in the system line instead of utilizing the Fill Syringe. Alternatively, additional pressure gauges could be installed at key locations in order to measure the pressure drop corresponding to the given flow rate (see Hagen-Poiseuille Equation - 42). Using Figure 3.1 as a reference, a pressure gauge placed at the tube entrance could be used to measure the ΔP within the Porous Ceramic Tube. Likewise, additional gauges at the entrance and exit of the Nutrient Reservoir Diaphragm could be installed to measure the corresponding pressure drop. These two pressure drops are desired since the theoretical "pressure situations" depicted in Figure 5.3 were not quantified. In addition, the magnitude of the ΔP existing in the ceramic tubes needs to be determined in order to evaluate the assumption of neglecting this effect in the current model equation.

The problems discussed earlier associated with Figure 4.1 can be alleviated if an alternative means of controlling the applied pressure is used. The method used in this research utilized the Pressure Adjustment Syringes which resulted in the variations in the volumetric flow rates. The other method which could have been used involved the Flow Control Valve which was maintained fully open during the experiments. The problem with this second method was that this valve was highly insensitive and, therefore, difficult to control to obtain the desired pressure readings. If a more sensitive valve could be installed in the current experimental apparatus, then this would represent an optimum means of controlling the applied pressure in the ceramic tubes. Once this is accomplished, further experiments to improve and verify the model equation can be conducted not only here on Earth but in alternative gravitational environments as well.

The thermistor based moisture sensor device converted the heat dissipation into a millivolt reading using an analog-to-digital converter (Bean, et al., 1990). Instead of utilizing a voltmeter to measure the sensor signal, a data acquisition computer could be programmed to continuously monitor the signals sent by the sensory device (Miles, 1990). This computer could then process the data by comparing the readings to a standardized curve (Δ Sensor Reading vs. ΔP) and adjust the pressure control valve accordingly. These types of plots would be similar to those derived earlier in Figures 4.3.1 to 4.3.4. However, as is evident from these curves, this particular sensory device does not give consistent results between uses and any previous calibrations may be useless. In addition, the time required by this device to measure dynamic changes in the moisture content can be as long as 35 seconds (for the 10.0 micron tube). This time requirement translates into a lag time which would exist between the acquisition of the voltage data and the corresponding adjustments to the applied pressure by the computer. Therefore, the thermistor based moisture sensor device may not represent the best method of measuring "wetness" due to its inconsistency and long response times.

Before a final verdict on the applicability of this device to the PCTPNS can be made, further evaluations should be made particularly after the redesign of the hydroponic system. With pressure gauges installed at both ends of the Porous Ceramic Tube, the sensor can be more accurately correlated with a corresponding pressure drop. This comparison to a physical occurrence was used as the third criterion in the evaluation of this device. Perhaps the most telling evaluative experiment in this research which should be expanded upon is the comparison of the sensor readings to the absorption rate into sections of germination paper. As was seen in Figure 5.5.1, the relationship between these two results was nonlinear for the 10.0 micron tube. However, the 0.3 micron pore sized tube gave results which were indicative of a linear relationship. Since this sensor cannot discern between the different pore sizes of the ceramic tubes, then there should only exist a single functional relationship between these two parameters. In order to test this hypothesis, other applied suction pressures which are closer to zero should be used to obtain a wider range of results for the 0.3 micron

tube. The linear results obtained in this research may only represent the lower half of a non-linear relationship such as is exhibited in the lower half (160 to 200 mv) of Figure 5.5.1. In addition, since only the extreme pore sized tubes were tested, the intermediate tubes could also be included in these experiments in order to obtain clearer results in the transition region between these two trends. These recommendations are just extensions of the experiments conducted in this research as well as those conducted by Thomas Dreschel. In addition, these experiments will further confirm the consistency (or lack of it) associated with this moisture sensor device.

If all of the problems that arise from utilizing this device on the PCTPNS cannot be resolved satisfactorily, then a new method of measuring "wetness" would be required. The average level of liquid must be known in order to verify the mathematical model developed in this research. For the sample verification calculation discussed earlier, h became a known quantity since weeping conditions were occurring. However, under normal operating conditions, this variable would need to be measured in order for the model to be checked completely. The criteria necessary to design a sensor for this application should include remote sensing to maintain steady state conditions, stability and consistency in measurements, rapid response times to compensate for dynamic changes, and a direct relationship to physical phenomena. One solution which is currently being investigated and could meet all of these requirements is the use of an infrared (IR) sensor. For the last criterion, since water absorbs light in the IR region (Bromberg, 1984), projecting a known quanta of IR band light at the moist tube should result in an absorption related to the "wetness" Using an IR sensor, the quantity of light reflected off of the moist surface could be used to back-calculate the amount absorbed. Using several different pressures resulting in several different liquid levels, each tube could be tested to obtain the necessary calibration curves with this remote device. As for the stability, consistency, and response time of this proposed sensor, tests will have to be conducted in future evaluations.

In the long term operation of the PCTPNS such as those required for plant growth, the force due to the evaporation of liquid may have a profound influence on the system. This force is similar

to the forces exerted by the surface tension and pressure differential in that it is directionally independent. In the experiments of this research, this factor was considered negligible since the time durations were relatively short. In addition, the polyethylene wrap shown schematically in Figure 2.3 - Second Design was designed to maintain a near 100% relative humidity at the tube surface and to reduce the degree of evaporation (Dreschel, et al., 1988). However, during a long term operation of this system, substantial losses of liquid to the surrounding atmosphere could result and is recommended to be investigated further.

One of the key factors in this investigation would be the determination of the rate of evaporation of liquid from the PCTPNS. As liquid evaporates, the total volume in the system decreases thus resulting in an increase in the suction pressure. Therefore, batch experiments can be designed to measure the change in pressure from initial to final values and compared to the corresponding rate of evaporation. This rate can be calculated by measuring the change in the total volume of liquid in a given amount of time ($\Delta V_{total}/\Delta t$). Various environmental humidities can be set (such as in a sealed chamber) and used in these experiments in order to obtain a calibration curve between these two factors. Once this calibration is completed, a steady state degree of "wetness" can be maintained in the system by continuously adjusting the pressure applied. The method which would be used to continuously control the pressure would be the maintenance of the total volume of liquid by continuous (or step-wise) replenishments from the Pressure Adjustment Syringes. Therefore, the redesigned experimental apparatus would still require this portion to compensate for the unsteady state influence of the evaporation of liquid from the PCTPNS.

Once the influences of the pressure drop in the tubes and evaporation of liquid from the tubes are elucidated, further adjustments can be made to the models. Verification of the mathematical model could then be conducted here on Earth and under other gravitational forces utilizing either NASA's KC-135 parabolic, weightless simulation flights or a space shuttle mission. An accelerometer would have to be used to measure the changes in

the specific gravity, g, and then a corresponding pressure could be applied to maintain containment of the liquid (i.e. $\phi < \pi/2$ radians). Of course this implies that an accurate means of measuring the average height of liquid in the porous matrix would have to be available. In addition, the controlling device between the "wetness" sensing device and the pressure control valve would have to be designed beforehand.

6.3. Plant Growth Considerations

The ultimate goal of any research conducted on the PCTPNS is the growth of higher plants in an alternative gravitational environment. Up until now, this issue has not been addressed in this research paper but has been restricted to the physical, non-biological system itself. The reasons behind this decision stem from the current lack of knowledge characterizing the flow through the porous ceramic tube. Although this research paper only involved the flow of water, the next step should utilize a hydroponic plant nutrient solution. The ionic interactions between the material make-up of the tubes and the nutrient elements needs to be elucidated prior to any biological influences. Once this investigation has been completed, the complex issue of the effects of plant physiology should be examined in detail. Not only should analytical experiments be conducted to determine the degree of influence of plant roots on the accumulation of elements at the root-tube interface but adjustments due to the stage of growth should be examined as well. These will lead to the final forms of the physical and mathematical models that should be used to charactenze the PCTPNS.

From the literature review, certain components of the nutrient solution have been shown to accumulate at the root-tube interface whiles others maintain absorption into the plant biomass (Dreschel, 1988; Olson, et al., 1989). Possible reasons behind this phenomenon may be due to an interaction with the ceramic material as discussed earlier, but more than likely, the reasons stem from the physiology of the plant root membrane (Dreschel, 1988). The PCTPNS is ideal for an investigation of these occurrences since the plant roots are physically separated from the bulk nutrient solution. Therefore, the

solution contained in the meniscus between the tube surface and the plant root (Wright and Bausch, 1984) can be collected and compared to the bulk concentrations. This would not be possible with conventional hydroponic systems since the plant roots are normally exposed directly to the nutrient solution (Resh, 1987).

Procedures for analyzing the elemental composition of the bulk solution and the solution accumulated on the tube exterior have been established and conducted (Dreschel, 1988; Dreschel and Sager, 1989). Using atomic absorption spectrophotometry, weekly samples of the bulk solution were monitored to show the timed variations in the cation concentrations while daily replenishments of the solution were used. In addition, the solution contained on the roots was pressed using a barrel of clear PVC pipe with a plastic holder used to filter the solution on the pressed roots. This allowed the concentrations of each element present in the run-off to be recorded at harvest time. Similar procedures are recommended to be conducted using nutrient solutions with varying amounts of a specific element. In particular, several elements were shown to accumulate at the root-tube interface at concentrations which were orders of magnitudes greater than the initial conditions (Dreschel, 1988). Thus if a lower content of the nutrient were utilized initially, then the corresponding accumulation may not be prevalent. This would lead to a conclusion that the particular element had an excess availability in the original solution and led to the accumulation at the root outer membrane. On the other hand, if a substantial accumulation still occurred after a reduced quantity was used to grow the plants, then a comparison of the respective concentrations would be required. If a proportional decrease occurs in the bulk and in the meniscus then this would not be a simple factor of availability but could indicate an interaction with another element (i.e. charge balance) or with the plant root membrane itself (i.e. concentration gradient). In order to obtain a more exact elemental species balance, these experiments could be complemented with analyses of the nutrient contents in the plant tissues, particularly the roots. Specific procedures to analyze plant tissues for various elements have been developed (N: Nelson and Sommers, 1973; P,K,Ca,Mg,Fe,Mn,Zn,Cu,B,Mo: Jones, 1985; S: Hafez, et al., 1991) and could be conducted in conjunction with the spectrophotometric readings. These types of experiments would lead

to a clearer understanding of the physiological requirements and mechanisms of plant roots.

An extension of this investigation could be conducted to include an analysis of the variations in nutrient requirements dependent upon the stage of growth of the plant. Current nutrient replenishment techniques only utilize a single set solution mixture throughout the entire growth cycle (Resh, 1987). The only exceptions to this occur when a fractional strength nutrient solution is used to germinate seeds or to cultivate plant seedlings. However, the nutrient solution for the remaining stages of the plant life cycle is either replenished as a whole or periodically maintained at prespecified concentrations. Using various lengths of growth times, the variations in the rates of utilization of specific elements by the plants can be determined and compared to the stage of growth.

When plants are grown on the PCTPNS, appropriate adjustments would have to be made to the physical models of this system. A depiction of the contact of the roots to the tube surface would have to be made and added to Figure 5.1. In particular, the meniscus of liquid under non-biological conditions would be different than when plant roots are in contact with the tube surface. In addition, the development of root hairs by the plant (Salisbury and Ross, 1985) can lead to a perpendicular orientation of the root-tube interface instead of the usual parallel arrangement (see Figure 2.1). Again, microscopic observations of the root zone environment could be conducted under these situations in order to make the appropriate adjustments to the model.

As for the mathematical model of the PCTPNS, since nutrient solution will be absorbed by the roots as plants grow, an additional term would have to be included in the model equation. In particular, the force exerted by the absorption of liquid by the plant roots would have to be formulated on a force per unit area of contact basis. This basis makes this force similar to the pressure differential effects but should also take into account the time dependency of the absorption. Since certain nutrient elements absorb continuously while others accumulate in the liquid meniscus outside of the root, individual species balances would have to be formulated in

conjunction with the total solution balance. Furthermore, these species balances will have to include charged interactions between elements, concentration gradients between the bulk and the meniscus regions, and diffusion of elements from one medium to another. The inclusion of these complexities derived from the physiology of plants into the model equation(s) would represent the ultimate explanation of plant growth on the PCTPNS.

6.4. Requirements to Conduct Future Research

The following list summarizes the major items required to conduct the research plans designed to explain the growth of plants on the PCTPNS.

I. Correspondence: Osmonics, Inc.
- Information on Materials
- Ceramic Tubes and Disks
- Ceramic Constituents

II. PCTPNS Components: (see Figure 6.1)
Ceramic Tubes
- Various Pore Sizes
- Various Physical Dimensions (ID, OD, Length)
Reservoir Diaphragms
Pumps
Negative Pressure Gauges
Interconnecting Tubing (Opaque)
Flow Control Valves

III. Sensors: Thermistor Based Moisture Sensor
IR Based Moisture Sensor/IR Source
pH Probe

IV. Biological Materials: Plant Seeds

V. Chemicals: Nutrient Solution Constituents
                  - Macro-Nutrients
                  - Micro-Nutrients
                 Nitric Acid and Ammonium Nitrate (pH Control)
                 Analytical Reagents   •

VI. Analytical: Atomic Absorption Spectrophotometer
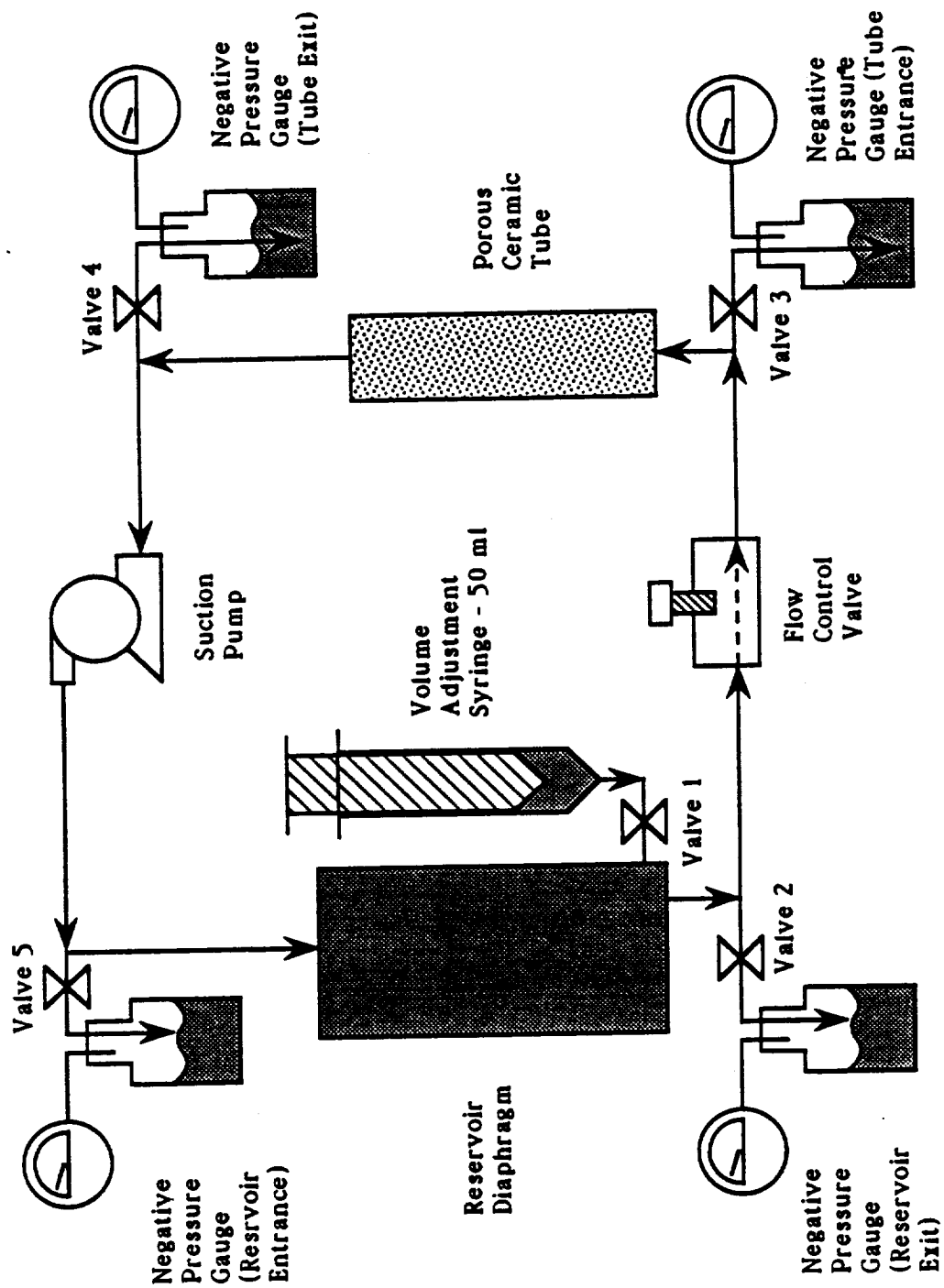   Glassware (Tissue Analysis)
                 Root Press

Figure 6.1. Redesigned Porous Ceramic Tube Plant Nutrification System (PCTPNS)

7. REFERENCES

Averner, M. M., R. D. MacElroy, and D. T. Smernoff: Controlled Ecological Life Support System - Section II. Ames Research Center, Moffett Field, CA., 1984.

Bausch, W. C. and B. D. Wright: Wright, B. D. Thesis Submitted to the Agricultural and Chemical Engineering Department at Colorado State University, Fort Collins, CO., 1985.

Bean, L., G. Clark, B. Finger, P. Severson, and A. Speicher: Porous Medium Wetness Sensing, 1990.

Berry, W. L., G. Goldstein, T. W. Dreschel, R. M. Wheeler, J. C. Sager, and W. M. Knott: Water Relations, Gas Exchange, and Nutrient Response to a Long Term Constant Water Deficit. UCLA, Los Angeles, CA., 1990.

Bird, R. B., W. E. Stewart, and E. N. Lightfoot: Transport Phenomenon. John Wiley & Sons, Inc., New York, NY., 1960.

Bromberg, J. P.: Physical Chemistry, 2nd Edition. Allyn and Bacon, Inc., Boston, ME., 1984.

Dreschel, T. W., R. P. Prince, C. R. Hinkle, and W. M. Knott: Paper #87-4025 presented to the ASAE. Baltimore, MD., June 28-July 1, 1987.

Dreschel, T. W.: NASA Technical Memorandum 100988. NASA, John F. Kennedy Space Center, FL., 1988.

Dreschel, T. W., J. C. Sager, and R. M. Wheeler: Paper #88-4524 presented to the ASAE. Chicago, IL., Dec. 13-16, 1988.

Dreschel, T. W. and J. C. Sager: Hort Science, Vol. 24, No. 6, pp. 944-947, 1989.

Dreschel, T. W., R. M. Wheeler, J. C. Sager, and W. M. Knott: Factors Affecting Plant Growth in Membrane Nutrient Delivery. In: "Controlled Ecological Life Support Systems: CELSS '89 Workshop," R. D. MacElroy, ed. Ames Research Center, Moffett Field, CA., 1990a.

Dreschel, T. W., C. S. Brown, C. R. Hinkle, J. C. Sager, and W. M. Knott: Paper #90-4533 presented to the ASAE. Chicago, IL., Dec. 18-21, 1990b.

Dreschel, T. W., R. P. Prince, W. M. Knott, and C. R. Hinkle: Unpublished Paper. NASA, John F. Kennedy Space Center, FL., no date.

Geankoplis, C. J.: Transport Processes and Unit Operations, 2nd Edition. Allyn and Bacon, Inc., Boston, ME., 1983

Hafez, A. A., S. S. Goyal, and D. W. Rains: Agronomy Journal, Vol. 83, pp. 148-153, 1991.

Humble, G. D. and K. Raschke: Plant Physiology, Vol. 48, pp. 447-453, 1971.

Jones, J. B.: Horticulture Review, Vol. 7, pp. 1-68, 1985.

Koontz, H. V., R. P. Prince, and W. L. Berry: Hort Science, Vol. 25, No. 6, p. 707, 1990.

MacElroy, R. D.: Draft Permeable Membrane Plant Nutrient Experiment Statement of Work. Ames Research Center, Moffett Field, CA., 1991.

Miles, G. E.: Automatic Data Acquisition and Analysis. In Press, 1990.

Morrison, R. T. and R. N. Boyd: Organic Chemistry, 4th Edition. Allyn and Bacon, Inc., Boston, ME., 1983.

Nelson, D. W. and L. E. Sommers: Agronomy Journal, Vol. 65, pp. 109-112, 1973.

No Name: "Plant Root Support and Nutrient Delivery by a Porous Steel Plate," 1991.

Olson, R. L., M. W. Oleson, and T. J. Slavin: Experiment and Technical Plan. Boeing Aerospace and Electronics, Kent, WA., 1989.

Orbisphere Corporation: Experimental Growth of Plants on Membranes. Orbiterre - A Division of Orbisphere Corporation, Geneva, Switzerland, 1988.

Osmonics, Inc. Product Bulletin: Controlled Porous Ceramics. Osmonics, Inc., Minnetonka, MN., 1988.

Resh, H. M.: Hydroponic Food Production. Woodridge Press, Santa Barbara, CA., 1987.

Salisbury, F. B. and C. W. Ross: Plant Physiology, 3rd Edition. Wadsworth Publishing Company. Belmont, CA., 1985.

Schwartzkopf, S. H., M. W. Oleson, and H. S. Cullingford: Paper #891586 of the Society of Automotive Engineers, Inc., 1989.

Spiegel, M. R.: Theory and Problems of Statistics. Schaum's Outline Series. McGraw-Hill Book Company, New York, 1961.

Tibbitts, T. W., et al.: WCSAR Annual Report Fiscal Year 1989. University of Wisconsin - Madison, WI., 1989.

Wright, B. D. and W. C. Bausch: Paper #84-2524 presented to the ASAE. New Orleans, LA.. Dec. 11-14, 1984.

Wright, B. D., W. C. Bausch, and W. M. Knott: Transactions of the ASAE. Vol. 31, pp. 440-446, 1988.

REPORT DOCUMENTATION PAGE

1. AGENCY USE ONLY *(Leave blank)*	2. REPORT DATE July 1992	3. REPORT TYPE AND DATES COVERED

4. TITLE AND SUBTITLE
Development of Physical and Mathematical Models for the Porous Ceramic Tube Plant Nutrification System (PCTPNS)

5. FUNDING NUMBERS
NAS10-11624

6. AUTHOR(S)
*D. Teh-Wei Tsao, *M.R. Okos, **J.C. Sager, ***T.W. Dreschel

7. PERFORMING ORGANIZATION NAME(S) AND ADDRESS(ES)
*Purdue University, West Lafayette, IN, **NASA, John F. Kennedy Space Center, FL, ***The Bionetics Corporation, John F. Kennedy Space Center, FL

8. PERFORMING ORGANIZATION REPORT NUMBER

9. SPONSORING / MONITORING AGENCY NAME(S) AND ADDRESS(ES)
NASA, Biomedical Operations and Research Office, John F. Kennedy Space Center, FL

10. SPONSORING / MONITORING AGENCY REPORT NUMBER
NASA TM 107551

11. SUPPLEMENTARY NOTES

12a. DISTRIBUTION / AVAILABILITY STATEMENT
Publicly available

12b. DISTRIBUTION CODE

13. ABSTRACT *(Maximum 200 words)*

A physical model of the Porous Ceramic Tube Plant Nutrification System (PCTPNS) was developed through microscopic observations of the tube surface under various operational conditions. In addition, a mathematical model of this system was developed which incorporated the effects of the applied suction pressure, surface tension, and gravitational forces as well as the porosity and physical dimensions of the tubes. The flow of liquid through the PCTPNS was thus charaterized for non-biological situations. One of the key factors in the verification of these models is the accurate and rapid measurement of the "wetness" or holding capacity of the ceramic tubes. This study evaluated a thermistor based moisture sensor device and recommendations for future research on alternative sensing devices are proposed. In addition, extensions of the physical and mathematical models to include the effects of plant physiology and growth are also discussed for further research.

14. SUBJECT TERMS
Porous ceramics, plants, hydroponics, wetness, pressure, surface tension

15. NUMBER OF PAGES
115

16. PRICE CODE

17. SECURITY CLASSIFICATION OF REPORT	18. SECURITY CLASSIFICATION OF THIS PAGE	19. SECURITY CLASSIFICATION OF ABSTRACT	20. LIMITATION OF ABSTRACT
Unclassified	Unclassified	Unclassified	